Carter, R.M., McCave, I.N., Richter, C., Carter, L., et al., 1999
Proceedings of the Ocean Drilling Program, Initial Reports Volume 181

9. Site 1125: Productivity under the Subtropical Convergence on North Chatham Slope[1]

Shipboard Scientific Party[2]

BACKGROUND AND OBJECTIVES

Site 1125 lies on the north slope of Chatham Rise, 600 km east of Kaikoura, South Island, at a water depth of 1360 m (Fig. F1). The site lies under the northern edge of the Subtropical Convergence (STC), a zone of high productivity, and the surface waters above are swept by the East Cape Current (Heath, 1985), which runs south along eastern North Island before turning east along the Chatham Rise. The STC zone is also supplied with water (and suspended sediment) by the Southland Current (Heath, 1972; Chiswell, 1996), which flows up the eastern South Island coast and then turns east in two branches, one north (derived through the Mernoo Saddle) and one south of the crest of Chatham Rise. The crest of Chatham Rise, therefore, is supplied with sediment from five quite different sources: (1) biopelagic snow, generated by high productivity within the vigorously mixing water masses along the STC (Bradford-Grieve et al., 1998); (2) suspended terrigenous sediment derived from river flooding in eastern North Island (East Cape Current); (3) similar terrigenous sediment from the South Island (Southland Current); and, intermittently, (4) direct airfall tephra from major explosive eruptions in the central North Island (e.g., Carter et al., 1995), or (5) occasional rafted iceberg debris (Cullen, 1965). Despite these potentially prolific sediment sources, the crest of the Chatham Rise is mostly shallower than 500 m, and vigorous currents (e.g., Chiswell, 1994) inhibit sediment deposition there. It is well established that only a thin discontinuous layer of upper Neogene sediment occurs on the crest of the rise, which is underlain at shallow subseafloor depths by Miocene chalks and glauconitic marls (Lewis et al., 1985;

F1. Locality map for Site 1125, p. 28.

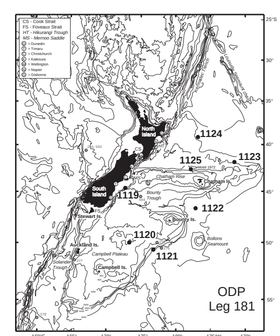

[1]Examples of how to reference the whole or part of this volume.
[2]Shipboard Scientific Party addresses.

Ms 181IR-109

Wood et al., 1989). Phosphatized, glauconitized, and bored pebbles of Miocene limestone are commonly dredged from the Chatham Rise seafloor (Karns, 1976; Cullen, 1980).

Before Leg 181, the ultimate depocenter for material winnowed off the top of the Chatham Rise was unknown, but it seems likely that sediment becomes trapped in topographic lows in deeper waters on both the north and south flanks of the Rise. Site 1125 was drilled at the end of Leg 181 as an alternate site for which only an outdated, reconnaissance seismic line was available (Fig. F2). On the basis of this unsatisfactory seismic record, it was anticipated that the hole would traverse the shallowly dipping lower Miocene chalks that underlie the crest of Chatham Rise, penetrating beyond that to perhaps retrieve a sequence of unaltered upper Paleogene biopelagic sediments suitable for isotope analysis. In the event, Site 1125 proved to contain a thick sequence of rhythmic upper Neogene hemipelagic and biopelagic sediment, and undoubtedly represents a major rise-flank depocenter that has trapped sediment for at least the last 10 m.y. The site is a close counterpart to Deep Sea Drilling Project (DSDP) Site 594, located on the south side of the Chatham Rise at a similar depth (1204 m).

F2. Seismic line through Site 1125, p. 29.

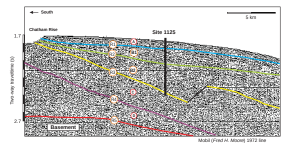

DSDP Site 594 and Ocean Drilling Program (ODP) Site 1125 both lie within lower Antarctic Intermediate Water (AAIW). In the North Atlantic Ocean, intermediate water has been shown to increase in depth range and speed during glaciations, concomitant with a decrease in North Atlantic Deep Water production in the Norwegian-Greenland Sea (Labeyrie et al., 1992). Analogously, in the Southern Ocean, Pudsey et al. (1992) have shown that Antarctic Bottom Water production also diminished during glaciations, in which case AAIW production may also have become greater at the same time. If the vigor of global deep circulation decreased during glaciations, then upper Circumpolar Deep Water from both the Indian and Pacific oceans may have become even more nutrient enriched and oxygen depleted than it is today. Material from Site 1125 will be used for oxygen isotope, carbon isotope, and trace-element analysis to reconstruct through time the changing paleochemistry and paleoproductivity of the site.

Recent paleoceanographic studies have suggested that the STC remained fixed in its general position along the crest of the Chatham Rise throughout the major glacial/interglacial fluctuations of the late Quaternary (Fenner et al., 1992; Weaver et al., 1998). If the STC was similarly stable during the last 10 m.y., then global ocean chemistry shifts, such as the late Miocene carbon isotope excursion at ~6.5 Ma (Loutit and Kennett, 1979) and changing CO_2 fluxes (Compton and Mallinson, 1996), should be able to be sharply delineated and studied in stratigraphic context. The recovered upper Neogene sequence from Site 1125 will thus provide a record of AAIW paleohydrography and of the changing patterns of paleoproductivity that relate either to migrations of the position of the STC or to global ocean chemistry changes.

OPERATIONS

Hole 1125A

The 198-nmi voyage to Site 1125 (proposed site SWPAC-3A) was accomplished at an average speed of 9.0 kt. The vessel proceeded directly to the Global Positioning System coordinates of the location. The hydrophones and thrusters were lowered and the advanced hydraulic piston corer/extended core barrel (APC/XCB) bottom-hole assembly (BHA) was assembled using a 9⅞-in PDC bit and deployed. Hole 1125A was spudded with the APC at 0352 hr on 3 October. The recovery indicated a water depth of 1364.6 m below sea level (mbsl). APC coring advanced without incident to refusal, which was at 203.5 mbsf when Core 22H failed to achieve full stroke. The Adara heat-flow shoe was deployed at 42.5 mbsf (5H), 61.3 mbsf (7H), 80.3 mbsf (9H), 99.3 mbsf (11H), and 118.3 mbsf (13H). The computed heat-flow gradient was 64.9°C/km. The bit was pulled back to 168.0 mbsf, where the top drive was set back. The drill string was pulled out in stands, clearing the seafloor at 2000 hr on 3 October, ending operations at Hole 1125A.

Hole 1125B

The vessel was offset 30 m to the north. To obtain a stratigraphic overlap with the previous hole, the bit was lowered by 5 m from the spudding depth of Hole 1123A, and Hole 1125B was spudded with the APC at 2130 hr on 3 October. The recovery indicated a seafloor depth of 1365.6 mbsl. APC coring advanced without incident to 188.8 mbsf (Table **T1,** also in **ASCII format**). Cores were oriented starting with Core 3H. The hole was deepened with the XCB to 552.1 mbsf, when coring time expired for the leg at 0315 hr on 6 October.

T1. Site 1125 expanded coring summary, **p. 61.**

Logging Operations in Hole 1125B

In preparation for logging, an aluminum go-devil was dropped and the hole was circulated with a 60-barrel flush of high-viscosity mud and displaced with 186 barrels of sepiolite. The bit was pulled back to 512 mbsf and the top drive set back. The bit was placed at the logging depth of 96 mbsf. Logging operations began at 0600 hr on 6 October and ended at 1300 hr the same day. Logging operations were limited to only one full pass of the triple combination tool (see "**Downhole Measurements,**" p. 29, in the "Explanatory Notes" chapter) because of time constraints. There was ~1–2 m of heave throughout operations and the wireline heave compensator was used during all measurements. Logging was carried out from the bottom of the hole at 524 mbsf to the bit at 78 mbsf (picked up from 96 mbsf). The condition of the borehole was good, and the data quality was excellent. The hole had a fairly uniform diameter of 12 in throughout, except near the top, where the hole widened to greater than 18 in.

Following the rigging down from logging, the drill string was recovered and the BHA disassembled for secure stowage during the final transit of the leg. Following the recovery of the beacon, the hydrophones and thrusters were retracted, and the vessel began the transit to Wellington, New Zealand, at 1730 hr on 6 October.

LITHOSTRATIGRAPHY

Introduction

The crest of Chatham Rise marks the position of the STC, separating warm subtropical waters in the north from cooler, more nutrient-rich subantarctic waters in the south. Although designated a convergence, the STC is a region of intense mixing, eddy generation, and upwelling. The result is enhanced productivity of plankton, which become an important contributor to the sediment flux (Bradford-Grieve et al., 1998; Nodder, 1998). However, the proximity of Chatham Rise to New Zealand, and the presence of two current systems to transport the terrigenous load to the Rise (the East Cape Current flowing east along the northern flanks of the Rise and the Southland Current passing along the southern Rise), have ensured that a supply of terrigenous material reached Site 1125 (Mitchell et al., 1989; Neil, 1998).

Apart from an old (1972) industry seismic line (Mobil vessel *Fred H. Moore,* line 72-21) and a single 3.5-kHz profile (National Institute of Water and Atmospheric Research [NIWA] cruise 3011), the only other information on the sediments is provided by a single kasten core from NIWA station R657 at 1408 m depth. This is immediately downslope of Site 1125. Stable isotopes and calcium carbonate profiles, together with foraminiferal assemblage analyses and flux estimates for R657, reveal changes in intermediate-depth water masses and changes in fluxes that are a response to paleoclimatic cycles going back to isotope Stage 6 (Neil, 1998; Weaver et al., 1998; Carter et al., unpubl. data). These data assisted in the choice of Site 1125 as providing a historical record of AAIW and sediment fluxes, in particular the paleoproductivity record associated with the STC. Furthermore, Site 1125 and DSDP Site 594 on the south side of Chatham Rise, provide control points with which to evaluate the long-term position of the STC (e.g., Nelson, 1986).

F3. Generalized lithologic log for Site 1125, p. 30.

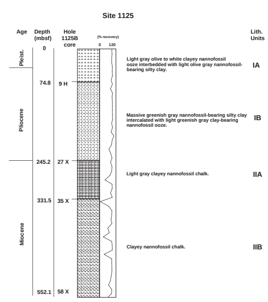

Description of Lithostratigraphic Units

Cores from Site 1125 recovered a succession of clay-rich nannofossil ooze and chalk with interbeds of more terrigenous silty-clay. The sedimentary sequence is divided into two basic lithologic units that are recognized on the basis of changes in the calcareous biogenic and noncarbonate components along with variations in bedding and color. The division of the lithologic units is supported by estimates of core composition from smear slides (see the **"Core Descriptions"** contents list), together with shipboard measurements of calcium carbonate, physical properties, light reflectance, and bulk mineralogy using X-ray diffraction. The generalized characteristics of the lithostratigraphic units are summarized in Figure **F3**, and a more specific set of logs, combining biostratigraphic and magnetostratigraphic data, is presented in Figure **F4.**

F4. Summary log for 1125, p. 31.

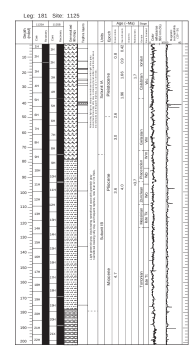

Light reflectance at 550-nm wavelength (Fig. **F5**) is presented as a proxy of $CaCO_3$, the relationship being based on data collected at Sites 1120 to 1124. Calcium carbonate data specific to Site 1125 are still required.

Unit I

Unit I extends from the present seafloor to 245.2 mbsf and represents an interglacial/glacial cyclic sedimentation pattern of alternating nannofossil ooze and silty clay that can be divided into Subunits IA and IB on the basis of lithology and color.

F5. Reflectance profile for 550-nm wavelength, p. 34.

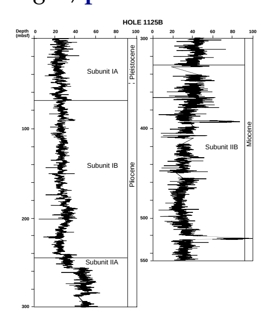

Subunit IA

Interval: Sections 181-1125A-1H-1 through 9H-1; Sections 181-1125B-1H-1 through 9H-1
Depth: 0–70.8 mbsf (Hole 1125A); 0–74.8 mbsf (Hole 1125B)
Age: Pliocene to Pleistocene

Subunit IA, extending from 0 to ~75 mbsf, is a sequence of light and darker colored layers consisting of light gray (5Y 7/2) to white (5Y 8/1) clayey nannofossil ooze interbedded with light olive-gray (5Y 6/2) to olive-gray (5Y 5/2) nannofossil-bearing silty clay. Beds are distinguished by color variations with layers typically between 0.5 and 1.5 m thick. Contacts are generally bioturbated.

The accessory components of the clayey nannofossil oozes, which are regarded as interglacial deposits, include foraminifers in "Present" to "Common" abundance, as well as a small component of sponge spicules and biogenic siliceous fragments. The darker olive-gray nannofossil-bearing silty clay layers are distinguished by an increased abundance of quartz/feldspar and a larger biosiliceous component of radiolarians, diatoms, and spicules together with fewer foraminifers. These layers are interpreted as representing glacial periods. Below ~30 mbsf (Core 181-1125A-4H), pyrite is found as smears or frequently as aureoles around and infilling burrows. Glauconite is locally a significant constituent of the sediment.

Pervasive bioturbation exists throughout Subunit IA and identified ichnofauna include *Zoophycus, Chondrites, Planolites, Thalassinoides,* and *Skolithos* (Fig. F6). This assemblage shows a succession from a dominant *Cruziana* facies in the upper ~37 m of the sequence to an alternating and finally dominant *Zoophycos* facies below ~50 m.

F6. Trace-fossil assemblages for Site 1125, p. 35.

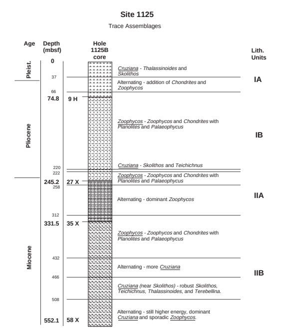

Numerous macroscopic tephra layers are present in Subunit IA (Table T2; Fig. F7), ranging in thickness from <1 cm to a maximum of ~20 cm. Tephra layers are typically pinkish gray (5YR 5/1 to 5YR 6/1) to light pinkish gray (5YR 7/1) and are darkened occasionally by the presence of authigenic pyrite. As with Sites 1122, 1123, and 1124, layers commonly have sharp bases, normal grading, and bioturbated upper contacts. Below basal contacts, reworked tephra often infills burrows, particularly those of *Thalassinoides*. The composition of the tephra layers (dominantly fresh glass and phenocrysts of plagioclase), the absence of Bouma-sequence sedimentary structures, particularly ripples, and the location of the site downwind of the Central Volcanic Region source, indicate the tephra accumulated from airfall rather than turbidity currents. A total of 26 tephra layers were recorded in Subunit IA. In addition, dark green, silty clay laminae are dispersed throughout the subunit and probably represent alteration of thin basic tephras, as previously described by Gardner et al. (1986) and Nelson et al. (1986).

T2. Macroscopic tephra, p. 77.

F7. Distribution of macroscopic tephra, p. 36.

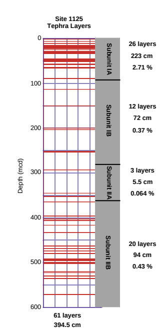

Core disturbance is minimal through Subunit IA, with only a small amount of flow-in present in Cores 181-1125A-5H and 7H.

Subunit IB

Interval: Sections 181-1125A-9H-1 through 22H-CC; Sections 181-1125B-9H-1 through 27X-1
Depth: 70.8–203.52 mbsf (Hole 1125A); 74.8–245.2 mbsf (Hole 1125B)
Age: late Miocene to late Pliocene

Subunit IB extends from 74.8 to 245.2 mbsf. It consists of massive beds (up to ~8 m thick beds) of greenish gray (5GY 5/1 to 5GY 6/1) nannofossil-bearing silty clay intercalated with equally thick light greenish gray (5GY 7/1 to 5BG 7/1) clay-bearing nannofossil ooze. Below ~206 mbsf (Core 181-1125B-23X), the sediments become sufficiently indurated to be classified as nannofossil-bearing mudstone and clay-bearing nannofossil chalk, respectively.

The *Zoophycos* ichnofacies, seen toward the base of Subunit IA, continues downcore through Subunit IB. However, a reappearance of *Cruziana* assemblage occurs between ~220 to 222 mbsf, albeit with slightly different trace fossils, which include *Palaeophycus, Teichichnus,* and *Skolithos* (Fig. **F6**).

A noticeable difference between Subunits IA and IB is the paucity of tephra in the latter. Only 12 macroscopic tephra beds (1–20 cm thickness) were detected, all of which occur in the unlithified section of Subunit IB. Furthermore, only a single green lamina is noted in Subunit IB (Section 181-1125B-23X-5).

The change from APC to XCB coring at around 189 mbsf (Core 181-1125B-21X) suggests the sediment becomes lithified through the formation of carbonate cement at that level, some 17 m below the lithologic determination of the change from ooze to chalk. This transition is also marked by a decrease in the foraminiferal abundance and the inception of drilling biscuits.

Unit II

Unit II consists of mainly clayey nannofossil chalk and extends from 245.2 mbsf through to the base of Hole 1125B at 552.10 mbsf. The unit is divided into Subunits IIA and IIB on the basis of lithology and color.

Subunit IIA

Interval: Sections 181-1125B-27X-1 through 35X-CC
Depth: 245.2–331.5 mbsf (Hole 1125B)
Age: late Miocene

The sedimentary sequence between 245.2 and 331.5 mbsf is a monotonous, very light gray (5Y 7–7.5/1) clayey nannofossil chalk. Subunit IIA is recorded as an increase in light reflectance (Fig. **F5**), which is most likely associated with higher carbonate percentages. Glauconite is dispersed throughout the sequence and is locally concentrated in sandy beds. The site is well above the modern regional carbonate compensation depth (~4500 m), and so the carbonate-rich sediments are well preserved. Bioturbation is common through this subunit and, for the most part, is dominated by a *Zoophycos* ichnofacies containing *Chondrites, Planolites,* and *Zoophycos*. The pervasive occurrence of *Chondrites* is highlighted by the presence of pyrite, which commonly fills these burrows. Only below ~312 mbsf does the sporadic appearance of *Teichichnus* and *Skolithos* suggest an alternation with *Cruziana* ichnofacies (Fig. **F6**).

A total of three macroscopic tephra layers, ranging in thickness from ~1 to 2.5 cm, are present in Subunit IIA. All show the typical form described previously.

Subunit IIB

Interval: Sections 181-1125B-35X-CC through 58X-CC
Depth: 331.5–552.10 mbsf (Hole 1125B)
Age: late Miocene

Subunit IIB has a dominant lithology of clayey nannofossil chalk, in various shades of gray (light gray 5Y 7/1 and light greenish gray 5GY 7/1 to greenish gray 5GY 6/1). This subunit is distinguished from its overlying counterpart by an abundance of pale yellow (5Y 7/3) zones that are interpreted as infilled burrows. This fill consists of clayey nannofossil chalk with a conspicuous biosiliceous component of radiolarians, diatoms, and spicules. Contacts are generally bioturbated, but the abundant biscuiting and brecciation makes the positioning of many contacts subjective. Cyclicity in the color layering is intermittently present but in general it is too subtle for visual identification in split core.

The pale yellow burrow fills highlight the trace fossils, which show notable changes downcore. Initially, fossil assemblages belong to the *Zoophycos* ichnofacies containing *Zoophycos, Chondrites,* and the widespread *Planolites* and *Palaeophycus*. Between ~432 and 466 mbsf, alternating zones of *Zoophycos* and *Cruziana* facies are present, whereas below 466 mbsf *Cruziana* dominates with robust assemblages containing *Skolithos, Teichichnus, Thalassinoides,* and *Terebellina*. Although this facies is placed in the *Cruziana* category, it is close to being a *Skolithos* assemblage and is therefore indicative of an even more energetic and well-ventilated water mass. From ~508 mbsf to the base of Hole 1125B, the dominant high-energy *Cruziana* ichnofacies is interspersed with zones of *Zoophycos*.

Another feature is the abundant tephra layers; a total of 20 are recognized in Subunit IIB (Fig. **F7**). Some layers have been disturbed by drilling biscuits, and their estimated thicknesses range from 1 to 10 cm. Of note in these tephra layers is the presence of fine planar laminae, which is probably evidence of bottom-current activity in the unit. This is consistent with the ichnofauna assemblages described above.

Discussion

Like other sites whose sediments are predominantly a varying mixture of terrigenous and calcareous biogenic components, sediments of Site 1125 have a cyclicity that is well displayed in the 550-nm reflectance profiles (Fig. **F5**). Such cycles are a response to changes in the burial flux of the two main sediment components, and, on the basis of data from nearby piston core R657, these changes are directly correlatable to isotope stages (at least for Stages 1–6 measured in R657 by Weaver et al., 1998). Therefore, it is tempting to relate the cycles to Milankovitch frequencies, but such a correlation must await development of an astronomically tuned time scale for the site. These cycles are superimposed on longer term changes. Of particular note is the gradual, long-term increase in reflectance/carbonate in the late Miocene (10.5 to 5.5 Ma), followed by a sharp reduction to a level that is more or less maintained through the late Miocene to Holocene (Fig. **F5**). These data, together with lithologic and faunal information, suggest that Site 1125 sediments evolved as follows.

Around 10.5 Ma, northern Chatham Rise received nannofossil ooze (now chalk) and a lesser amount of terrigenous sediment. The biogenic siliceous component was relatively minor. Up to 6 Ma, the rate of accumulation decreased gradually in response to a reduction in the terrigenous supply, as suggested by a concomitant decrease in reflectance values and the lack of visually identifiable sedimentary cycles (note the spectrophotometer-detected color cyclicity was invisible to the naked eye). A high-energy environment prevailed for the first half of Subunit IIB as suggested by the dominance of a *Cruziana* ichnofacies (see Pemberton and MacEachern, 1995). Bioturbation was extensive and produced the strongly mottled nannochalk with its characteristic large, pale yellow burrows. However, the upper reaches of Subunit IIB marked a change to the *Zoophycos* ichnofacies, heralding a less energetic setting.

Around 6 Ma, sedimentation rates increased markedly (see **"Age Models and Sedimentation Rates,"** p. 18). The continued increase in the already-dominant nannofossil ooze is consistent with the enhanced production of biogenic carbonate caused by warmer ocean temperatures and increased upwelling at the STC (Kennett and von der Borch, 1986). Higher sedimentation rates, together with fluctuating benthic conditions, may also have influenced the change in bioturbation style seen in Subunit IIA (i.e., the replacement of large, pale yellow burrows by smaller less conspicuous traces belonging to ichnofacies that alternated between *Zoophycos* and *Cruziana*).

The change to Unit I occurred around 5.5 Ma and is proximal to an abrupt decrease in reflectance values at 241 and 256 mbsf (Fig. **F5**). This decrease marks the first appearance of terrigenous mud and of visually obvious color cycles (as opposed to cycles measured only by reflectance). There is also a change in the overall sediment color from light gray in Unit II to green gray in Unit I. The enhanced terrigenous supply followed a major reorientation of the motion of the New Zealand plate boundary. Around 6.4 Ma, the plate motion changed from predominantly strike slip to one with a major compressive component (Walcott, 1998). As a result, uplift increased, erosion accelerated, and more sediment was introduced to the eastern South Island. The reason for the suddenness of the terrigenous influx at Site 1125, 0.9 m.y. after the change in plate motion, is not clear. Biostratigraphic data provide no evidence for a hiatus between Units I and II. However, an abrupt reduction of the diatom flora as a result of corrosion suggests a change in oceanographic conditions, that is, inflow of waters undersaturated in silica (see **"Biostratigraphy,"** p. 9). Thus, the influx of terrigenous sediment may reflect a change in the circulation, in particular, in the path of the Southland Current.

Reflectance/carbonate increased slightly in the early Pliocene but did not reach the levels recorded in Unit I. However, the increase was short lived. Around 5 Ma, carbonate reduced to a general level that remained fairly constant until Holocene times. The reduction in carbonate was accompanied by a gradual reduction of the overall sedimentation rate, suggesting a cause-and-effect mechanism. This may be the case, but the overall sedimentation rate continued to decline gradually into the Pleistocene at a time when the terrigenous influx from New Zealand increased as a result of greater tectonic uplift along the plate boundary, progressive exposure of readily erodible rocks, and increasing severity of glaciations (e.g., Carter and Carter, 1993). Furthermore, there was a significant contribution from tephra, with macroscopic tephra contributing up to 2.7% of Unit IA's thickness. It would appear that following the burst of deposition between 5 and 6 Ma, northern Chatham Rise either became increasingly isolated from the terrigenous input from New Zealand or conditions on the Rise became less conducive to deposition. This is inferred from a change to more energetic conditions suggested by the *Cruziana* ichnofacies in the Pleistocene. However, the presence of well-formed grains of glauconite in Unit I indicates that the crest of Chatham Rise, a site of extensive greensand deposits (Cullen, 1987), provided detritus to Site 1125. Presumably, such interchanges occurred mainly during lowstands of sea level when reaches of the crest would be affected by storm waves and currents.

Superimposed on the general reduction in sedimentation are prominent cycles (Fig. **F5**) which, on the basis of data from Neil (1998) and Weaver et al. (1998), are probably related to glacial/interglacial periods. Their results reveal that the carbonate flux increased in interglacial periods, whereas the terrigenous-biogenic silica flux dominated during glaciations. In core R657, the greatest difference between fluxes occurred during Stage 2 with terrigenous detritus increasing markedly and the carbonate input decreasing to near zero. Such a difference was in part caused by dissolution of planktonic foraminifers, possibly by corrosive AAIW (Weaver et al., 1998). In contrast, Stages 4–6 had carbonate and terrigenous-biogenic silica fluxes that were similar, both being within a fairly narrow range of 0.5–1.0 g/cm²/ky. However, further dissolution events were detected sporadically in core-catcher samples from the Pleistocene section of Site 1124.

BIOSTRATIGRAPHY

Summary

Site 1125, drilled on the northern slopes of the Chatham Rise in 1360-m water depth, contained rich Neogene planktonic faunas and floras with calcareous nannofossils, foraminifers, and radiolarians. The benthic foraminifers comprise a diverse lower bathyal fauna. The calcareous microfaunas and -floras are well preserved, with recrystallization of the calcareous microfossils below Core 181-1125B-47X. Radiolarians are well preserved down to Core 181-1125B-54X. Diatoms are very scarce in the upper 160 mbsf and are missing because of dissolution below Core 181-1125B-53X. The preservation deteriorates strongly below Core 181-1125B-46X.

Rich diatom floras indicating high primary productivity, presumably upwelling conditions, are present in the upper Miocene (160 to 430 mbsf). High productivity is also indicated by the dominance of small coccoliths throughout the lower Pliocene and upper Miocene from 120 to 430 mbsf.

Reworking of older forms is less common compared to other sites. Single reworked valves of diatoms occur only sporadically. At least half of the samples investigated for calcareous nannofossils contain minor amounts of reworked specimens.

The biostratigraphy of Site 1125, as determined by the four major microfossil groups, is summarized in Figure F8. The 75 datums determined from these microfossil groups allow the construction of a detailed age-depth curve (compare Fig. F16) and demonstrate very high sedimentation rates, in excess of 200 m/m.y., for levels near the Miocene/Pliocene boundary (6.0 to 5.0 Ma).

The following major intervals have been determined by consensus results from all groups:

1. late Pleistocene–Holocene (0–~0.8 Ma), 0 to 15 mbsf, lithostratigraphic Subunit IA;
2. early Pleistocene (0.8–1.8 Ma), 15 to 40 mbsf, lithostratigraphic Subunit IA;
3. late Pliocene (1.8–3.8 Ma), 40 to 100 mbsf, lithostratigraphic Subunits IA and IB, possible hiatus or condensed interval (~2–3 Ma), 43–51 mbsf;
4. early Pliocene (3.8–5.3 Ma), 100 to 245 mbsf, lithostratigraphic Subunit IB, possible hiatus representing a short time interval separating Subunit IB and Unit II is indicated by a dissolution event documented in the diatom assemblages; and
5. late Miocene (5.3–10.7 Ma), 245 to 548 mbsf (total depth), lithostratigraphic Unit II.

F8. Biostratigraphic summary chart, p. 37.

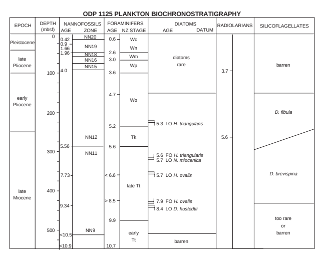

For the late Miocene interval, the following age-depth relationships have been determined:

5.7 Ma at ~290 mbsf;
6.6 Ma at ~360 mbsf;
8.0 Ma at 400 mbsf;
9.4 Ma at ~435 mbsf;
10.0 Ma at ~475 mbsf; and
10.7 Ma at ~548 mbsf.

Age

The biostratigraphy of Site 1125 is mostly based on the study of core-catcher samples. Samples from Hole 1125A were used for the upper part of the section, and samples from Hole 1125B for the lower part. Additional samples were taken from within selected cores to address specific age and paleoenvironmental questions. The absolute ages assigned to biostratigraphic datums follow the references listed in Tables T2, p. 59, T3, p. 60, T4, p. 63, and T5, p. 64, all in the "Explanatory Notes" chapter.

Calcareous Nannofossils

Calcareous nannofossil biostratigraphy of Site 1125 is based upon examination of core-catcher samples taken from Cores 181-1125A-1H to 22H and Cores 181-1125B-23X to 58X. Several additional samples from within cores in the upper part of the section were also examined to increase resolution. Nannofossils are abundant and well preserved throughout the sequence, except for the lowermost portion, where nannofossil assemblages show signs of dissolution and overgrowth (Table T3). Fourteen datum levels were recognized (Table T4). Most of the age markers are in the upper Pliocene–Pleistocene section (0 to 94.85 mbsf), whereas the major part of the sequence belonging to the upper Miocene and lower Pliocene (95 to 547 mbsf) is poorly resolved.

T3. Identification and relative abundance of nannofossils, p. 78.

T4. Nannofossil datum levels identified and age estimates, p. 80.

The first sample (181-1125A-1H-CC; 4.21 mbsf) is definitely older than 0.15 Ma, based upon the presence of *Helicosphaera inversa*. This sample is dominated by the medium-sized *Gephyrocapsa oceanica* and *Gephyrocapsa caribbeanica*. There are a few specimens that may look similar to *Emiliania huxleyi*. But, because of their small size and scarcity, we are not confident in determining whether this sample indeed contains *Emiliania huxleyi* and, therefore, is still within Zone NN21, and, in other words, younger than 0.24 Ma. The occurrence of abundant, typical *Pseudoemiliania lacunosa* (first occurrence [FO] 0.42 Ma) in the upper part of the next core, Sample 181-1125A-2H-2, 54 cm (4.84 mbsf), however, suggests that the topmost Pleistocene is missing, or, alternatively, the top part of the sequence is very condensed and has a sedimentation rate of less than 1 cm/k.y. Judging from the clay-rich, hemipelagite lithology of this section, and the overall high sedimentation rates (~6 cm/k.y.) in the lower part of the sequence, the latter explanation is less likely.

Several age-diagnostic markers were found for the Pleistocene section. In Sample 181-1125A-3H-CC (23.6 mbsf) two short-ranged species were found: *Reticulofenestra asanoi* (last occurrence [LO] 0.85 Ma) and *Gephyrocapsa parallela* (FO 0.95 Ma). The coexistence of these two species constrains the age of this sample as between 0.85 to 0.95 Ma. *Heli-*

cosphaera sellii occurs in the next sample (181-1125A-4H-CC; 32.83 mbsf), indicating an age older than 1.26 Ma.

In Sample 181-1125A-5H-3, 150 cm (35.8 mbsf), only a few medium-sized *Gephyrocapsa* were found and they disappear downsection. With the absence of any discoasterids, this sample is estimated to be very close to the origin of the medium-sized *Gephyrocapsa* at ~1.67 Ma. In the core-catcher of the same core (181-1125A-5H-CC; 42.58 mbsf), a few *Discoaster brouweri* are present without the companionship of other *Discoaster* species. This indicates that this sample is very close to the extinction level of *Discoaster,* dated at 1.96 Ma. The Pliocene/Pleistocene boundary (1.81 Ma) is therefore between these two samples at ~37.5 mbsf.

Part of the uppermost Pliocene is missing, as suggested by the occurrence of *Discoaster tamalis* (LO 2.76 Ma) in the next sample (181-1125A-6H-CC; 51.57 mbsf) (Fig. **F9**). The sporadic occurrence of discoasterids downcore during the Pliocene at this site precludes the usage of other *Discoaster* data. The occurrence of abundant small-sized *Gephyrocapsa* (2–3.5 µm in size) together with *Reticulofenestra pseudoumbilicus-gelida* in Sample 181-1125A-9H-CC (80.76 mbsf) in the Pliocene is somewhat unusual. The hemipelagic setting and perhaps the high biological productivity associated with the Subtropical Convergence at this site have probably combined to yield this assemblage. As shown by Rio's (1982) detailed study, this is the so-called "mid-Pliocene small *Gephyrocapsa* bloom," which occurred below the base of the Gauss Chron and higher than the Cochiti Event, namely between 3.58 and 4.18 Ma. The FO of *Pseudoemiliania lacunosa* (4.0 Ma) in the next sample (Sample 181-1125A-10H-CC; 89.91 mbsf) is consistent with this age assignment.

F9. Age-depth relationships at Site 1125, **p. 38.**

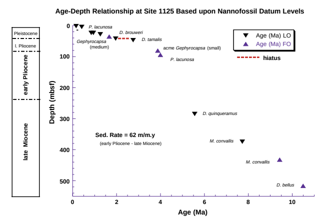

Discoasterids are present in the section to the bottom of the hole, but major key species are either missing or sporadic. We can only tentatively use the LO of *D. quinqueramus* in Sample 181-1125B-31X-CC (288.28 mbsf) as an age marker to date the latest Miocene. Within the long sequence downward to the bottom, only the persistent occurrence of *Minylitha convallis* from Samples 181-1125B-40X-CC to 45X-CC (379.02 mbsf to 427.81 mbsf) provides good age control. The sedimentation rate for this interval, calculated based upon the LO (7.73 Ma) and FO (9.43 Ma) of this species, is ~34 m/m.y.

The presence of *Discoaster bellus* in Sample 181-1125A-54X-CC (512.73 mbsf) suggests that this interval is at least younger than its first occurrence at 10.5 Ma (in the lower part of magnetic Chron 5n.2n) (Gartner, 1990). The next few samples down to the bottom of the hole contain moderately preserved nannofossil assemblages in which only a few badly preserved discoasterids were found. Therefore, the apparent FO of *D. bellus* at Sample 181-1125B-54X-CC may not be a genuine first appearance. Nevertheless, the absence of *Coccolithus miopelagicus* (LO 10.94 Ma) from the lowest part of the sequence does suggest that the bottom of the hole is younger than 10.94 Ma, which agrees with the age assignments based upon *Minylitha convallis* and *Discoaster bellus*. However, the bottom of the core is probably only a few meters away from the middle/late Miocene boundary (11.2 Ma)

In summary, nannofossil biochronology indicates that the upper Pliocene and Pleistocene is incomplete and has been truncated by at least two hiatuses, one in the upper Pliocene (2 to 3 m.y. missing?) and the other on the very top of the sequence (topmost Pleistocene missing). The lack of proper age markers for the lower Pliocene and upper Miocene hampers dating the lower part of the sequence in detail. The boundary between the Pliocene and Miocene (5.32 Ma) is estimated to be at ~240 mbsf (Fig. F9). The lower half of the sequence is represented by a thick sequence of upper Miocene. The average sedimentation rate for the late Miocene and early Pliocene is calculated to be 62 m/m.y. based upon two relatively reliable datum levels, the FOs of *Pseudoemiliania lacunosa* (4.0 Ma) and *Minylitha convallis* (9.43 Ma) (Fig. F9).

Foraminifers

Foraminiferal faunas throughout most of Site 1125 (Tables T5 and T6) are abundant to moderately abundant and are generally well preserved above ~400 m. Evidence of dissolution is only present in a few samples in the upper part of the hole. Recrystallization and flattening of some tests is evident in only the lower samples (Sample 181-1125B-46X-CC and below).

T5. Significant foraminiferal and bolboformid datums, p. 81.

T6. Identification and abundance of planktonic foraminifers and bolboformids, p. 82.

Late Pliocene–Quaternary

Samples 181-1125A-1H-CC to 5H-CC (0–42.6 mbsf) are late Pliocene and Quaternary in age (0–2.6 Ma; Nukumaruan, Castlecliffian, and Haweran Stages), based on the presence throughout of sparse keeled *Globorotalia crassaformis* forms (*G. crassula, G. crassacarina*). Accurate subdivision within this interval is difficult because of the diachronous ranges of the common *Globorotalia* species between the tropical-subtropical and subantarctic regions. All samples in this interval contain a mixture of common *Globorotalia inflata* and *Globorotalia puncticuloides* (the latter has a recorded LO in this region of ~0.6 Ma), suggesting that the first core may contain a condensed section or hiatus and that the remainder of the interval is 0.6–2.6 Ma. The following datums are observed within this interval.

The first occurrence of *Globorotalia truncatulinoides* is in Sample 181-1125A-3H-CC (FO ~2 Ma in the tropics-subtropics; ~0.8 Ma in the subantarctic). The last occurrence of *Stilostomella* and *Plectofrondicularia advena* (0.6–0.8 Ma) also occurs in Sample 181-1125A-2H-CC. These suggest that Sample 181-1124C-1125A-2H-CC is older than ~0.6 Ma.

Sample 181-1125A-4H-CC contains *Globigerinoides extremus,* which ranges up into planktonic foraminifer zone PL6, late Pliocene. Its LO varies between oceans but it may range up to ~1.8 Ma.

Sample 181-1125A-5H-CC contains the LO of *Globorotalia inflata triangula* (~2 Ma) and the FO of *Globorotalia crassula* (2.6 Ma). There appears to be a condensed section or hiatus within Core 181-1125A-6H of ~0.5 m.y.

Pliocene

Samples 181-1125A-6H-2, 130–135 cm, to 7H-CC (45.1–61.8 mbsf) contain the dextral coiling forms of unkeeled *Globorotalia crassaformis* (2.1–3.0 Ma). When coupled with the absence of *Globorotalia crassula* (FO 2.6 Ma) and presence of *Globorotalia tosaensis* (FO 3.0 Ma), this suggests an age of 2.6–3.0 Ma (late Pliocene, Mangapanian Stage) for this interval.

Samples 181-1125A-8H-CC to 11H-CC (70.4–99.8 mbsf) are late Pliocene (3.0–3.6 Ma, Waipipian Stage), based on the presence of *Globorotalia crassaconica* (LO 3.0 Ma), sinistral unkeeled *Globorotalia crassaformis* (last common occurrence [LCO] 3.0 Ma), *Globorotalia puncticuloides* (FO 3.6 Ma), *Globorotalia inflata* (FO 3.7 Ma), and *Globorotalia inflata triangula* (FO 3.6 Ma).

Samples 181-1125A-13H-CC to 181-1125B-25X-CC (118.8–234.7 mbsf) are early Pliocene in age (3.7–5.2 Ma, Opoitian Stage), based on the presence throughout of the zone species *Globorotalia puncticulata* (3.7–5.2 Ma) and *Globorotalia pliozea* (LO 3.6 Ma). This lower Pliocene interval can be divided into upper (3.7–4.7 Ma) and lower sections (4.7–5.2 Ma) at Sample 181-1125A-17H-CC, which contains the FO of *Globorotalia crassaconica* (FO 4.7 Ma) and the LO of *Globorotalia mons* (LO 4.8 Ma).

Late Miocene

Sample 181-1125B-25X-CC (234.7 mbsf) lies on the Kapitean/Opoitian Stage boundary, just above the Miocene/Pliocene boundary, because it contains the LO of *Globorotalia sphericomiozea* (LO 5.2 Ma) and FO of *Globorotalia crassaformis* (FO 5.2 Ma).

Samples from 181-1125B-25X-CC to 29X-CC (234.7–274 mbsf) are latest Miocene in age (5.2–5.6 Ma), based on the presence of *Globorotalia sphericomiozea* (5.2–5.6 Ma) and the following accompanying species, which assist in subdividing this short interval:

1. *Globorotalia juanai* (LO 5.2 Ma), Samples 181-1125B-26X-CC and lower;
2. *Globorotalia miotumida* (LO ~5.4 Ma), Samples 181-1125B-26X-CC and lower;
3. *Globorotalia pliozea* (FO 5.4 Ma), Samples 181-1125B-26X-CC and higher; and
4. *Globorotalia mons* (FO 5.5 Ma), Samples 181-1125B-27X-CC and higher.

Samples 181-1125B-31X-CC to 45X-CC (288–427.8 mbsf) are middle late Miocene in age (5.6–9.9 Ma), based on the abundant presence of sinistral *Globorotalia miotumida* (LO ~5.4 Ma) and the absence of *Globoquadrina dehiscens* (LO 9.9 Ma). Samples 181-1125B-37X-CC and above contain *Globorotalia juanai* (FO 6.6 Ma), providing a useful datum within this interval.

Sample 181-1125B-37X-CC has a temperate aspect with *Globorotalia explicationis* and *G. menardii.* Also present in the sample are *Bolboforma* spp. and common *Neogloboquadrina pachyderma.* A similar assemblage, but without *G. juanai* and with *Catapsydrax parvulus,* occurs in Sample 181-1125B-39X-CC.

Samples 181-1125B-41X-CC and lower are much more indurated ("chalky") than are the sediments above, with poor preservation, which persists to total depth in the hole. The assemblages in Samples 181-1125B-41X-CC to 46X-CC include *Globorotalia partimlabiata, Catapsydrax parvulus, Globigerinoides quadriloba, G. decoraperta,* common to abundant *Globorotalia miotumida* (both encrusted and nonencrusted forms), *Zeaglobigerina nepenthes, Neogloboquadrina pachyderma,* and *Globigerina quinqueloba* (often frequent). In this assemblage *N. pachyderma* (first common occurrence [FCO] 9.2 Ma, FO 11.3 Ma) is rare, but we are unsure whether this should be interpreted as an age older than 9.2 Ma or not. Its rarity may be an effect of dilution of the planktonic foraminiferal tests by abundant clays, since the late Miocene sedimentation rate is in excess of 100 m/m.y. (see **"Age Models and Sedimentation Rates,"** p. 18).

The bolboformids, *Bolboforma* aff. *metzmacheri* (8.5–10.5 Ma) and *B. pentaspinosa* (7–11.5 Ma), occur in Sample 181-1125B-45X-CC, which indicates that this level is probably older than 8.5 Ma.

Samples 181-1125B-48X-CC to 57X-CC (450.8–542.2 mbsf) are 9.9–10.7 Ma (late early Tongaporutuan Stage), based on the co-occurrence throughout of *Globoquadrina dehiscens* (LO 9.9 Ma), and common, sinistral-dominated *Globorotalia miotumida* (FO of sinistral form 10.7 Ma). *G. dehiscens* only becomes common in Sample 181-1125B-52X-CC and could possibly represent the calibrated datum at 9.9 Ma. Sporadic specimens referable to *Paragloborotalia mayeri* (LCO 11.25 Ma) occur in Samples 181-1125B-48X-CC and 57X-CC. However, with the weight of other evidence, we consider that these records must lie above the last consistent occurrence datum of this species.

Sample 181-1125B-57X-CC contains the LO of *Globorotalia panda* (LO 10.3 Ma). At the bottom of the hole (548.2 mbsf), Sample 181-1125B-58X-CC contains more dextral than sinistral specimens of *Globorotalia miotumida* (LO 10.7 Ma, FO 10.9 Ma), indicating an age not much older than 10.7 Ma. Consistent with this is the presence of common *Zeaglobigerina nepenthes* (FO 11.8 Ma) and small *Globorotalia scitula* (FO 11.5 Ma). Hence the hole bottomed in beds of early late Miocene age (~10.7–10.9 Ma).

Age Summary

We list below a summary of foraminiferal ages at Site 1125, in terms of the New Zealand stage classification, and local chronological calibration of these stages, according to Table T2, p. 59, in the "Explanatory Notes" chapter.

1. Nukumaruan (Wn), Castlecliffian (Wc), and Haweran (Wq), late Pliocene to Recent (0–2.6 Ma): down to Sample 181-1125C-5H-CC(0–42.6 mbsf), possibly top and bottom missing;
2. Possible hiatus (?2.0–2.6 Ma) in the top of Core 181-1125A-6H (43–51 mbsf);
3. Mangapanian (Wm), late Pliocene (2.6–3.0 Ma): Samples 181-1125A-6H-2, 130–135 cm, to 7H-CC (51.6–61.8 mbsf), probably with top missing;
4. Waipipian (Wp), mid-Pliocene (3.0–3.6 Ma): Samples 181-1125A-8H-CC to 11H-CC (70.4–99.8 mbsf);
5. Opoitian (Wo), early Pliocene (3.6–5.2 Ma): Samples 181-1125A-13H-CC to 181-1125B-25X-CC (118.8–234.7 mbsf);
6. Kapitean Stage (Tk), latest Miocene (5.2–5.6 Ma): Samples 181-1125B-25X-CC to 29X-CC (234.7–274 mbsf);
7. Late Tongaporutuan Stage (late Tt), late Miocene (5.6–9.9 Ma): Samples 181-1125B-31X-CC to 45X-CC (288–427.8 mbsf); and
8. Early Tongaporutuan Stage (early Tt), late Miocene (9.9–~10.7 Ma): Samples 181-1125B-48X-CC to 58X-CC (475–548.2 mbsf).

Diatoms and Silicoflagellates

Diatoms are present throughout the Neogene section recovered at this site on the upper slope of the northern Chatham Rise, except for the lower five cores (Cores 181-1125B-54X to 58X). Their preservation deteriorates and species diversity decreases from 440 mbsf (Core 181-1125B-47X) downward. In the upper 160 m of the profile, diatoms are too scarce to provide reliable stratigraphic information. But from Core 181-1125A-18H downward, that is, in the lowermost Pliocene to upper Miocene sediments, diatoms are abundant and the assemblages diverse. Silicoflagellate occurrence shows a similar pattern. The following species provide reliable datums in this interval:

Hemidiscus triangularis, LO 5.3 Ma, 181-1125B-24X-CC; *Hemidiscus triangularis,* FO 5.6 Ma, 181-1125B-35X-CC; *Nitzschia miocenica,* LO 5.7

Ma, 181-1125B-35X-CC; *Hemidiscus ovalis,* LO 5.7 Ma, 181-1125B-38X-CC; *Hemidiscus ovalis,* FO 7.9 Ma, 181-1125B-45X-CC; and *Denticulopsis hustedtii,* LO ?8.4 Ma, 181-1125B-47X-CC.

Within the Messinian interval of high primary productivity and high sedimentation rates, a dissolution event is documented in Core 181-1125B-27X in the diatom assemblages, which may indicate a hiatus, although it can only represent a relatively short time interval.

With silicoflagellates the Miocene/Pliocene boundary has to be placed between Cores 181-1125B-25X and 32X (Fig. F8). In Sample 181-1125B-25X-CC and above, *Mesocena quadrangula* occurs, whereas the presence of *Mesocena hexalitha* in Sample 181-1125B-32X-CC and the consistent occurrence of *Mesocena diodon borderlandensis* below proves a Miocene age from at least this core downward.

Occasional benthic diatoms are found, but hardly any older, reworked diatom valves or silicoflagellates were encountered.

Radiolarians

Radiolarian biostratigraphy at Site 1125 is based on the examination of 59 core-catcher samples. Radiolarian faunas are generally abundant and very well preserved throughout the section, except in the lowest part of the section (Samples 181-1125B-54X-CC to 58X-CC; 512.73–548.22 mbsf). The radiolarian faunas at Site 1125 are dominated mostly by cosmopolitan and middle latitude species associated with a few subtropical species. In addition, the faunas are characterized by the absence of Antarctic/subantarctic species (e.g., various species of *Antarctissa, Lithelius nautiloides,* and *Saccospyris antarctica*).

Sample 181-1125A-3H-CC (23.6 mbsf) contains a single specimen of *Stylatractus universus* associated with *Eucyrtidium calvertense, Lamprocyrtis heteroporos* (LO 1.8 Ma), *Theocorythium trachelium* (FO 1.6–1.7 Ma), and *Theocorythium vetulum* (LO 1.2–1.3 Ma). Although the age for the sample is estimated to be early Pleistocene (1.7–1.8 Ma), this age is rather older than the age indicated by other microfossils. Reworking is possible. This, as well as other factors, may be the reason that the top two core-catcher samples yielded only very rare or few radiolarians without age-diagnostic species. Rare specimens of *Eucyrtidium matuyamai* (LO 1.0 Ma and FO 2.0 Ma in Morley and Nigrini, 1995) occur in Sample 181-1125A-4H-CC (32.83 mbsf).

In Sample 181-1125A-6H-CC (51.57 mbsf), the radiolarian fauna includes few *Stichocorys peregrina, Lamprocyrtis neoheteroporos, Axoprunum angelium,* and *Theocorys redondoensis*. The last occurrence of *Sphaeropyle langii* is recorded in Sample 181-1125A-9H-CC (80.76 mbsf). In Sample 181-1125A-10H-CC (89.91 mbsf), the last occurrence of *Lychnodictyum audax* (LO 3.7 Ma) indicates the sample is of early late Pliocene age.

Sample 181-1125B-28X-CC (264.44 mbsf) contains a diversified radiolarian fauna, including *Lychnocanoma parallelipes* (LO 5.6 Ma), *Dictyophimus* aff. *splendence,* and *Didymocyrtis penultima*. This assemblage indicates a latest Miocene age (5.6 Ma) for the sample.

Paleoenvironment

Foraminifers

Dissolution of foraminiferal faunas by corrosive bottom waters is only sporadically apparent, as determined by the presence of fragmented planktonic foraminiferal tests, in some darker (colder) intervals in the upper Pliocene to Holocene section. Elsewhere the assemblages contain rich, oceanic planktonic (>95% of foraminifers) faunas and diverse, lower to mid-bathyal benthic foraminiferal faunas. Many samples from the interval younger than ~8 Ma contain abundant, small *Neogloboquadrina pachyderma* and *Globigerina bulloides,* typical of cool temperate waters. The larger size fraction of the fauna is typically dominated by warm temperate *Globorotalia* forms (e.g., *G. inflata, G. puncticuloides, G. puncticulata, G. mons, G. pliozea,* and *G. miotumida*), although their abundance varies. More detailed quantitative work on the faunas is likely to provide better paleoenvironmental interpretations.

Diatoms

The diatom assemblages are oceanic and dominated by species of the genera *Thalassionema* and *Thalassiothrix,* indicating high productivity. Temperate to subtropical species prevail.

High productivity or upwelling conditions are indicated especially for the time interval between 5.0 and 6.0 Ma. But also in the sediments above and below, with considerably lower sedimentation rates, these same species are dominant. But here they do not indicate high productivity because the overall abundance of diatoms and the diversity of the diatom assemblages is low. This indicates silica dissolution. Winnowing is not a probable explanation as calcareous nannofossils abound in these sediments.

PALEOMAGNETISM

Core archive halves from Hole 1125A and Cores 181-1125B-1H to 39X from Hole 1125B were measured on the shipboard pass-through cryogenic magnetometer. Declination, inclination, and intensity of natural remanent magnetization (NRM) and 10-mT (for a few cores only) and 20-mT alternating-field (AF) demagnetization steps were routinely measured at 5-cm intervals on core from Hole 1125A. For Hole 1125B, cores were only measured at the 20-mT step because of the time constraints. Measurements were stopped after Section 181-1125-39X-4 because the intensity of remanence had dropped below the noise level of the shipboard cryogenic magnetometer. In situ Tensor tool data were collected from APC cores from Hole 1125A (from Cores 181-1125A-3H through 22H and 181-1125B-4H through 20H). Only inclination could be used to determine magnetic polarity of Holes 1125A and 1125B. At least two oriented discrete samples were collected from the working half of each core interval in Holes 1125A and 1125B (up to Section 181-1125B-39X-4) for shore-based progressive AF and thermal demagnetization and rock magnetic studies. Whole-core magnetic susceptibility was routinely measured on all cores using a Bartington susceptibility loop on the automated multisensor track (MST).

The NRM intensity in Site 1125 averages between 10^{-4} and 10^{-5} A/m. Higher remanence spikes (10^{-2} A/m) occur in the vicinity of tephra layers (Fig. **F10**). As for other sites on Leg 181, a steep downcore drilling-induced remanent magnetization dominates the NRM (Fig. **F11**). No rock-magnetic investigation has been conducted because of the time constraint at this site.

AF demagnetization of 20 mT reduces the intensity of magnetization to 10^{-5}–10^{-6} and mostly removes the steep downcore overprint. At such

F10. NRM intensity at Site 1125, **p. 39.**

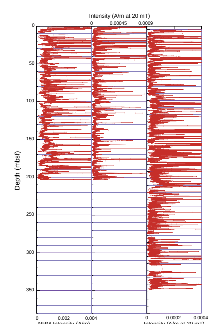

F11. Inclinations of remanence in Holes 1125A and 1125B, **p. 40.**

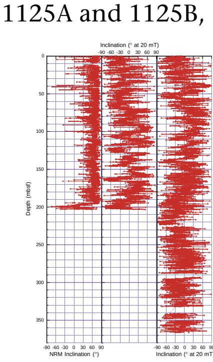

weak intensities, the inclination data are very noisy and polarity interpretation is difficult. However, between 50 and 140 mbsf, inclination directions in Holes 1125A and 1125B show some polarity changes. These are slightly better defined in Hole 1125A.

The inclination record between 0 and 14 mbsf is mostly normal. The LO of the nannofossils *Helicosphaera inversa* (0.16 Ma, 2.05 mbsf) and the LO of *Pseudoemiliania lacunosa* (0.42 Ma, 4.53 mbsf) suggest it most likely represents the Brunhes (C1n) Chron. Inclination between 14 and 39 mbsf is most likely positive (reversed polarity), but includes two possible normal events. Because it immediately underlies the Chron (C1n), and because it contains the LO of the nannofossils *Reticulofenestra asanoi* (0.85 Ma, 23.6 mbsf) and *H. sellii* (1.26 Ma), and the FO of the nannofossils *Gephyrocapsa parallela* (0.95 Ma, 23.6 mbsf) and *Gephyrocapsa* (medium) (1.67, 28.2 mbsf), it is most likely to be Chron C1r (upper Matuyama). The two normal polarity excursions are possibly the Jaramillo (C1r.1n) and Cobb Mountain (C1r.2r–1n) Subchrons. Another normal polarity is identified at ~40 mbsf, which might be the Olduvai (C2n) Chron. Between 42 and 48 mbsf, the LOs of the nannofossils *Discoaster brouweri* (1.96 Ma, 42 mbsf) and *D. tamalis* (2.76 Ma, 47.1 mbsf) suggest that this interval should be within Chron C2r; however, the inclinations are ambiguous and further investigation is needed to confirm the polarity.

Between 48 and 70.5 mbsf, polarity is dominantly normal and may represent the Gauss normal chron (C2An). Two short reversed subchrons exist within Chron C2An of the Geomagnetic Polarity Time Scale (Cande and Kent, 1995; Berggren et al., 1995). However, these are not obvious in the inclination record at Site 1125. Polarity is ambiguous between 70.5 and 93 mbsf. The inclination record between 93 and 203 mbsf is more variable, with alternating normal and reversed polarity. The acme of the nannofossil *Gephyrocapsa* (small) (3.88 Ma) and the FO of the nannofossil *P. lacunosa* (4.0 Ma) at 80.8 and 94.9 mbsf respectively and the LO of the diatom *Hemidiscus triangularis* (5.3 Ma, ~220 mbsf) suggest that the interval between 93 and 200 mbsf should be within the Gilbert Chron (C2Ar, C3n, and C3r). Several polarity changes may represent the subchrons of C3n but the inclination record is too ambiguous for this level of interpretation. These tentative chron assignments are summarized in Fig. F12.

Hole 1125B was advanced to 547 mbsf by XCB coring, but paleomagnetic interpretation was not possible beneath 200 mbsf as intensity of remanence was below the noise level of the shipboard cryogenic magnetometer. Further shore-based research is necessary before more detailed magnetic polarity interpretation can be made.

F12. Preliminary magnetic polarity interpretation for Hole 1125B, p. 41.

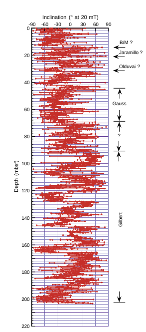

COMPOSITE DEPTHS

Composite Section and Splice

The composite section for Site 1125 yielded overlapping records for the upper ~238 meters composite depth (mcd) using data from Holes 1125A and 1125B. Two high-resolution data sets proved most useful for correlation at this site: magnetic susceptibility (MS) measured on whole cores on the MST, and spectral reflectance at 550 nm (the center wavelength of the range measured), measured on split cores. At other sites it was possible to concentrate on one parameter and use alternatives for checking correlations. However, in the case of Site 1125 both reflectance and MS had such low variability that it was only possible to complete the splice by frequent alternation between parameters. In some cases the "signal" from one parameter (e.g., reflectance) was not reproduced at the corresponding level in the adjacent hole, despite excellent correlation with the alternative parameter (e.g., MS). Data were edited to remove information collected over voids as identified by very low gamma-ray attenuation porosity evaluator (GRAPE) density values; the final composite section is illustrated in Figure F13.

Downhole core offsets in the composite section follow a model of 15% stretch between the mbsf and mcd depth scales (Fig. F14). It is not known why the offset increases at a rate of 15% rather than the more typical 10%. Table T7 (also in ASCII format) contains the offsets between the mbsf and mcd scales that result from composite section construction.

The continuous spliced record, based on MS and reflectance data (reflectance percentage) (Fig. F15), extends to 238 mcd. Wherever possible, splice tie points (Table T8, also in ASCII format) were picked at well-defined maxima or minima where the overlap in data from Holes 1125A and 1125B are strongly correlated. Typically, parameter values differed by less than 10% at tie levels. In all cases, ties were selected so that the spliced record was as free from noise (high-frequency variability) as possible.

F13. Composite sections for magnetic susceptibility and color reflectance, p. 42.

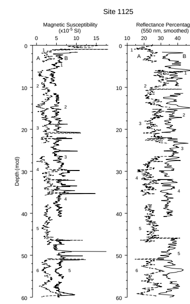

F14. Downhole depth offsets between the mbsf and mcd scales, p. 46.

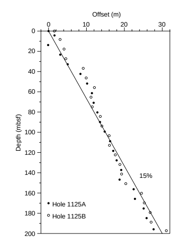

AGE MODELS AND SEDIMENTATION RATES

The North Chatham Slope Site 1125 was drilled to a depth of 552.1 mbsf, in upper Miocene through Pleistocene pelagic/hemipelagic sediments. The combined nannofossil, foraminifer, diatom, and radiolarian biostratigraphy at Site 1125 yielded 38 event levels with a preliminary age assignment, using the shipboard stratigraphic framework (see Table T2, p. 59, in the "Explanatory Notes" chapter). The age dates derived from the biostratigraphy are listed in Table T9. The setting of the site, in the area of the subtropical convergence on the Chatham Rise and with a relatively high-sedimentation rate, has the potential to yield a relatively high-resolution record of paleoproductivity.

The number of events observed is not particularly high, in comparison to the data from the other Neogene sites drilled during Leg 181, and a larger than usual number of dates are minimum or maximum age estimates, rather than being a single date. In general, the high sedimentation rate at the site requires detailed study of relatively large samples to acquire event levels, and postcruise studies will be essential to refine the stratigraphic record.

A graphical illustration of the age-depth data is in Figure F16. A large spread in age estimates, uncertainty in ages and event levels, and "bunching" of events near the 5.6 Ma level, degrade the reliability of the age-depth track (i.e., the net sediment accumulation curve). There is no doubt that the hole ended in strata immediately above the base of the upper Miocene, in an interval dated in the range 10.5–11.2 Ma, by the presence of common right-coiling *Globorotalia miotumida*.

Stratigraphic resolution in the upper part of the Miocene is less certain. According to the diatom record, a hiatus is indicated at 240 mbsf, near 5.4 Ma, a silica dissolution period. It is not apparent from the age-depth record of the events near this depth level that there is a stratigraphic hiatus. Indeed it falls in the most rapidly deposited section at the entire site.

T7. Composite depth section, Site 1125, p. 84.

F15. Spliced record for Site 1125, p. 47.

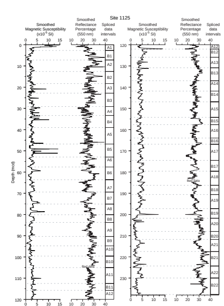

T8. Splice tie points, Site 1125, p. 90.

T9. Biostratigraphic events identified at Site 1125, p. 91.

Sedimentation at the site shows two cycles of high sedimentation rate declining to low values. In the upper Miocene, rates are 130 m/m.y. and then decrease to ~21 m/m.y. by the uppermost Miocene (~6.5 Ma). The second cycle occupies the Pliocene and Pleistocene, starting at 150 m/m.y. at 5.5 Ma, declining to ~19 m/m.y. for the last 2 m.y. This appears to reflect and date tectonic movements in New Zealand. The earlier period of rapid sedimentation may reflect the onset of severe strike-slip movement and uplift of mountains, whereas the second appears to coincide with the period of sharp change in the pole of rotation, increase in compression, and uplift of the Southern Alps (Walcott, 1998).

F16. Age-depth plot, p. 48.

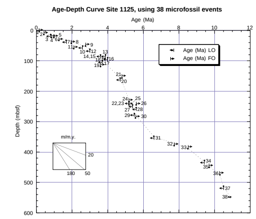

INORGANIC AND ORGANIC GEOCHEMISTRY

Interstitial Waters

Twenty-nine interstitial-water samples were collected at this site: 11 from Hole 1125A at depths ranging from 2.95 to 190.70 mbsf, and 18 from Hole 1125B between 197.70 and 545.45 mbsf. Sampling frequency is one per 20 m from the seafloor to 462.25 mbsf. Below 462.25 mbsf, one sample per 30 m was taken. Results from these two holes are considered to constitute a single depth profile and the data are plotted together in Figure **F17**. Analytical results are summarized in Table **T10** (also in **ASCII format**).

F17. Depth profiles of interstitial-water constituents, p. 49.

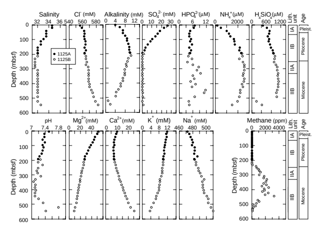

T10. Composition of interstitial waters at Site 1125, p. 92.

Salinity, Chloride, pH, and Sodium

Salinities of the interstitial water decrease from 34.5 at 2.95 mbsf to 31.5 at 231.90 mbsf. Below 286.6 mbsf, salinities remain almost constant (32.0), with the exception of the lowermost sample (32.5; Fig. **F17**).

The chloride (Cl^-) concentrations increase gradually with depth from 556 mM at 2.95 mbsf to a maximum of 583 mM at the bottom of the hole. The increasing gradient in chloride in the bottom part of the hole, below 422.65 mbsf, is steeper than that of the middle part of the hole, between 38.75 and 422.65 mbsf. The higher Cl^- values below 422.65 mbsf may be attributed to the sediment reacting with the pore water (e.g., the hydration of clay minerals).

Interstitial water pH values decrease gradually from 7.51 at 2.95 mbsf to 7.09 at 443.35 mbsf. Below 443.35 mbsf, pH values increase downcore with a significantly high value of 7.79 at 519.65 mbsf. Although this high pH value seems to be erroneous, there is some possibility that this value represents the real pH value of the pore water. The pH profile is generally mirrored by that of dissolved silica and this high-pH sample shows a significantly low concentration of dissolved silica, as discussed below.

Sulfate, Alkalinity, Ammonium, and Phosphate

Sulfate, alkalinity, ammonium, and phosphate concentrations are controlled by organic matter decomposition processes including sulfate reduction and methanogenesis. The sulfate (SO_4^{2-}) concentration decreases gradually from 26.1 mM at 2.95 mbsf to zero at 190.70 mbsf; below this depth, sulfate remains zero or near-zero downcore. Small fluctuations of sulfate in the bottom part of the hole may be attributed to contamination resulting from drilling disturbance. Methane concentration starts increasing just below the top of the zero sulfate interval, suggesting methanogenesis resulting from anaerobic organic matter decomposition by fermentation.

The alkalinity of interstitial water increases with depth to 10.51 mM at 212.70 mbsf; below this depth alkalinity decreases downcore, showing the minimum value of 0.96 mM at 519.65 mbsf. The alkalinity maximum is relatively small compared to maxima observed at Sites 1119 (26.7 mM) and 1122 (40.5 mM) on this leg, where intensive sulfate reduction also occurs. The increase in alkalinity results from the production of bicarbonate ions during bacterial degradation of organic matter.

Ammonium (NH_4^+) concentrations generally track the profile of alkalinity. Ammonium values increase with depth from the subsurface value of 158 µM at 2.95 mbsf to a maximum of 2578 µM at 308.90 mbsf, which is located ~180 m below the alkalinity maximum. Below 308.90 mbsf, ammonium values decrease gradually downhole to the bottom. An increase in the ammonium concentration reflects the intensive bacterial degradation of organic matter, whereas a decrease may be the result of ion-exchange reactions with clay minerals and/or the subsequent incorporation into diagenetically formed clay minerals.

The phosphate (HPO_4^{2-}) concentrations decrease from a subsurface value of 6.8 µM at 2.95 mbsf to ~4 µM at 212.70 mbsf, at which depth the alkalinity maximum occurs. Below this depth, phosphate concentrations show relatively large fluctuations and these roughly correspond to the profile of methane concentrations, suggesting that leaching of the phosphate from organic matter has occurred during methanogenesis.

Dissolved Silica

Dissolved silica (H_4SiO_4) concentrations increase gradually from a value of 447 µM at 2.95 mbsf to a maximum value of 1100 µM at 385.60 mbsf. This is a result of diffusion, driven by the concentration difference between seawater and the sediments and/or upward pore-fluid migration resulting from burial compaction. Dissolved silica concentrations show a pronounced minimum of 181 µM at 519.65 mbsf. A local decrease of dissolved silica in the deeper part of the hole is usually attributed to chert formation (see **"Inorganic Geochemistry,"** p. 37, in the "Site 1123" chapter), although no chert layers are found at this site (see **"Lithostratigraphy,"** p. 3). However, this part of the section below 500 mbsf shows an abrupt increase in density and hardness (responsible for longer drilling times; see **"Physical Properties,"** p. 22), which may be indicative of incipient silica concentration. The preservation of the diatom and radiolarians is poor in core-catcher samples (Samples 181-1125B-54X-CC to 58X-CC; 512.73–548.22 mbsf) (see **"Biostratigraphy,"** p. 9), suggesting possible changes in paleoproductivity of siliceous planktonic organisms. It would be another explanation for the local decrease of dissolved silica. Low abundance of siliceous fossils mirrored by low silica concentrations in interstitial waters has been reported from Site 1123 of this leg (see **"Inorganic Geochemistry,"** p. 37, in the "Site 1123" chapter) and the Ceara Rise in the Atlantic (Mikkelsen and Barron, 1997). Yet another possible interpretation of the distinct spike of low dissolved-silica concentration is the localized enhancement of silica dissolution. As described above, the profile of dissolved silica is mirrored by that of pH in interstitial waters. High-pH conditions may result in a low saturation of opaline silica, which may enhance silica dissolution. However, the cause of high pH at this depth is not clear.

Calcium and Magnesium

The calcium (Ca^{2+}) concentrations decrease slightly from 10.0 mM at 2.95 mbsf to 6.62 mM at 111.75 mbsf and then increase gradually with depth to a maximum of 25.2 mM at the bottom of the hole. The carbonate precipitation caused by the increase of alkalinity resulting from the oxidation of organic matter is responsible for the decreasing trend of Ca^{2+} concentrations in the uppermost part of the core. On the other hand, the increasing concentrations of Ca^{2+} in the lower part of the core are attributed to the progressive dissolution of carbonate-rich sediment in the interstitial waters.

The magnesium (Mg^{2+}) concentrations decrease consistently with depth from 51.7 mM at 2.95 mbsf to 9.1 mM at the bottom of the hole. Decrease of magnesium concentrations with depth have been reported at most DSDP and ODP sites, and magnesium transport from the surface downhole is thought to be controlled by alteration reactions of volcanic or igneous minerals (Gieskes, 1981). The rate of decrease in the Mg^{2+} concentrations diminishes below 200 mbsf.

Potassium and Sodium

The potassium (K^+) concentration steadily decreases downhole from the subsurface volume of 11.8 mM at 2.95 mbsf to a minimum of 3.7 mM at 545.45 mbsf. Potassium normally decreases with increasing burial depth at deep-sea sites. Sodium (Na^+) concentrations increase steadily from 472 mM at 2.95 mbsf to a maximum value of 510 mM at 545.45 mM mbsf. The profile of Na^+ can generally be related to chloride concentration in interstitial waters.

Summary of Interstitial-Water Results

Sulfate reduction occurs intensively in the upper part of the hole (<200 mbsf), while the methanogenesis zone is located below the sulfate reduction zone. Sulfate decreases gradually with depth, to zero at ~200 mbsf and remains near zero to the total depth. Alkalinity shows a maximum value of 10.5 mM at 222 mbsf. Organic carbon degradation processes are inferred from the profiles of phosphate and ammonium. Phosphate shows a similar profile to that of methane concentration, whereas ammonium concentrations track the profile of alkalinity, with both ammonium and alkalinity showing gradual changes downcore. Dissolved silica concentrations show almost equilibrated values with respect to opaline silica in the lower part of the hole. A pronounced minimum in dissolved silica corresponds to the poor preservation of diatoms and radiolarians in the bottom part of the core. The increased hardness of the sediments suggests a high silica concentration in this horizon.

PHYSICAL PROPERTIES

Multisensor Track Measurements

The shipboard physical properties program at Site 1125 included nondestructive measurements of bulk density and magnetic susceptibility on whole sections of all cores using the MST (Fig. F18). Magnetic susceptibility was measured at 4-cm intervals and at high sensitivity (4-s measurement time) on core from all Site 1125 holes. High-amplitude fluctuations in magnetic susceptibility above 245 mbsf are associated with the occurrence of tephra layers (see "Lithostratigraphy," p. 3). The GRAPE bulk density measurements were made at 4-cm intervals in all Site 1125 cores. The GRAPE density increases gradually from a surface low of 1.6 to 1.85 g/cm³ at 188 mbsf. A break in the increasing trend at 188 mbsf may be related to a hiatus or a rapid change in deposition rate. The densities are generally low between 188 and 245 mbsf (245 mbsf is the boundary between lithologic Subunits IB and IIA) and correspond to high magnetic susceptibility values. With some exceptions, lithostratigraphic Unit II is characterized by a very flat density profile. Below 510 mbsf, the densities begin another gradually increasing trend down to 532 mbsf. An abrupt decrease in the GRAPE density at 532 mbsf corresponds to a similar decrease in the magnetic susceptibility record, possibly reflecting a depositional hiatus.

F18. MST measurements from Hole 1125C, p. 50.

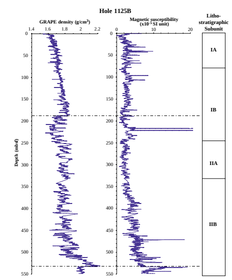

Thermal Conductivity and Heat Flow

Five downhole temperature measurements were taken with the Adara temperature tool at the position of Cores 181-1125A-5H, 7H, 9H, 11H, and 13H. The Adara temperature tool yielded good quality temperature estimates of 6.54°C from Core 5H, 7.10°C from Core 7H, 9.25°C from Core 9H, 9.42°C from Core 11H, and 11.65°C from Core 13H (Fig. F19). Based on temperature equilibration curves from Cores 5H, 7H, 9H, 11H, and 13H, the temperature estimate at the mudline is 3.60°C. Thermal conductivity was measured in the shipboard laboratory on the same core as the Adara temperature tool was used in; four measurements were made per core. A thermal gradient of 6.49°C/100 m was then calculated from the Adara and thermal conductivity measurements. Using an average thermal conductivity of 1.09 W/(m·K), heatflow was estimated to be 0.07 W/m².

F19. Plots of thermal gradient and temperature from Hole 1125A, p. 51.

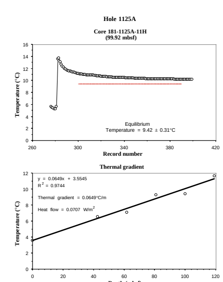

DOWNHOLE MEASUREMENTS

Logging Operations

Downhole logging was conducted in Hole 1125B. The drill string was placed at 96 mbsf as the logging tools were lowered to the bottom of the hole. During logging, the drill string was raised to 81 mbsf. The drill string had to be maintained at 81 mbsf to keep the upper hole wall from collapsing.

Operations began at 0600 hr on 6 October 1998 and ended at 1300 hr on the same day. Because of time constraints, logging operations were limited to one full pass of the triple combination tool string (Fig. F20) (see "Downhole Measurements," p. 29, in the "Explanatory Notes" chapter for details). There was ~1–2 m of heave throughout operations, and the wireline heave compensator was used during all

F20. Logging operations in Hole 1125B, p. 52.

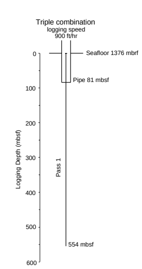

measurements. The hole conditions were generally good, with a relatively uniform borehole diameter (~12 in), except near the top where the hole widened to >18 in. As a result, the data quality for most of the hole is excellent. The principal results are shown in Figure **F21.**

F21. Log data and log units from Hole 1125B, **p. 53**.

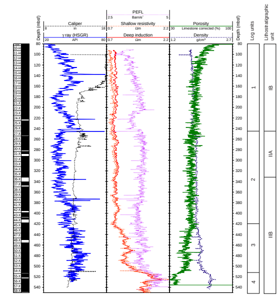

Data Quality/Preliminary Interpretation

The caliper reading from the lithodensity tool on the triple combination indicates that there are zones of fluctuating hole width (e.g., 250–275 mbsf). A plot of the caliper log with the occurrence of tephra beds shows that there is no systematic correlation between zones of increased hole width and tephra layers (Fig. **F22**). However, at 250–275 mbsf, there is a peak-to-peak correlation between the gamma-ray and caliper data, with lower gamma-ray values (sand-rich lithologies) corresponding to larger hole widths (Fig. **F22**).

F22. Comparison of the gamma-ray and caliper logs, **p. 54.**

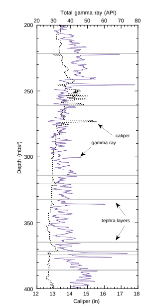

If the gamma-ray data are separated into their constituent parts (K, Th, and U) (Fig. **F23A**), a good correlation can be seen between Th and K, but U concentrations often fluctuate independently of the other two radioactive elements (e.g., 100–200 mbsf). This is partly because U is soluble under oxidizing conditions and is, therefore, often leached from the sediment, and partly because U is often present within a different component of the sediment: Th and K are likely to be contained within the clay mineral fraction, whereas the U has probably been adsorbed by organic matter. However, a plot of total natural gamma radioactivity (HSGR) against just Th and K radioactivity (HCGR) (Fig. **F23B**) shows that the signal is dominated by Th and K, indicating that fluctuations in clay content control gamma-ray variability. Because clay content appears to be controlling the natural gamma ray, compelling cyclical deposition of the clay emerges, with distinct low-frequency cycles (Fig. **F23**) (see also **"Logging Units,"** p. 24). Nevertheless, certain anomalously high spikes in natural gamma ray may well indicate the position of tephra horizons, as discussed at the end of this section.

F23. Spectral gamma-ray log, **p. 55.**

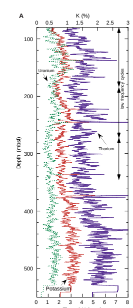

The good hole conditions allow for confident interpretation of the bulk density and neutron porosity logs. Inversion of the bulk density into a density-based porosity log, using a matrix density of 2.71 g/cm^3 (calcite) and fluid density of 1.03 g/cm^3 (seawater) (see **"Triple Combination Tool String,"** p. 29, in the "Explanatory Notes" chapter) gives the most reliable proxy for downhole porosity variability. Comparison of the density porosity with the neutron porosity shows a tight linear relationship (Fig. **F24**). This linear relationship shows several factors. First, the data is reliable because the two logs agree. Second, the absence of any significant deviation between the two indicates that the clay content of Hole 1125B is low enough not to adversely affect the density porosity/neutron porosity correlation. Since clays have bound water in their composition, regions of high clay content would cause the neutron porosity to give anomalously high values relative to the density porosity. This is not the case anywhere in Hole 1125B.

An apparent deviation from the 1:1 linear relationship at high-neutron porosities could be inferred in Figure **F24,** with the regression slope becoming gentler. This may be a result of variable instrument response in high-porosity sediments. The overall slight deviation from a pure 1:1 relationship at lower porosities may be caused by slight errors in the inversion parameters for computing density-porosity, as well as a small bias in the lithodensity tool between measured densities and the true values.

F24. Crossplot of density porosity and neutron porosity, **p. 57.**

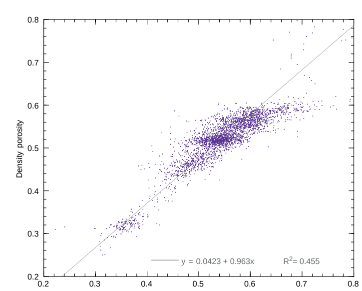

The failure of the MAXIS depth recorder software that occurred during the logging operations of Hole 1123B did not recur. Therefore, the temperature tool data is reliable. The temperature data from the Lamont Temperature Tool are shown in Figure F25. No zones of hydrothermal input are seen in the data and the increase of temperature with depth reflects a normal geothermal temperature increase downhole.

F25. Downhole variations in borehole temperature, p. 58.

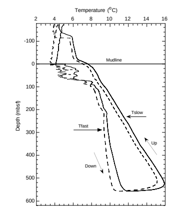

Logging Units

In common with the results from Site 1123, on the northeast margin of the Chatham Rise, the log data from Hole 1125B show relatively low-amplitude fluctuations (Fig. F21). Natural gamma-ray values range between 22 and 79 API, and shallow-resistivity values vary only between 0.73 and 2.21 Ωm. In fact, shallow-resistivity values appear to be relatively constant (0.86 ± 0.05 Ωm) in all but the bottom 130 m of the hole (Fig. F21). Nevertheless, distinct logging units can be assigned to this hole, mainly on the basis of changes in the character and rhythmicity of the data.

Log Unit 1: Base of Pipe to 245 mbsf

Within this unit cyclical fluctuations in the natural gamma are particularly pronounced. Two main frequencies can be recognized: a low-frequency cyclicity, with a wavelength of ~100 m; and a high-frequency cyclicity with a wave length of ~10 m (Fig. F26). The neutron-porosity values record a slight compaction trend in the upper ~40 m of this unit. The base of log Unit 1 corresponds to the boundary between lithostratigraphic Subunits IB and IIA (Fig. F21).

F26. Cyclical fluctuations in the natural gamma results from log Unit 1, p. 59.

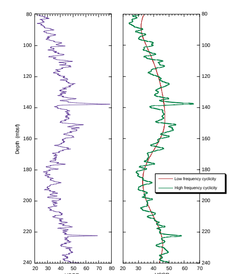

Log Unit 2: 245–420 mbsf

Below 245 mbsf, the character of the gamma-ray curve changes (Fig. F21). Between 245–360 m, low-frequency cycles are less apparent, because of a decrease in amplitude, and they appear to have a shorter wavelength (~60 m). Below 360 m (to the base of the log), the low-frequency gamma-ray cycles increase in amplitude again, but show a further reduction in wavelength to ~40 m. However, caution must be employed in comparing the nature of the gamma-ray curves above and below 360 m: it is at this depth that sedimentation rates decrease dramatically (see "Age Models and Sedimentation Rates," p. 18). Within log Unit 2, resistivity, photoelectric effect, density, and neutron porosity values all remain relatively constant (Fig. F21).

Log Unit 3: 420–512 mbsf

Resistivity values begin to rise within log Unit 3, from ~0.85 Ωm at the top to ~1.58 Ωm at the base. The increase in resistivity reflects an increase in compaction and lithification of the sediments. This compaction trend is also recorded in an increase in the neutron porosity and a decrease in the density, from the top to the bottom of log Unit 3.

Log Unit 4: 512–550 mbsf

The contact between log Units 3 and 4 is characterized by a sharp increase in resistivity and density, and a sharp decrease in neutron porosity. These log responses are again thought to be a response to increased compaction and induration. A concomitant increase in the photoelectric effect value at the top of log Unit 4 may reflect increased calcite cementation.

Discussion

As shown above, the low- and high-frequency cycles in the natural gamma results are indicative of a rhythmically fluctuating input of terrigenous clays at Hole 1125B. Post-cruise analysis of the natural gamma results from Hole 1125B will show if this cyclicity can be related to astronomical (Milankovitch) forcing. Cyclic sedimentation was also recorded in the reflectance data from the core (see **"Lithostratigraphy,"** p. 3) and was attributed to changes in the burial flux of the terrigenous and calcareous biogenic components of the sediment.

It is perhaps surprising that the numerous tephra layers sampled at this site, and at Sites 1123 and 1124, do not have a more distinctive signature in the logs. Rhyolitic volcanism from the North Island, New Zealand, could be expected to produce tephras that are relatively rich in radioactive Th, K, and U (Nelson et al., 1986), which should be evident in the natural gamma results. The relatively poor correlation between tephra horizons seen in the core, and spikes in the gamma log (Fig. **F22**) may be, in part, a result of the thinness of the tephra horizons (typically <0.1 m) and the relatively low resolution of the HNGS (~0.45 m). However, closer inspection of all the log data from Hole 1125B seems to indicate that some of the tephra horizons can be identified, especially considering there is likely to be a depth discrepancy between the core and log depths. Figure **F27** shows selected logging results from 200–250 mbsf and 350–400 mbsf. Tephra horizons at ~222, 365, 372, and 374 mbsf can be identified in the logs by increases in the natural gamma, particularly the potassium radioactivity, and decreases in the photoelectric effect and the density. A tephra horizon seen in the core at ~ 386 mbsf is not recorded in the logs. There is, however, strong evidence from the logs that a tephra horizon exists at ~245 mbsf, even though no tephra was recovered in the core at this depth. Although core recovery is recorded as 100% at this point, it is still possible that a tephra horizon could have been preferentially washed out, especially considering the "tephra horizon" seen in the logs at ~245 mbsf falls in between Cores 181-1125B-26X and 27X, at the boundary of a change in lithology and in an area where core recovery was biscuity (see **"Lithostratigraphy,"** p. 3).

F27. Comparison of tephra horizons and log responses, **p. 60.**

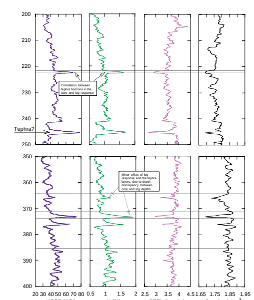

REFERENCES

Berggren, W.A., Kent, D.V., Swisher, C.C., III, and Aubry, M.-P., 1995. A revised Cenozoic geochronology and chronostratigraphy. *In* Berggren, W.A., Kent, D.V., Aubry, M.-P., and Hardenbol, J. (Eds.), *Geochronology, Time Scales and Global Stratigraphic Correlation*. Spec. Publ.—Soc. Econ. Paleontol. Mineral. (Soc. Sediment. Geol.), 54:129–212.

Bradford-Grieve, J., Murdoch, R.C., James, M., Oliver, M., and McLeod, J., 1998. Mesozooplankton biomass, competition and potential grazing pressure on phytoplankton during the austral winter and spring 1993 in the Subtropical Convergence region near New Zealand. *Deep-Sea Res.*, 45:1709–1737.

Cande, S.C., and Kent, D.V., 1995. Revised calibration of the geomagnetic polarity timescale for the Late Cretaceous and Cenozoic. *J. Geophys. Res.,* 100:6093–6095.

Carter, L., and Carter, R.M., 1993. Sedimentary evolution of the Bounty Trough: a Cretaceous rift basin, southwestern Pacific Ocean. *In* Ballance, P.F. (Ed.), *South Pacific Sedimentary Basins:* Amsterdam (Elsevier), Sedimentary Basins of the World Ser., 2:51–67.

Carter, L., Nelson, C.S., Neil, H.L., and Froggatt, P.C., 1995. Correlation, dispersal, and preservation of the Kawakawa Tephra and other late Quaternary tephra layers in the Southwest Pacific Ocean. *N. Z. J. Geol. Geophys.,* 38:29–46.

Chiswell, S.M., 1994. Acoustic doppler current profiler measurements over the Chatham Rise. *N. Z. J. Mar. Freshwater Res.,* 28:167–178.

————, 1996. Variability in the Southland Current, New Zealand. *N. Z. J. Mar. Freshwater Res.,* 30:1–17.

Compton, J.S., and Mallinson, D.J., 1996. Geochemical consequences of increased late Cenozoic weathering rates and the global CO_2 balance since 100 Ma. *Paleoceanography,* 11:431–446.

Cullen, D.J., 1965. Autochthonous rocks from the Chatham Rise, east of New Zealand. *N. Z. J. Geol. Geophys.,* 8:465–474.

————, 1980. Distribution, composition and age of submarine phosphorites on Chatham Rise, east of New Zealand. *Spec. Publ.—Soc. Econ. Paleontol. Mineral.,* 29:139–148.

————, 1987. The submarine phosphate resource on central Chatham Rise. *Div. Mar. Freshwater Sci. Rep.,* 2:1–22.

Fenner, J., Carter, L., and Stewart, R., 1992. Late Quaternary paleoclimatic and paleoceanographic change over northern Chatham Rise, New Zealand. *Mar. Geol.,* 108:383–404.

Gardner, J.V., Nelson, C.S., and Baker, P.A., 1986. Distribution and character of pale green laminae in sediment from Lord Howe Rise: a probable late Neogene and Quaternary tephrostratigraphic record. *In* Kennett, J.P., von der Borch, C.C., et al., *Init. Repts. DSDP,* 90 (Pt. 2): Washington (U.S. Govt. Printing Office), 1145–1159.

Gartner, S., 1990. Neogene calcareous nannofossil biostratigraphy, Leg 116 (Central Indian Ocean). *In* Cochran, J.R., Stow, D.A.V., et al., *Proc. ODP, Sci. Results,* 116: College Station, TX (Ocean Drilling Program), 165–187.

————, 1992. Miocene nannofossil chronology in the North Atlantic, DSDP Site 608. *Mar. Micropaleontol.,* 18:307–331.

Gieskes, J.M., 1981. Deep-sea drilling interstitial water studies: implications for chemical alteration of the oceanic crust, layers I and II. *In* Warme, J.E., Douglas, R.G., and Winterer, E.L. (Eds.), *The Deep Sea Drilling Project: A Decade of Progress*. Spec. Publ.—Soc. Econ. Paleontol. Mineral., 32:149–167.

Heath, R.A., 1972. The Southland Current. *N. Z. J. Mar. Freshwater Res.,* 6:497–533.

————, 1985. A review of the physical oceanography of the seas around New Zealand–1982. *N. Z. J. Mar. Freshwater Res.,* 19:70–124.

Karns, A.W., 1976. Submarine phosphorite deposits of Chatham Rise near New Zealand: summary. *AAPG Mem.,* 25:395–398.

Kennett, J.P., and von der Borch, C.C., 1986. Southwest Pacific Cenozoic paleoceanography. *In* Kennett, J.P., von der Borch, C.C., et al., *Init. Repts. DSDP,* 90 (Pt. 2): Washington (U.S. Govt. Printing Office), 1493–1517.

Labeyrie, L.D., Duplessey, J.-C., Duprat, J., Juillet-Leclerc, A., Moyes, J., Michel, E., Kallel, N., and Shackleton, N.J., 1992. Changes in the vertical structure of the North Atlantic Ocean between glacial and modern times. *Quat. Sci. Rev.,* 11:401–413.

Lewis, K.B., Bennett, D.J., Herzer, R.H., and von der Borch, C.C., 1985. Seismic stratigraphy and structure adjacent to an evolving plate boundary, western Chatham Rise, New Zealand. *In* Kennett, J.P., von der Borch, C.C., et al., *Init. Repts. DSDP,* 90: Washington (U.S. Govt. Printing Office), 1325–1337.

Loutit, T.S., and Kennett, J.P., 1979. Application of carbon isotope stratigraphy to late Miocene shallow marine sediments, New Zealand. *Science,* 204:1196–1199.

Mikkelsen, N., and Barron, J.A., 1997. Early Oligocene diatoms on the Ceara Rise and the Cenozoic evolution of biogenic silica accumulation in the low-latitude Atlantic. *In* Shackleton, N.J., Curry, W.B., Richter, C., and Bralower, T.J. (Eds.), *Proc. ODP, Sci. Results,* 154: College Station, TX (Ocean Drilling Program), 483–490.

Mitchell, J.S., Carter, L., and McDougall, J.C., 1989. New Zealand region sediments (1:6,000,000). *N. Z. Oceanogr. Inst. Chart, Misc. Ser.,* 67.

Morley, J.J., and Nigrini, C., 1995. Miocene to Pleistocene radiolarian biostratigraphy of North Pacific Sites 881, 884, 885, 886, and 887. *In* Rea, D.K., Basov, I.A., Scholl, D.W., and Allan, J.F. (Eds.), *Proc. ODP, Sci. Results,* 145: College Station, TX (Ocean Drilling Program), 55–91.

Neil, H.L., 1998. Late Quaternary variability of surface and deep water masses, Chatham Rise, SW Pacific [Ph.D. thesis]. Univ. of Waikato, Hamilton, New Zealand.

Nelson, C.S., 1986. Lithostratigraphy of Deep Sea Drilling Project Leg 90 drill sites in the Southwest Pacific: an overview. *In* Kennett, J.P., von der Borch, C.C., et al., *Init. Repts. DSDP,* 90: Washington (U.S. Govt. Printing Office), 1471–1491.

Nelson, C.S., Froggatt, P.C., and Gosson, G.J., 1986. Nature, chemistry, and origin of late Cenozoic megascopic tephras in Leg 90 cores from the southwestern Pacific. *In* Kennett, J.P., von der Borch, C.C., et al., *Init. Repts. DSDP,* 90: Washington (U.S. Govt. Printing Office), 1161–1171.

Nodder, S.N., 1998. Particulate fluxes in the Subtropical Convergence region and other marine environments of New Zealand [Ph.D. thesis]. Univ. of Waikato, Hamilton, New Zealand.

Pemberton, S.G., and MacEachern, J.A., 1995. The sequence stratigraphic significance of trace fossils: examples from the Cretaceous Foreland Basin of Alberta, Canada. *In* Van Wagoner, J.C., and Bertram, G.T. (Eds.), *Sequence Stratigraphy of Foreland Basin Deposits.* AAPG Mem., 64:429–475.

Pudsey, C.J., 1992. Late Quaternary changes in bottom water velocity inferred from grain size in the Northern Weddell Sea. *Mar. Geol.,* 107:9–33.

Rio, D., 1982. The fossil distribution of coccolithophore genus *Gephyrocapsa* Kamptner and related Plio-Pleistocene chronostratigraphic problems. *In* Prell, W.L., Gardner, J.V., et al., *Init. Repts. DSDP,* 68: Washington (U.S. Govt. Printing Office), 325–343.

Sato, T., and Kameo, K., 1996. Pliocene to Quaternary calcareous nannofossil biostratigraphy of the Arctic Ocean, with reference to late Pliocene glaciation. *In* Thiede, J., Myhre, A.M., Firth, J.V., Johnson, G.L., and Ruddiman, W.F. (Eds.), *Proc. ODP, Sci. Results,* 151: College Station, TX (Ocean Drilling Program), 39–59.

Walcott, R.I., 1998. Modes of oblique compression: late Cenozoic tectonics of the South Island of New Zealand. *Rev. Geophys.,* 36:1–26.

Weaver, P.P.E., Carter, L., and Neil, H., 1998. Response of surface watermasses and circulation to late Quaternary climate change, east of New Zealand. *Paleoceanography,* 13:70–83.

Wood, R.A., Andrews, P.B., Herzer, R.H., et al., 1989. Cretaceous and Cenozoic geology of the Chatham Rise region, South Island, New Zealand. *N. Z. Geol. Basin Stud.,* 3:1–76.

Figure F1. Locality map of Site 1125, showing location of seismic line through the site.

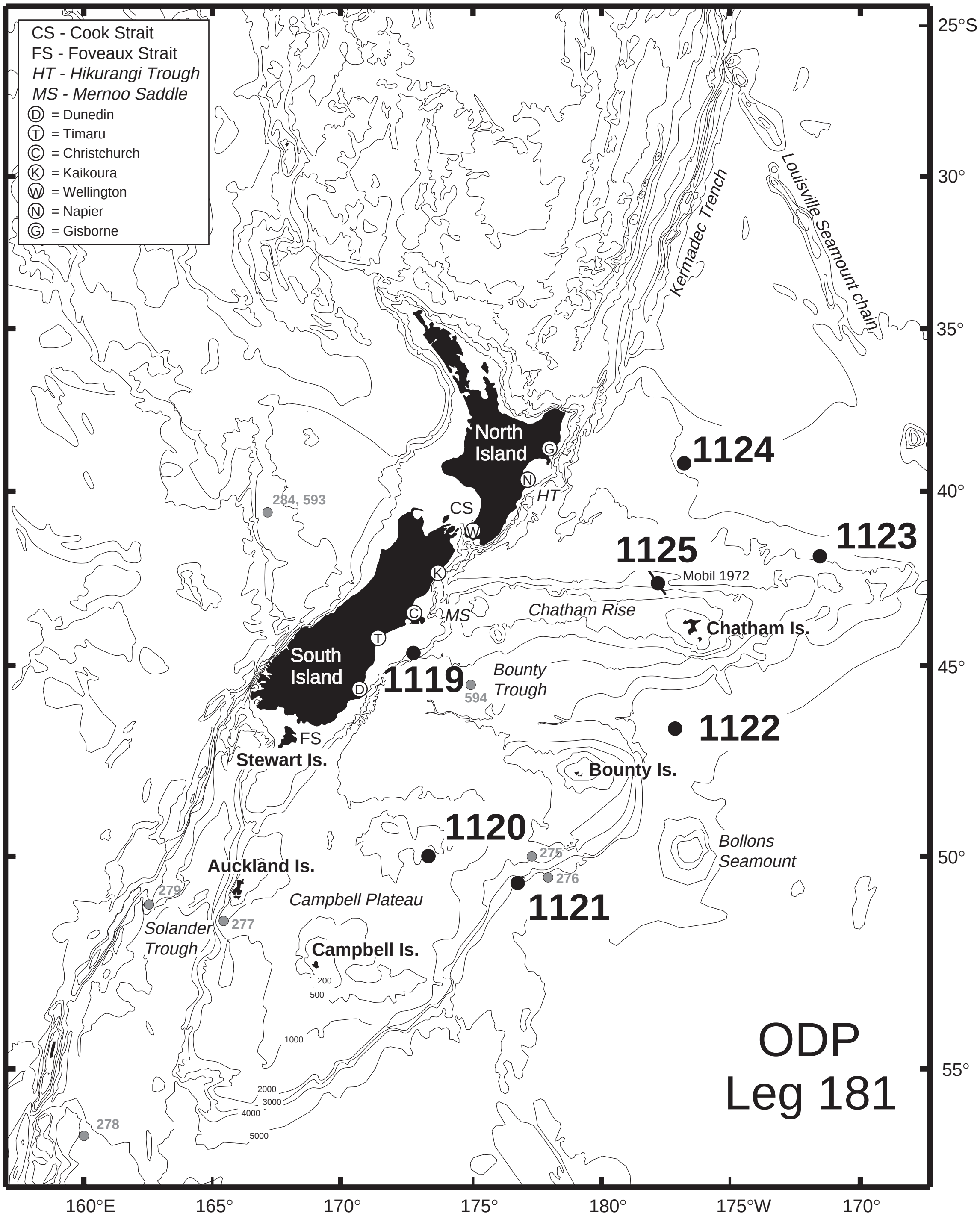

Figure F2. Portion of reconnaissance seismic line Mobil (*Fred H. Moore*) 1972.

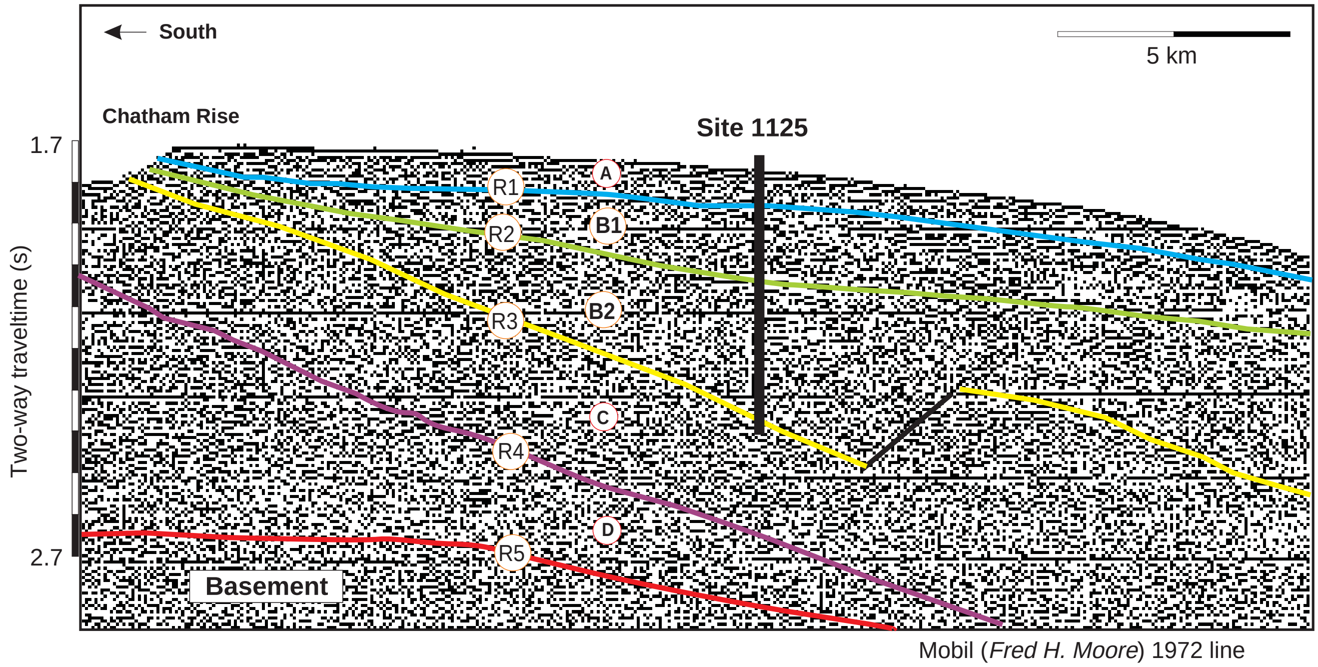

Figure F3. Generalized lithologic log for Site 1125.

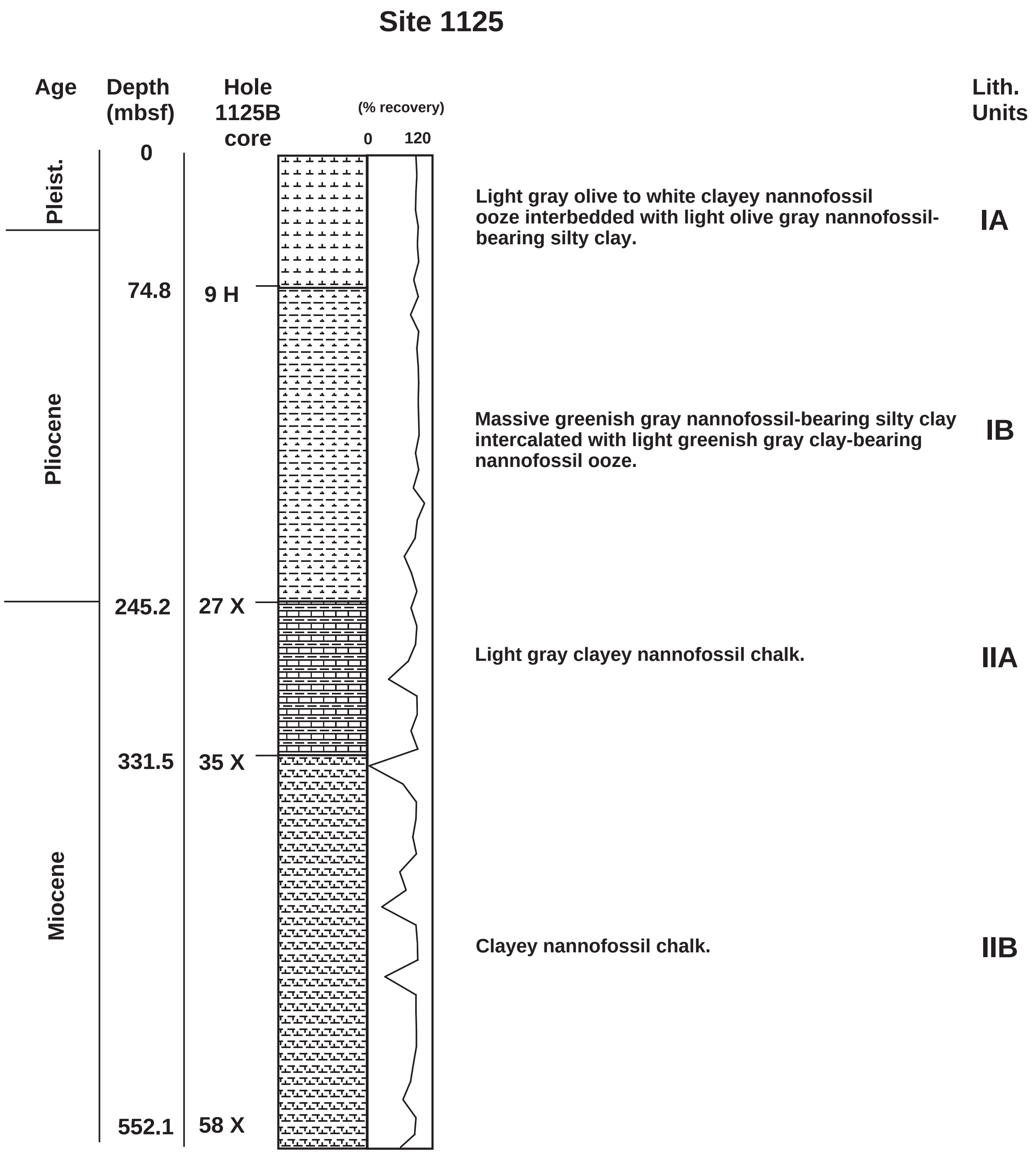

Figure F4. Summary log for Site 1125. (Continued on next two pages.)

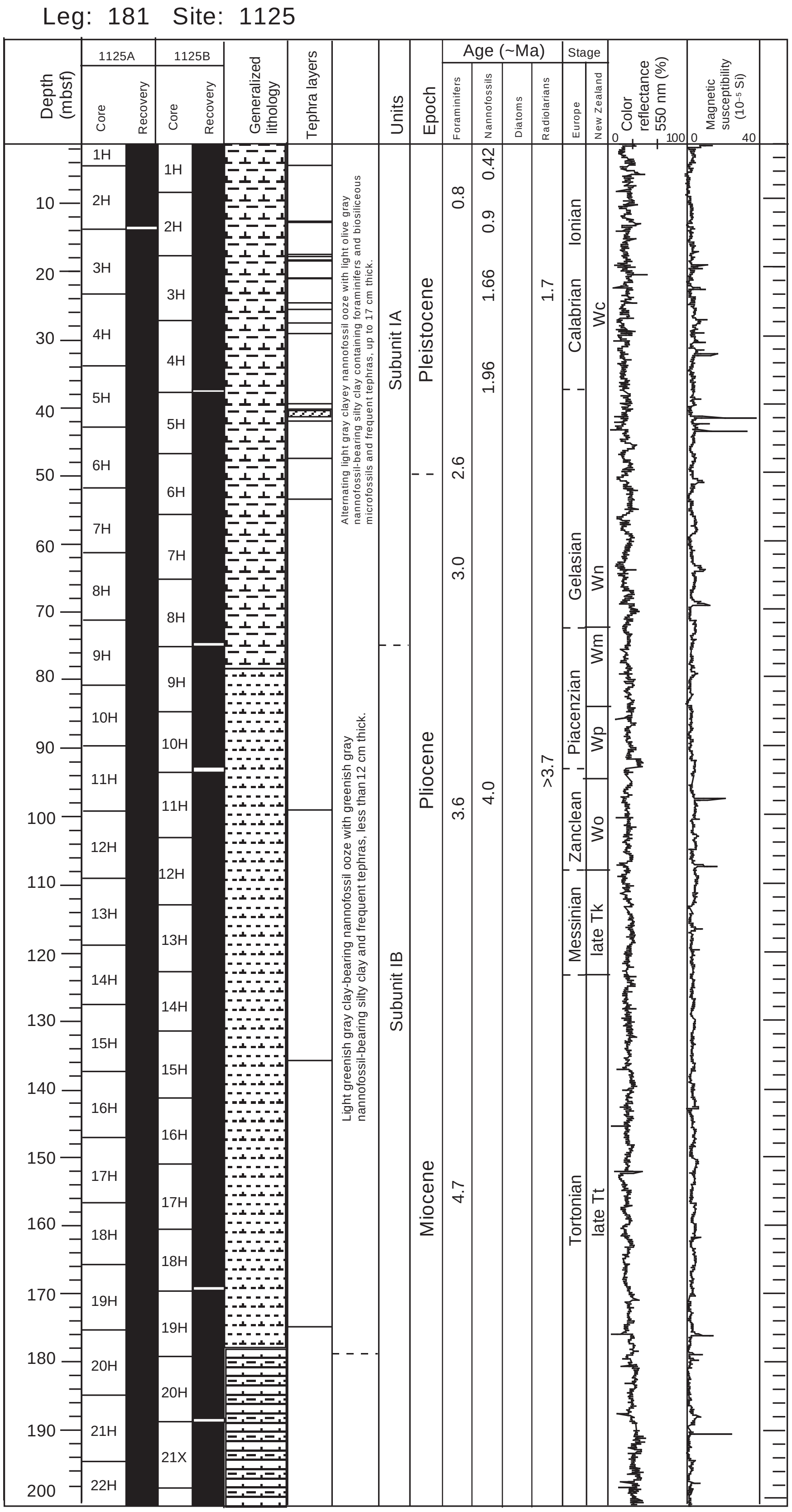

Figure F4 (continued).

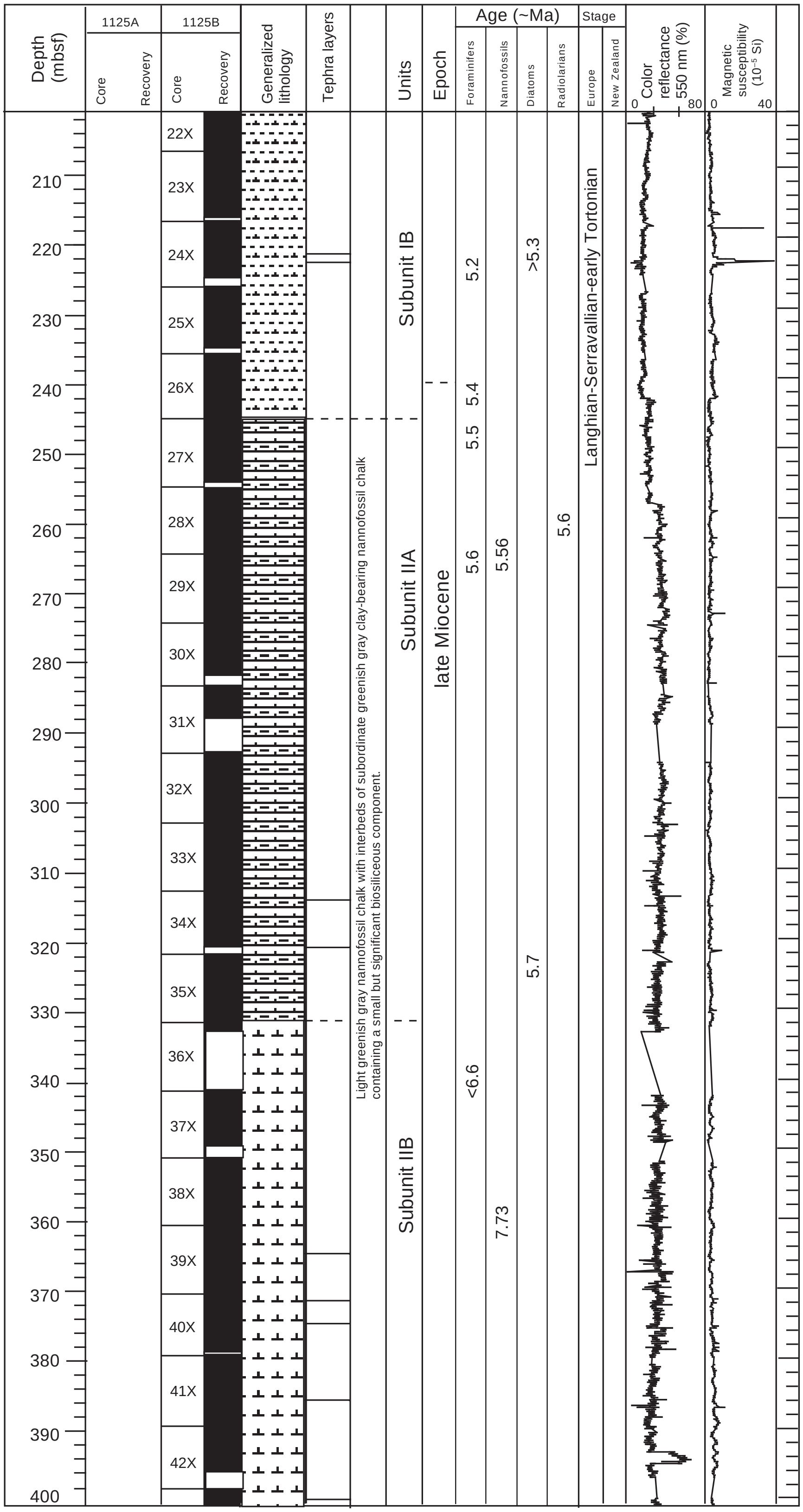

Figure F4 (continued).

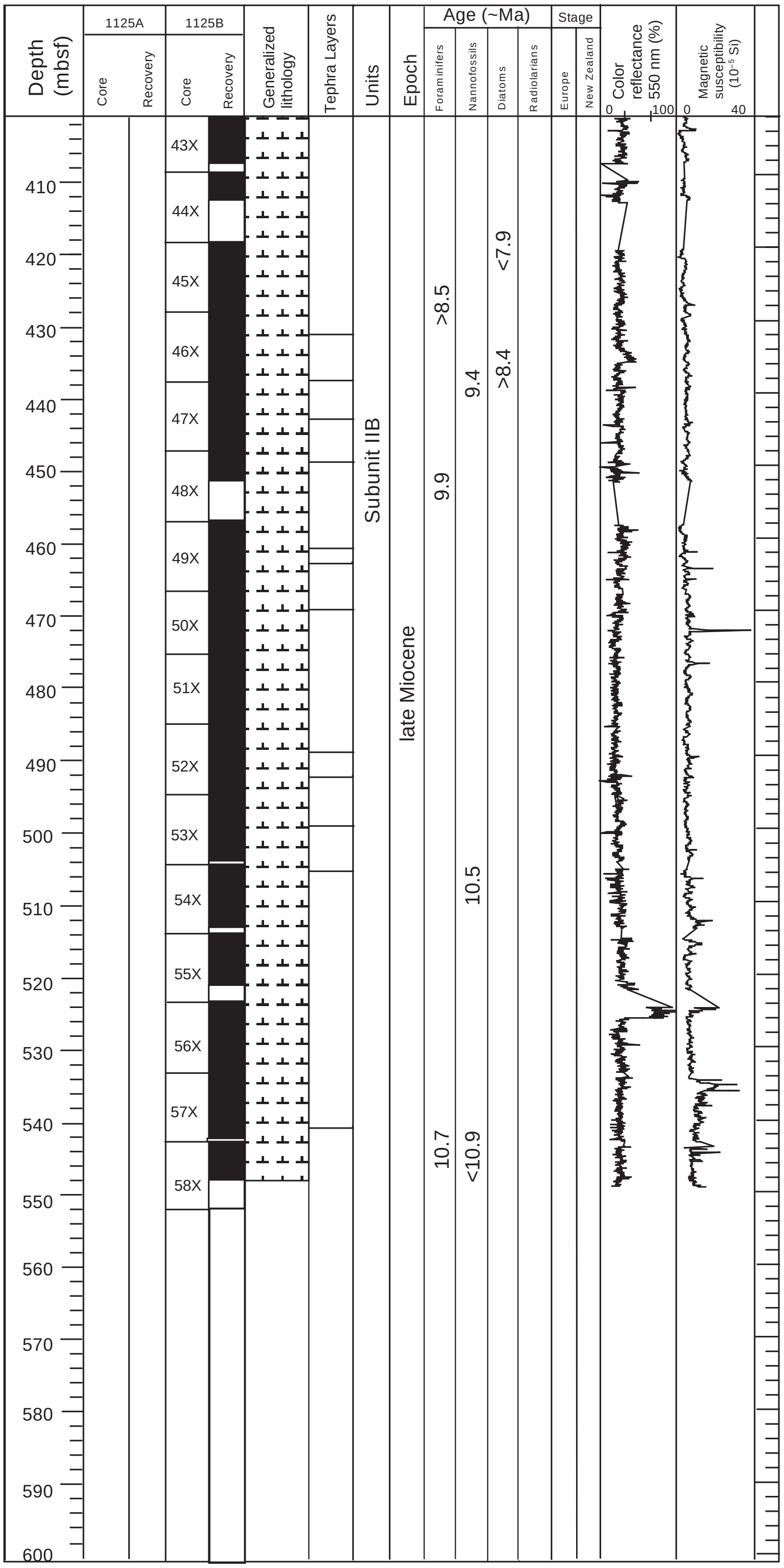

Figure F5. Reflectance profile for 550-nm wavelength, Hole 1125B.

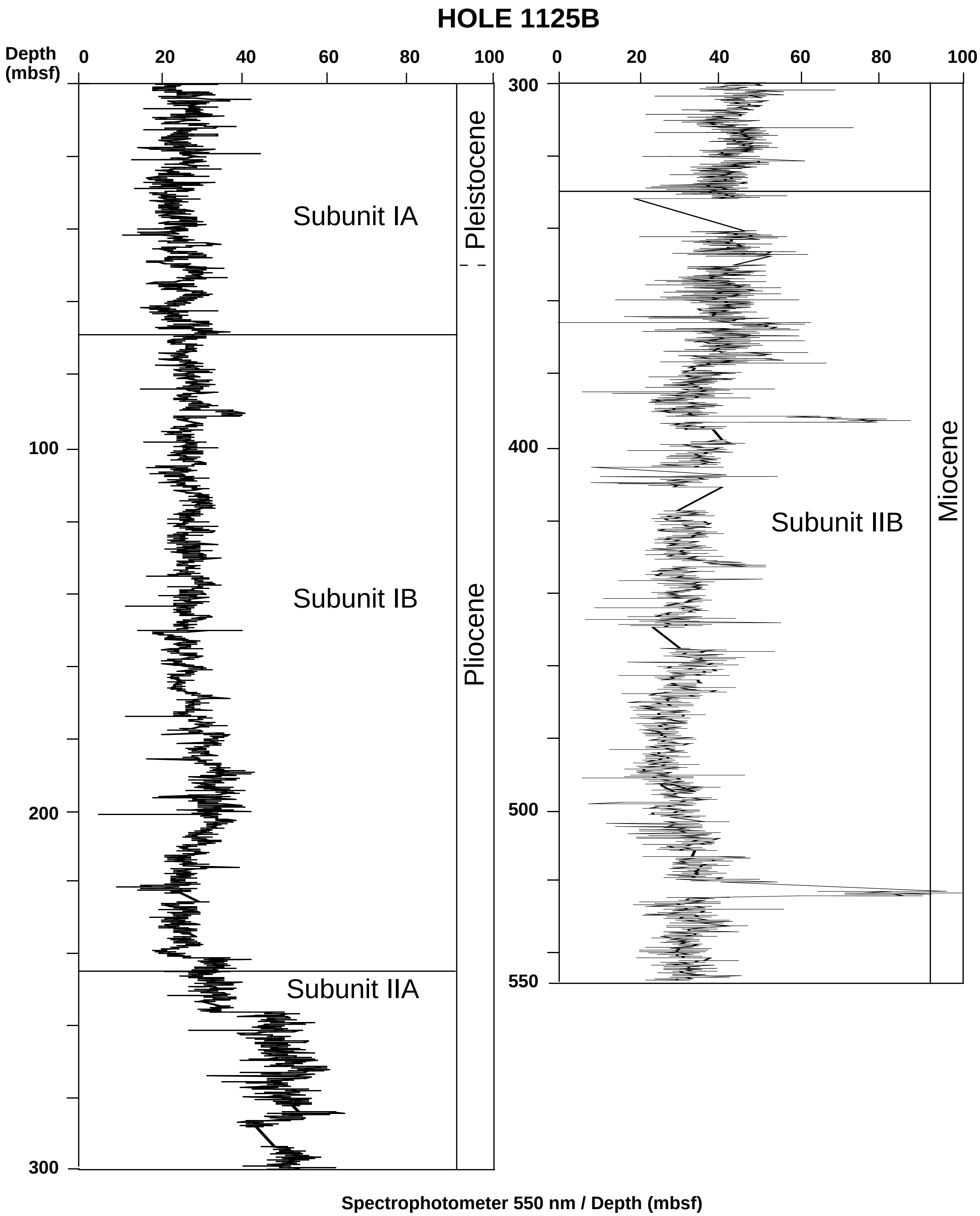

Figure F6. Trace-fossil assemblages with ichnofacies (underlined) for Site 1125.

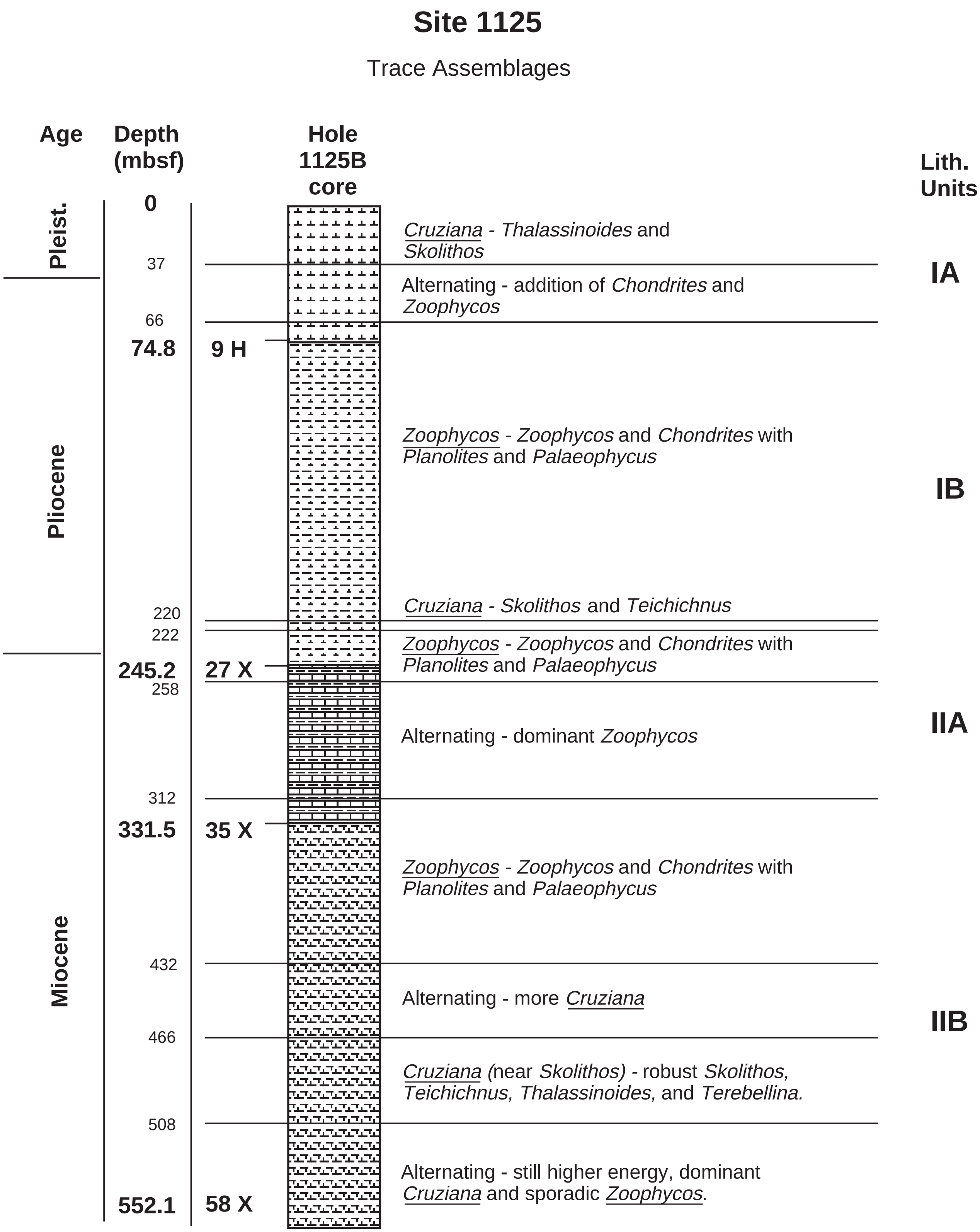

Figure F7. Distribution of macroscopic tephra, with total thickness of tephra in each subunit (e.g., 223 cm in Subunit IA) and thickness percentage of each subunit.

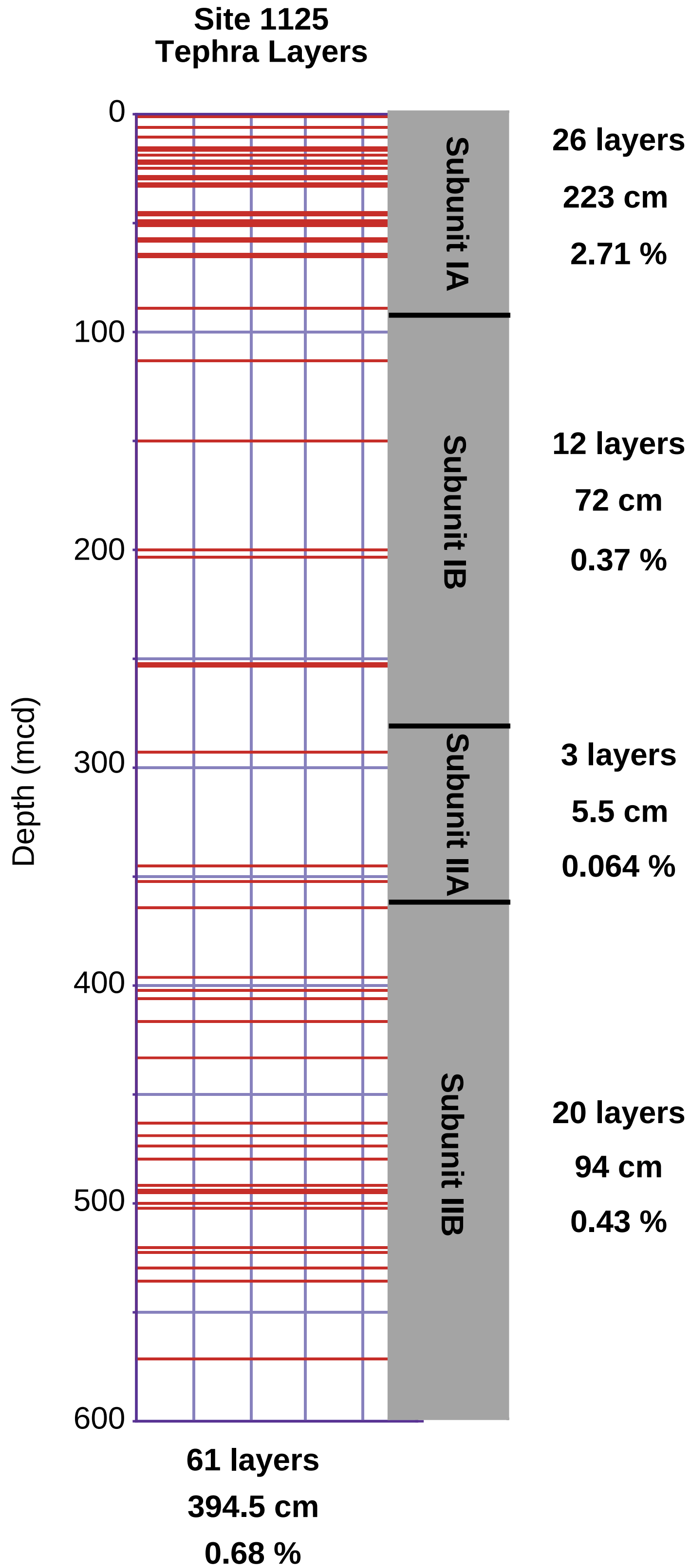

Figure F8. Biostratigraphic summary chart of Site 1125.

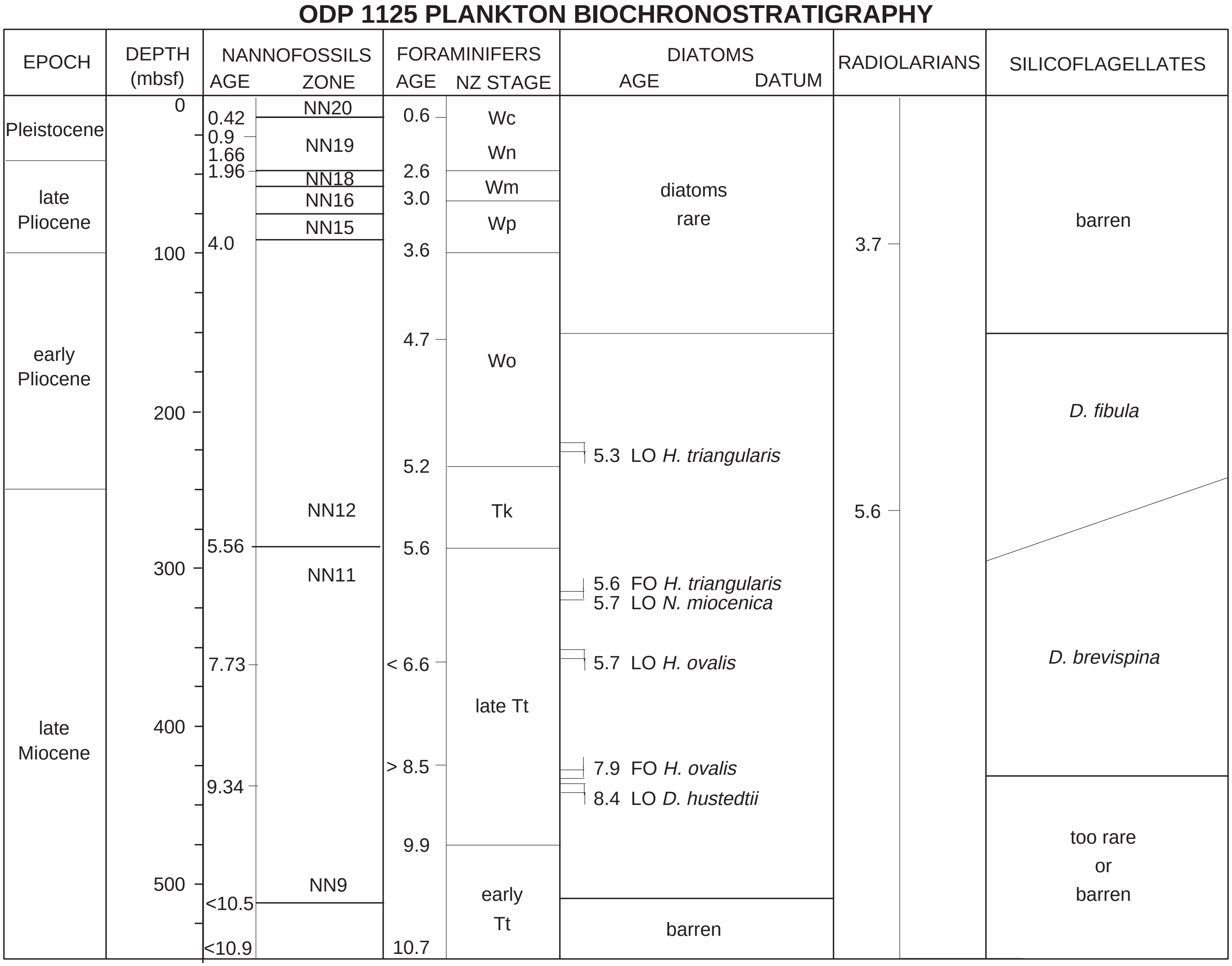

Figure F9. Age-depth relationships at Site 1125, based upon nannofossil datums.

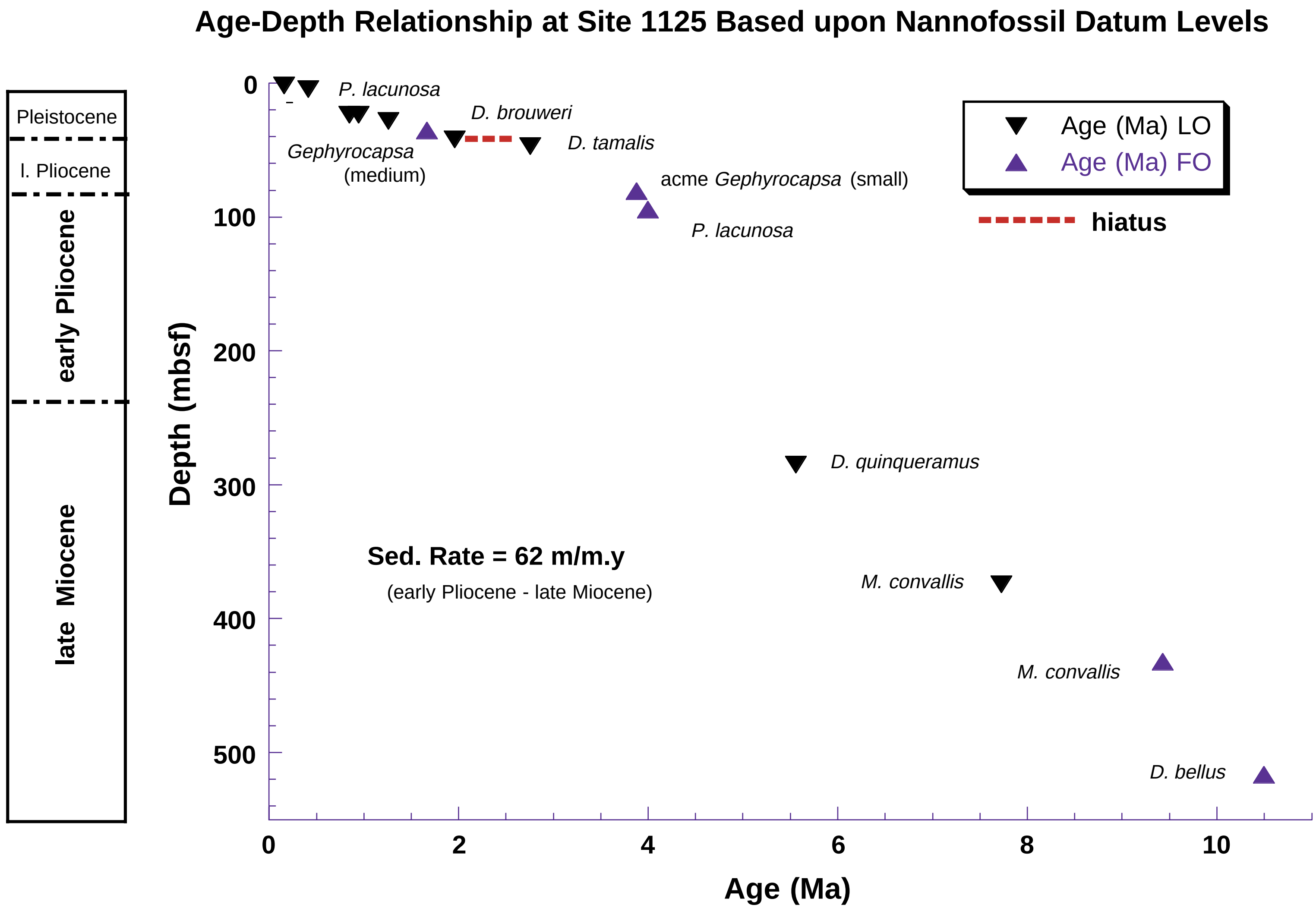

Figure F10. Intensity of remanence in Holes 1125A (NRM and after 20 mT of demagnetization) and 1125B (after 20 mT of demagnetization). NRM intensity averages between 10^{-4} and 10^{-5} A/m. After 20-mT AF demagnetization, the intensity decreases to 10^{-5}–10^{-6} A/m.

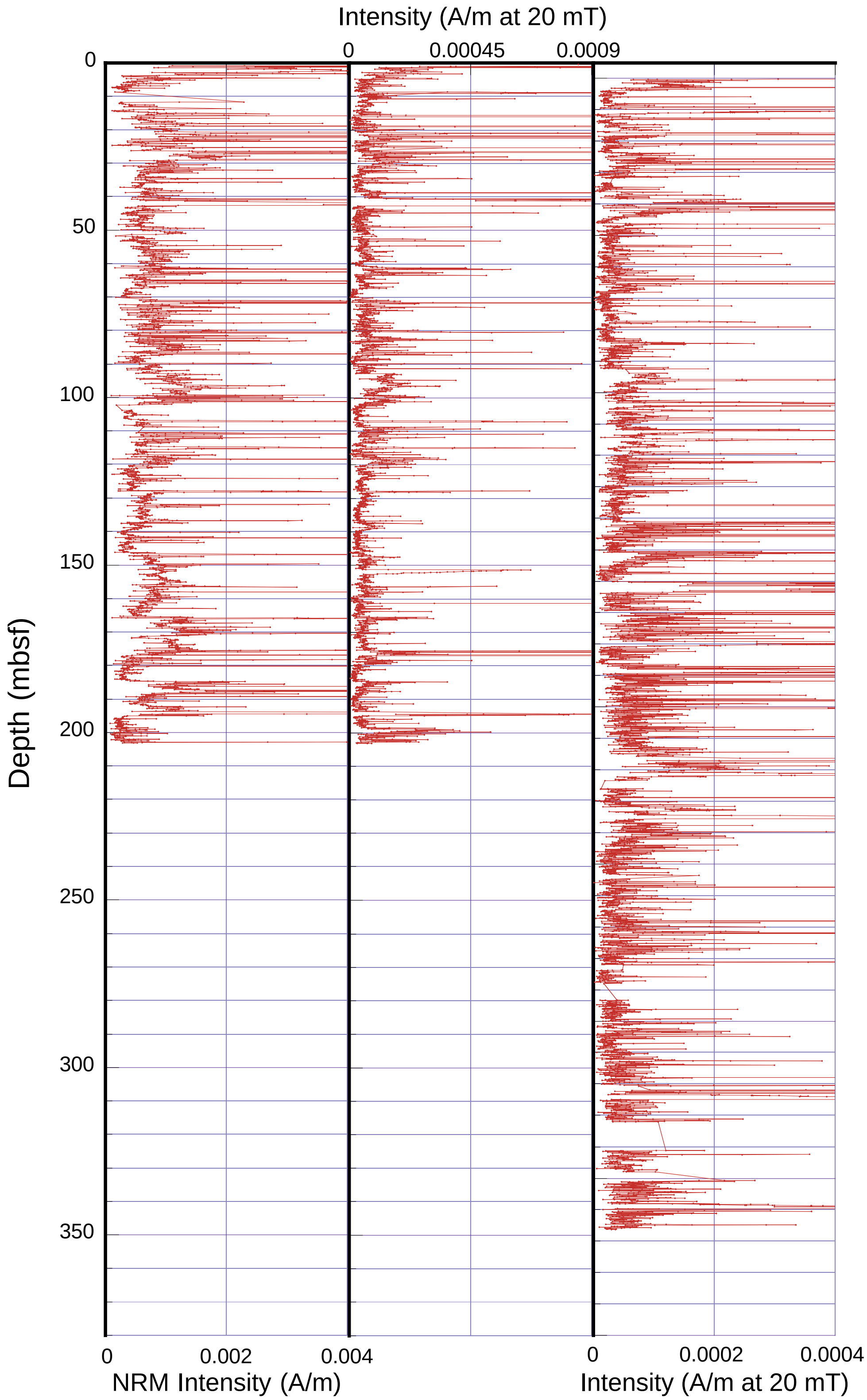

Figure F11. Inclinations of remanence in Holes 1125A and 1125B. NRM inclination in Hole 1125A is steep and downcore in direction, indicating that a strong drilling-induced component dominates the NRM. After 20-mT AF demagnetization, inclination is more variable, which indicates cleaning of the drilling-induced overprint despite weak intensities.

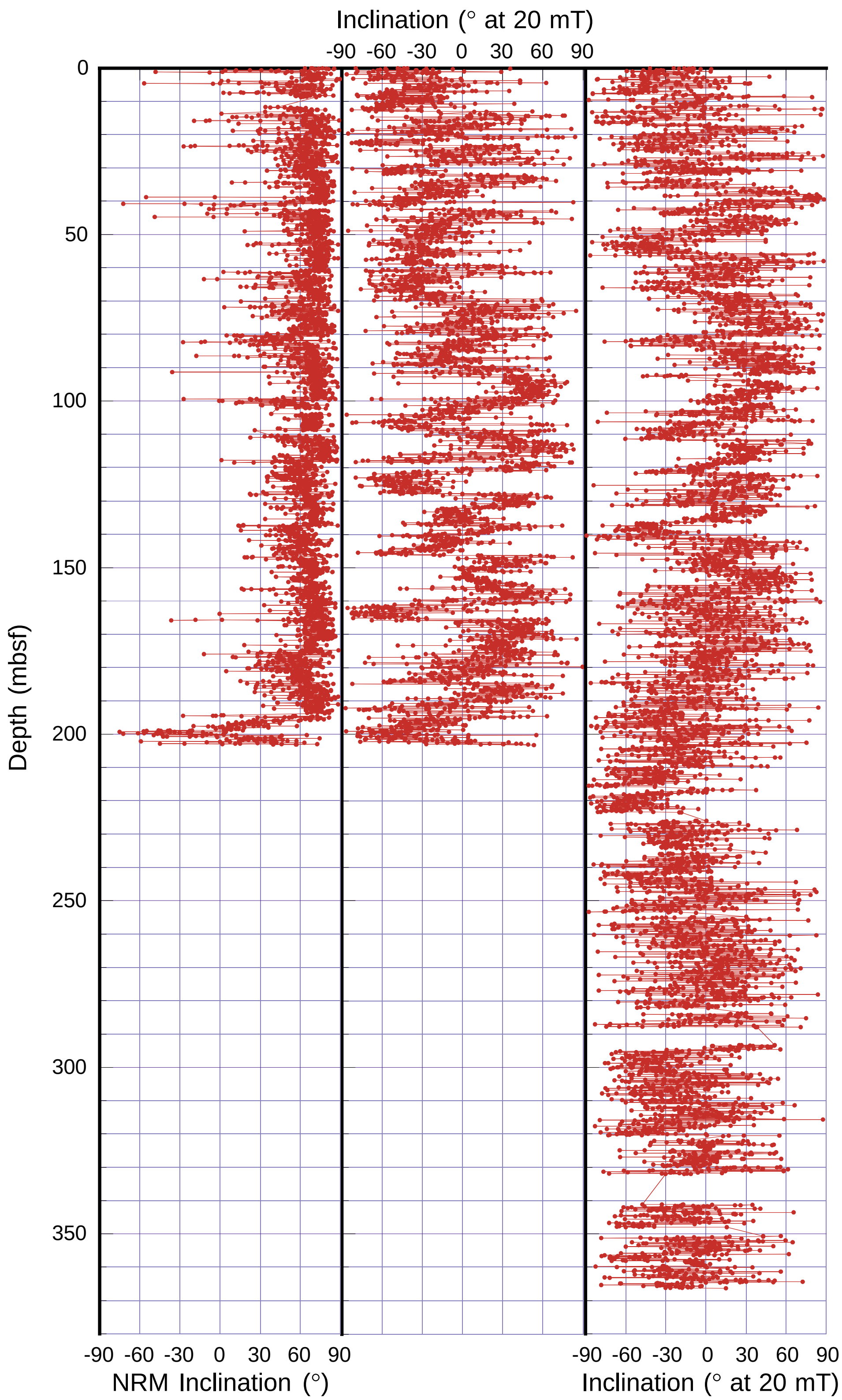

Figure F12. Preliminary interpretation of magnetic polarity for Hole 1125B.

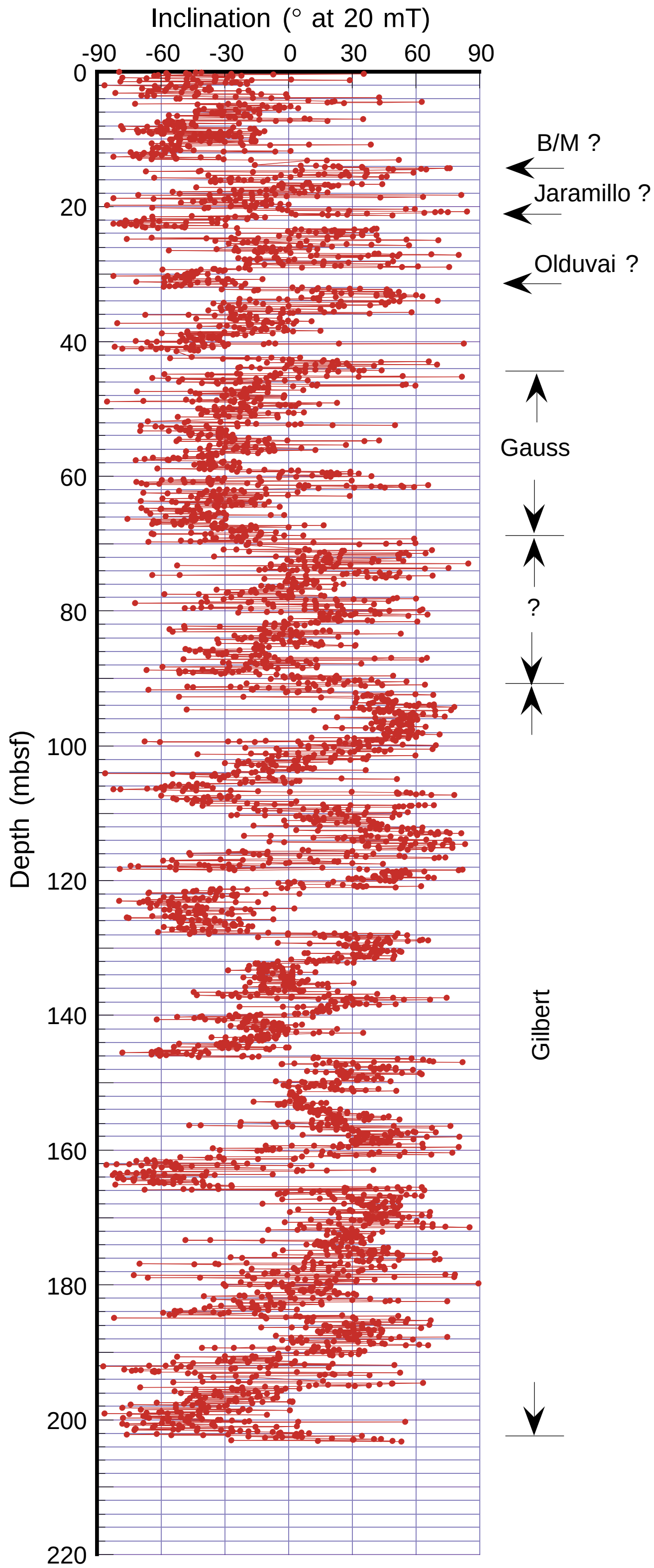

Figure F13. Composite sections for MS and reflectance percentage at 550 nm. For convenience, MS values from Hole 1125B are offset by 3×10^{-5} relative to data from Hole 1125A. Similarly, reflectance values from Hole 1125B are offset by 10%. Cores are indicated by small numbers. (Continued on next three pages.)

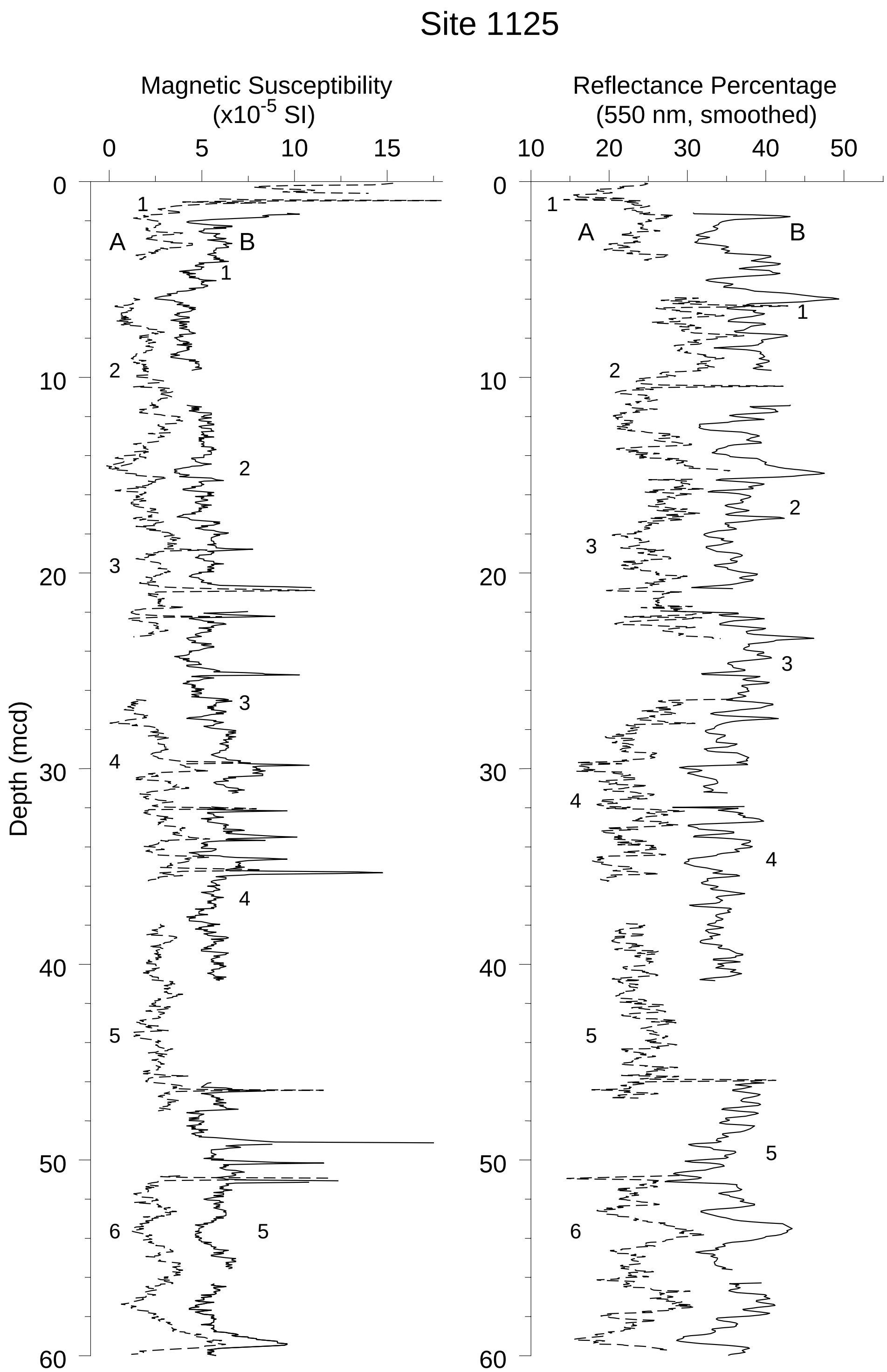

Figure F13 (continued).

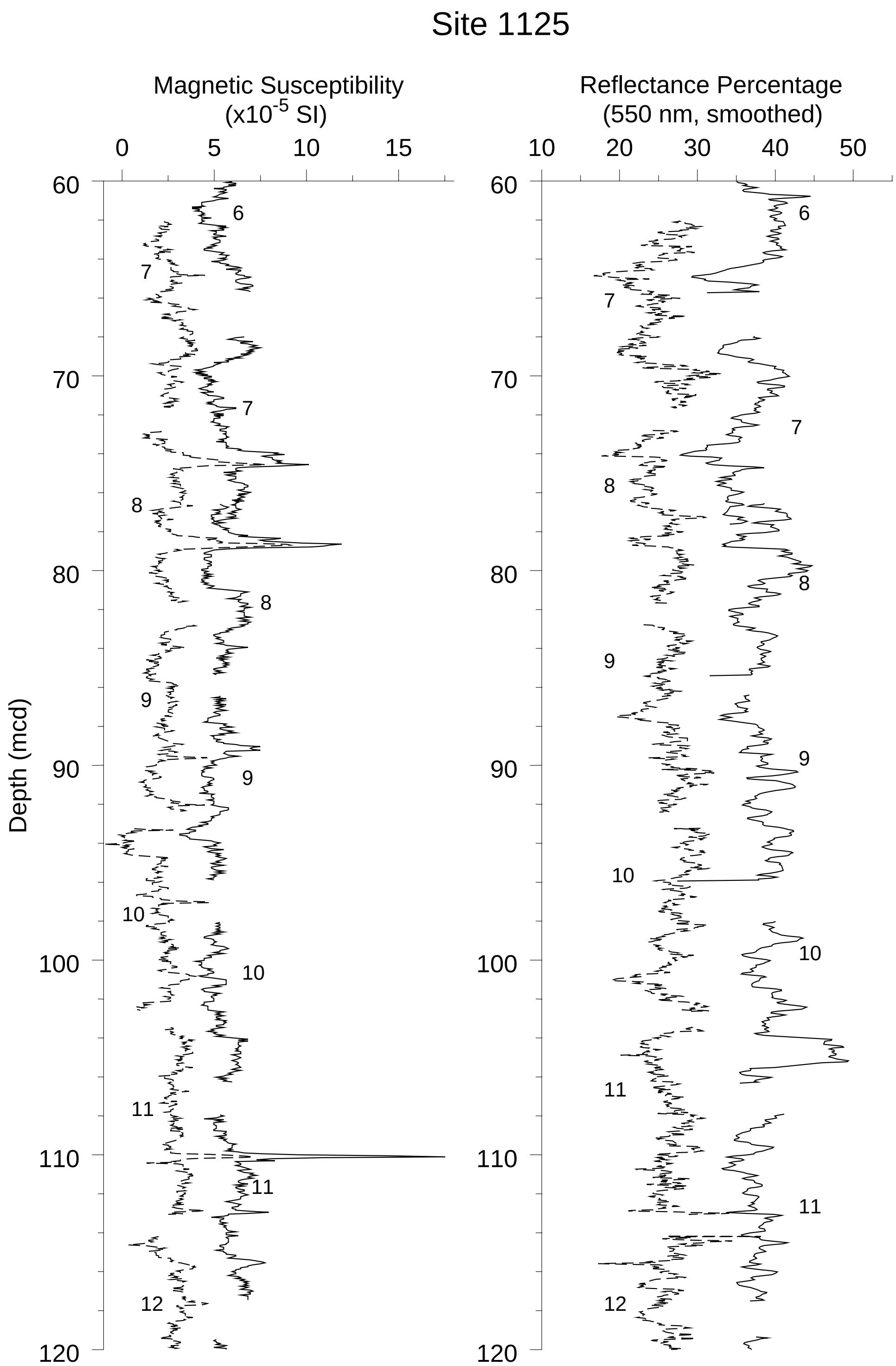

Figure F13 (continued).

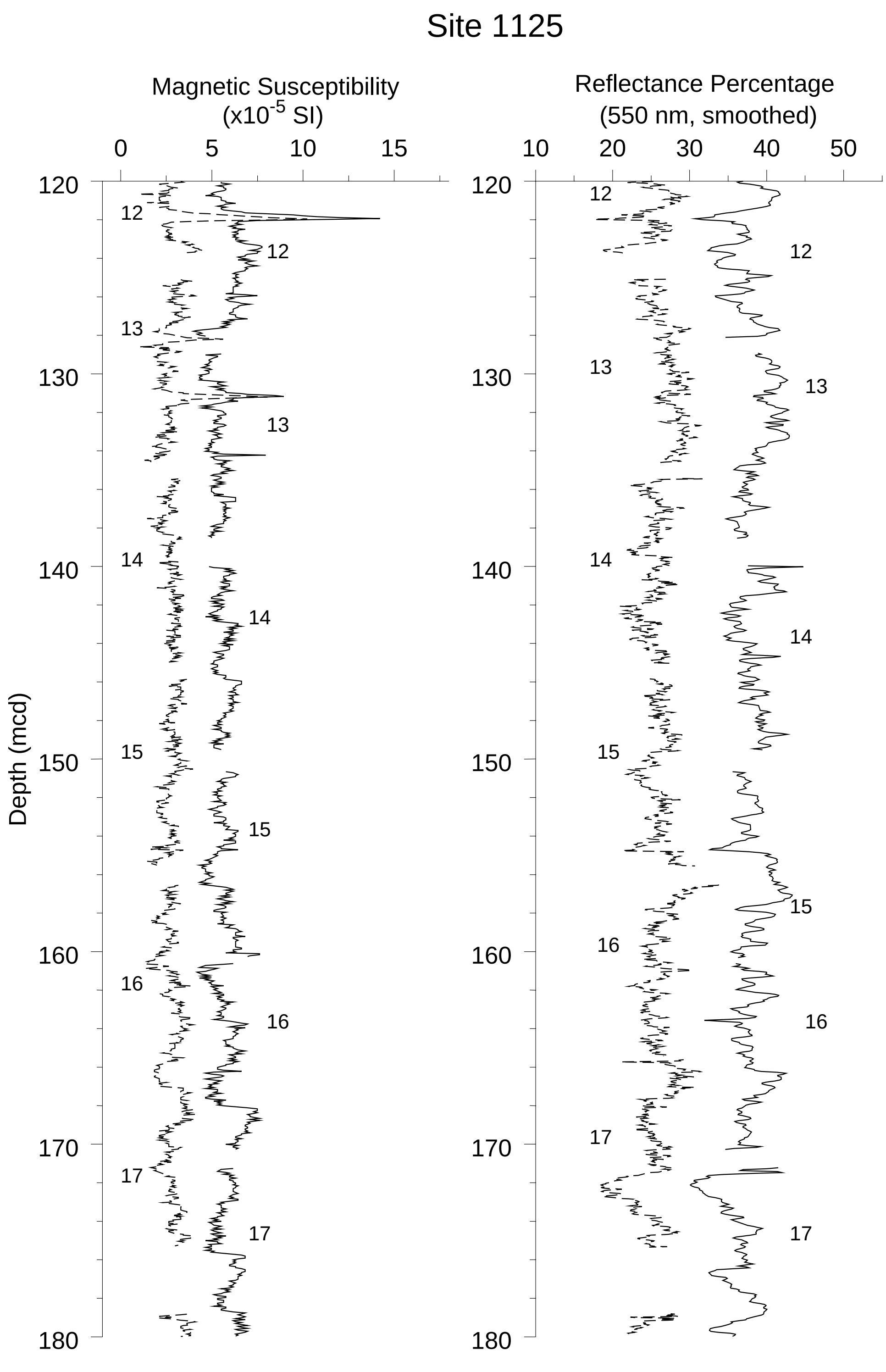

Figure F13 (continued).

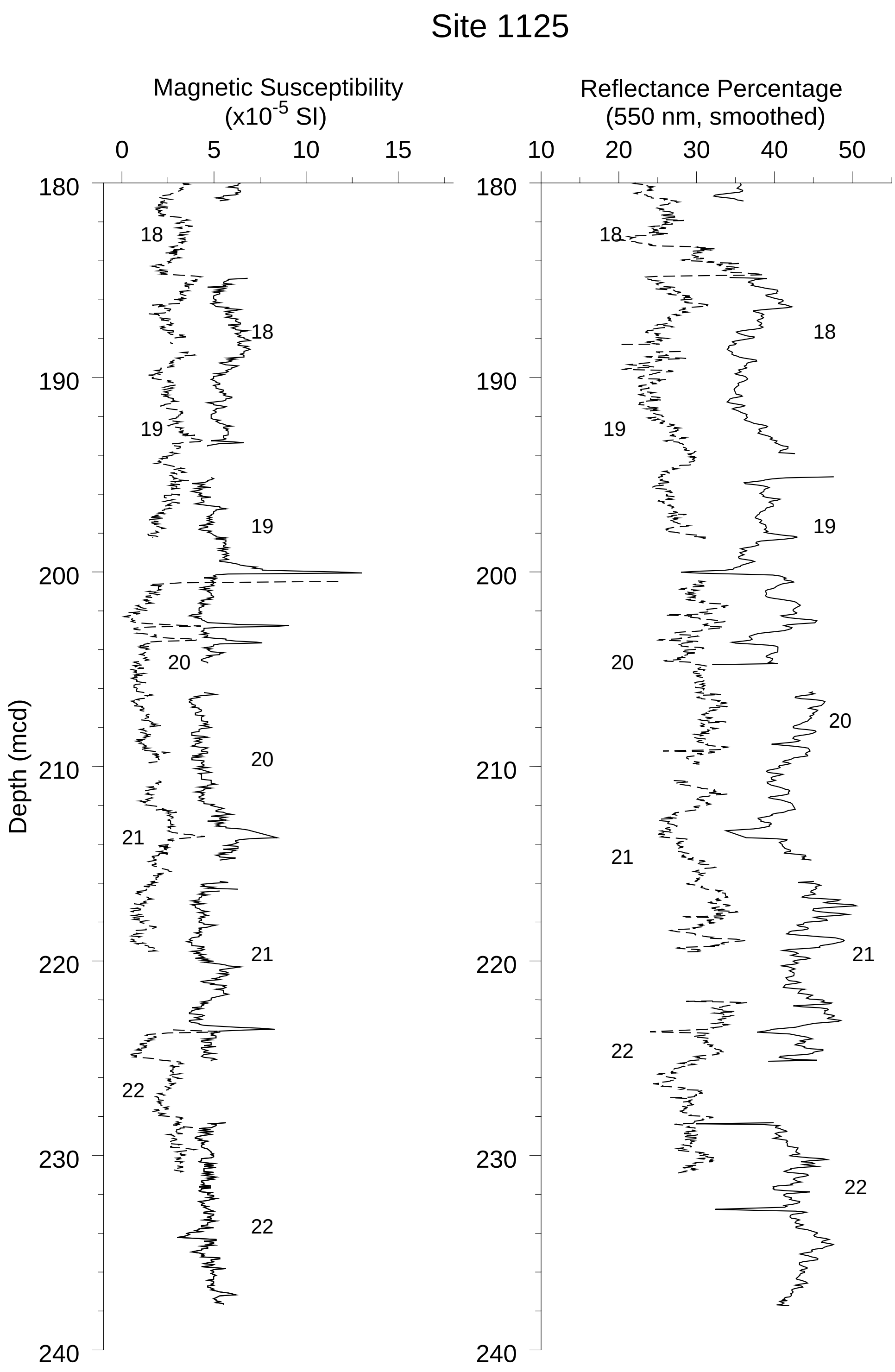

Figure F14. Downhole depth offsets between the mbsf and mcd scales for Site 1125. The offsets follow the solid line, indicating the trend for a model of 15% stretch between mbsf and mcd depths.

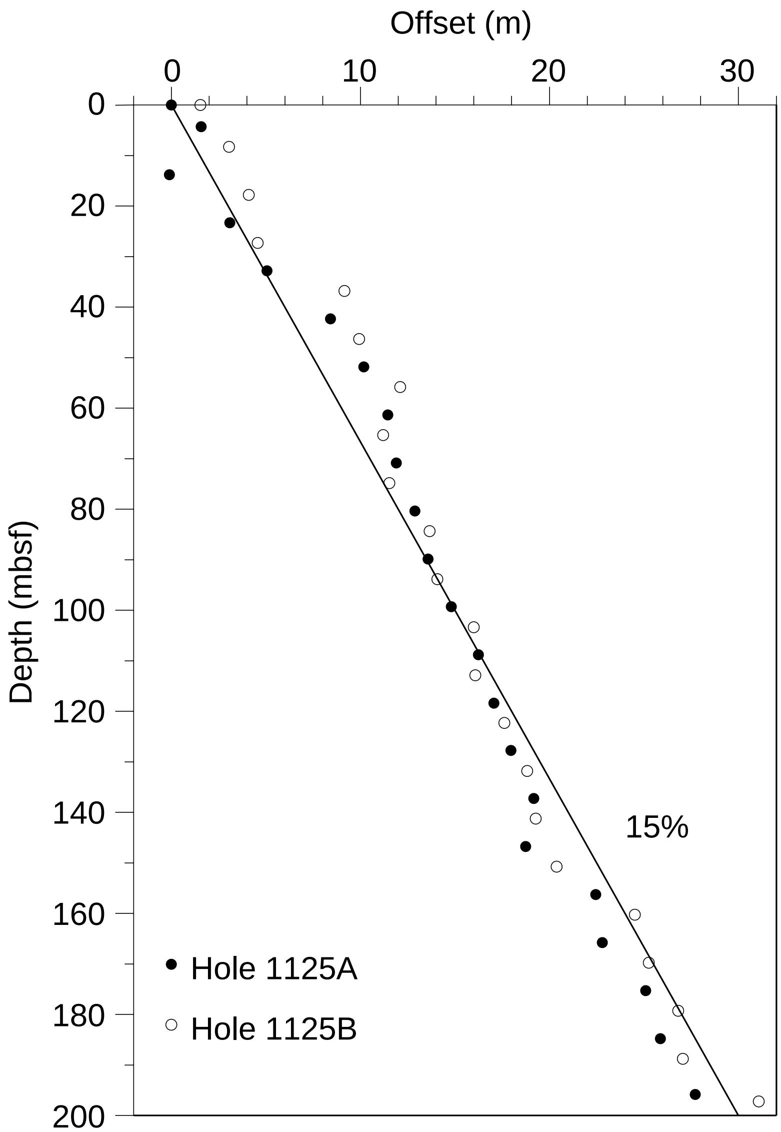

Figure F15. Spliced record for Site 1125. To reduce noise, all data illustrated were smoothed with a 5-point Gaussian window. A1 = Core 181-1125A-1H, B2 = Core 181-1125B-2H, and so on.

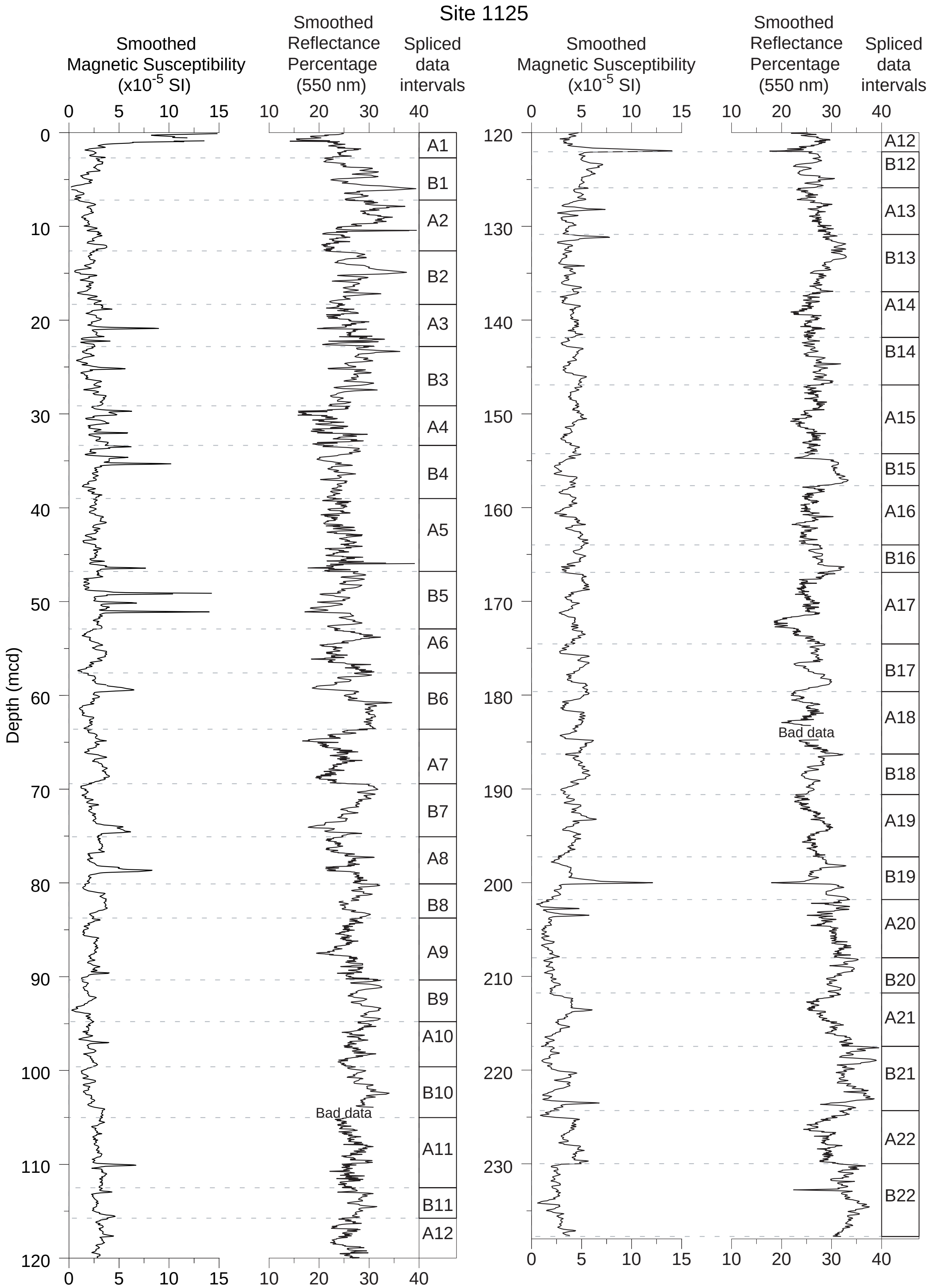

Figure F16. Age-depth plot, using the diatom, radiolarian, foraminifer, and nannofossil age assignments for Site 1125, as shown in Table T9, p. 91.

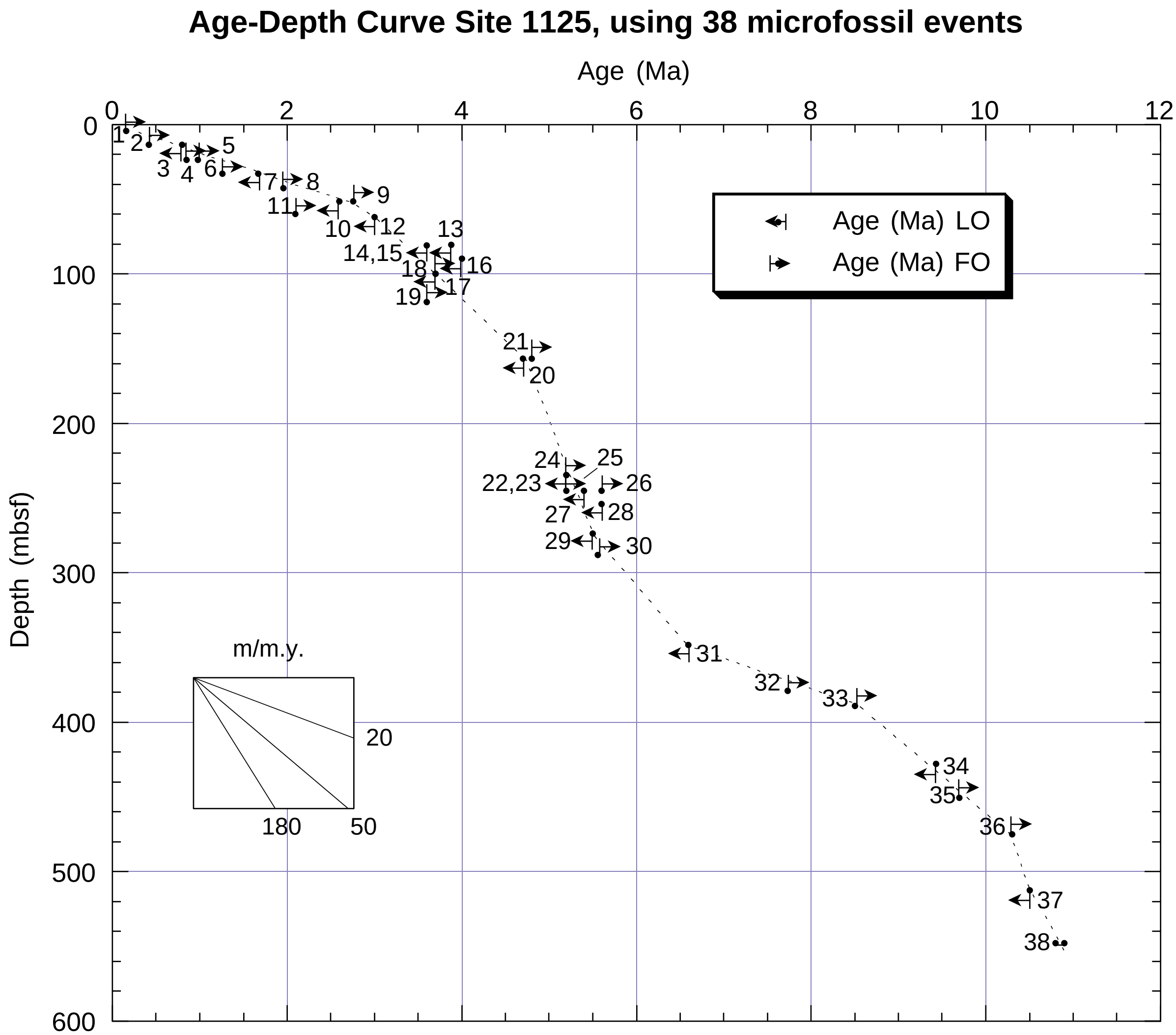

Figure F17. Depth profiles of interstitial-water constituents and methane at Site 1125.

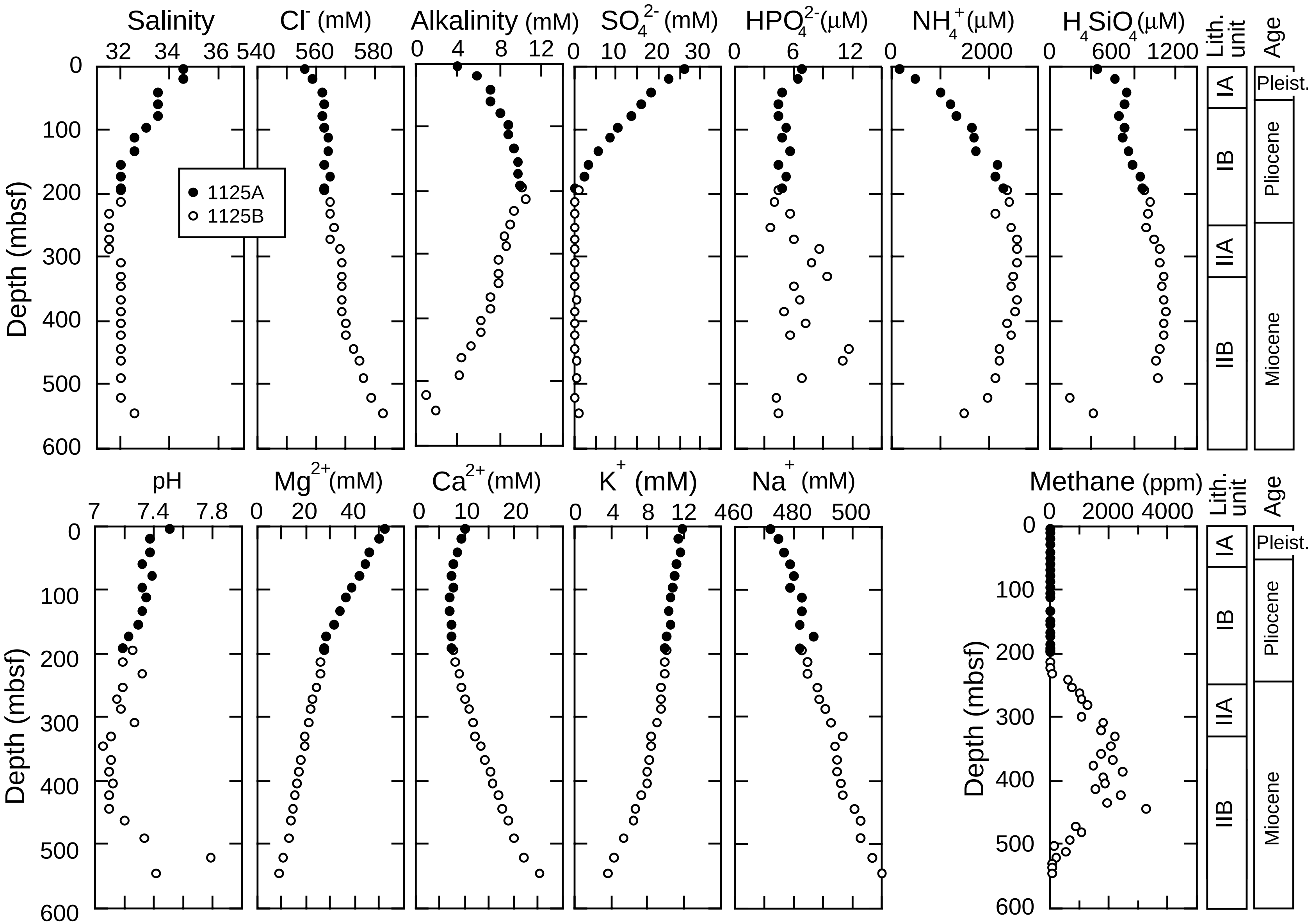

Figure F18. Multisensor track measurements from Hole 1125C, including MS and GRAPE density.

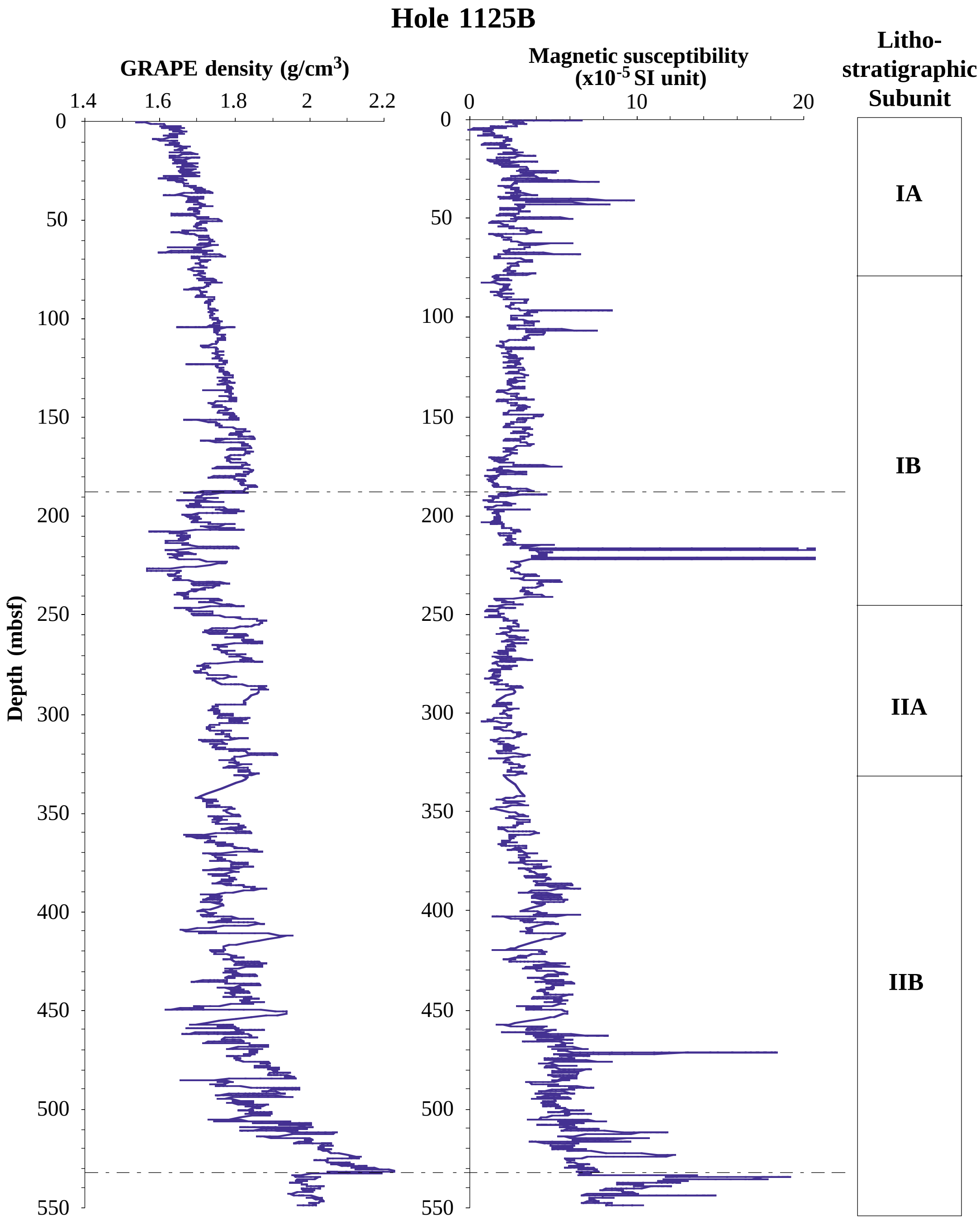

Figure F19. Plots of temperature measurement by the Adara temperature tool on Core 181-1125A-11H and thermal gradient for Hole 1125A.

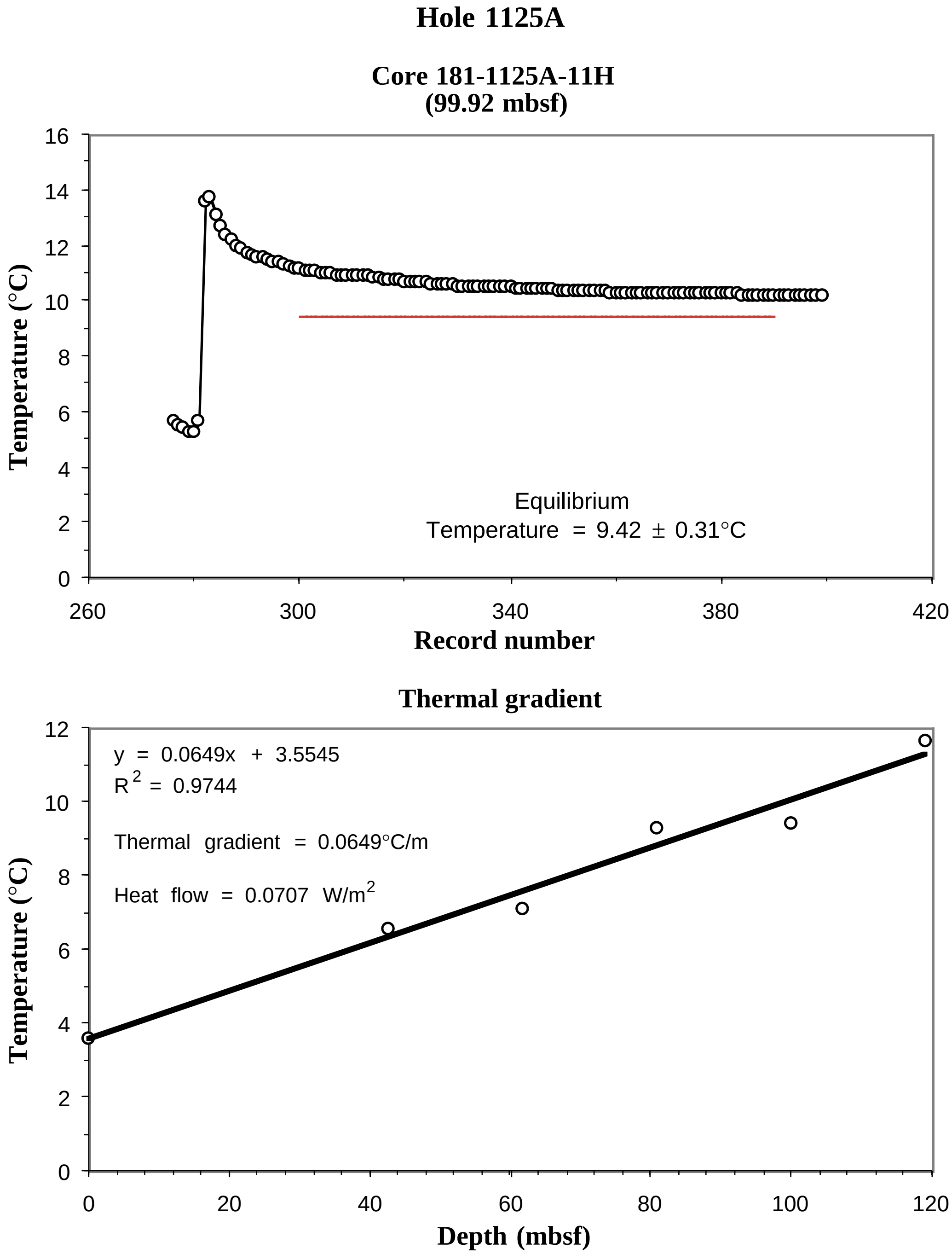

Figure F20. Logging operations in Hole 1125B.

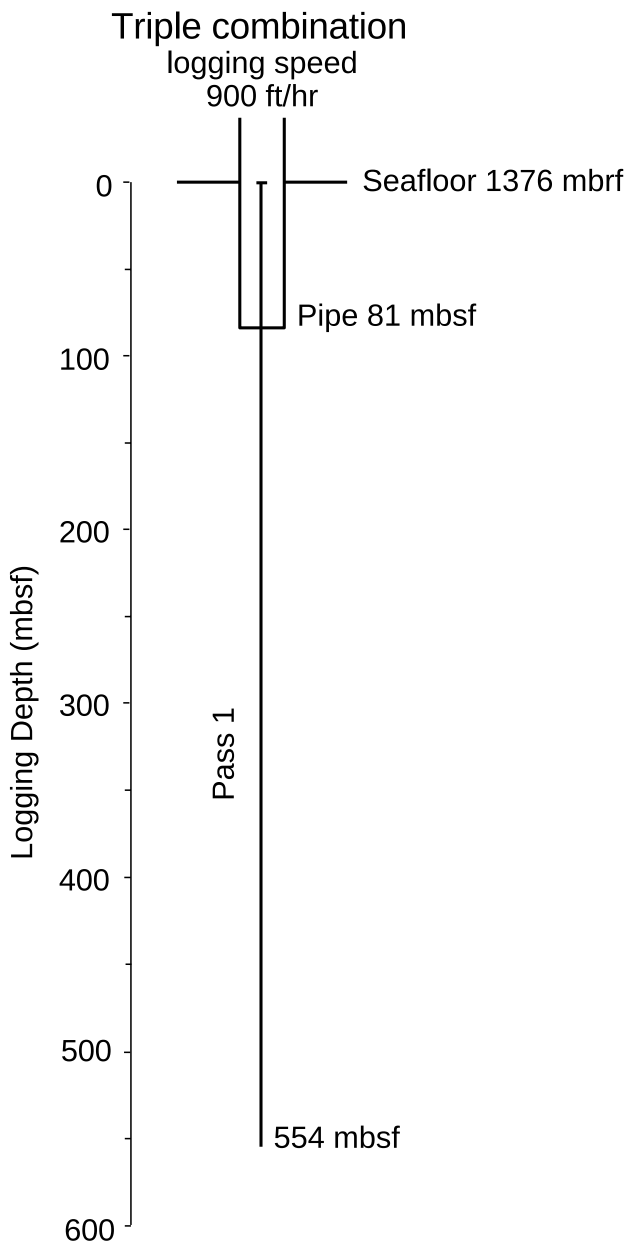

Figure F21. Log data and log units from Hole 1125B.

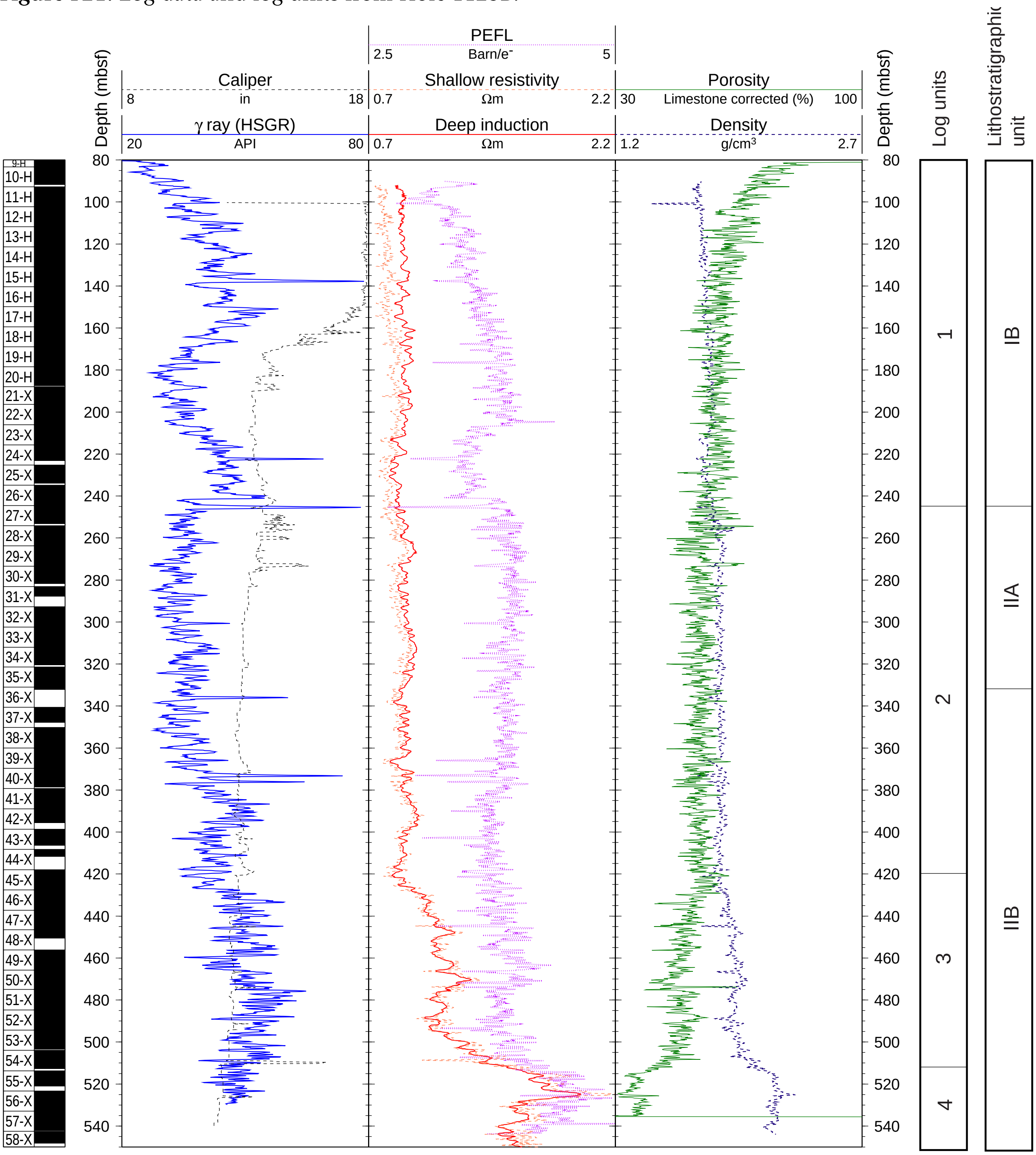

Figure F22. Comparison of the gamma-ray and caliper logs between 200 and 400 mbsf, with the position of tephra layers marked, in Hole 1125B. Note that the tephra layers are not responsible for sudden changes in hole width, yet the shift to more sandy or shaly lithologies, recorded by the gamma-ray log, is responsible for some of the hole width changes (e.g., 250–275 mbsf).

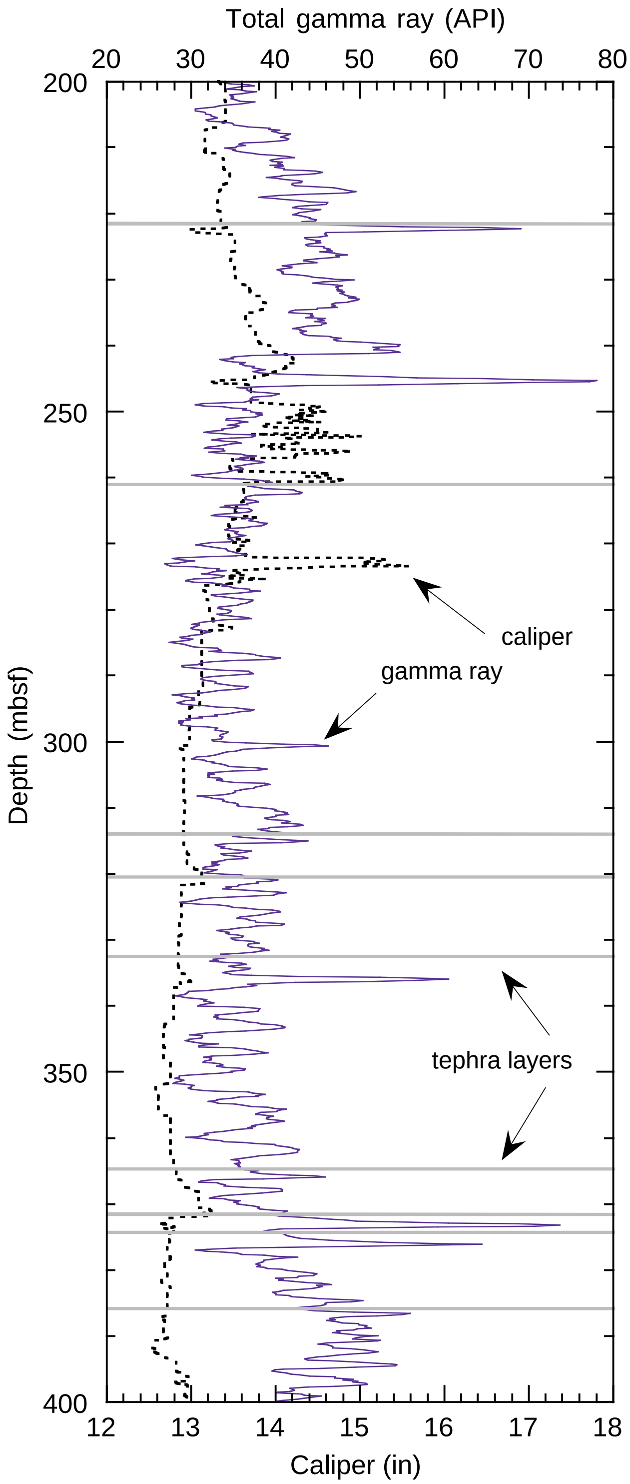

Figure F23. A. Spectral gamma-ray log (Th, K, and U) for Hole 1125B. Low-frequency cyclicity is marked on the graph. (Continued on next page.)

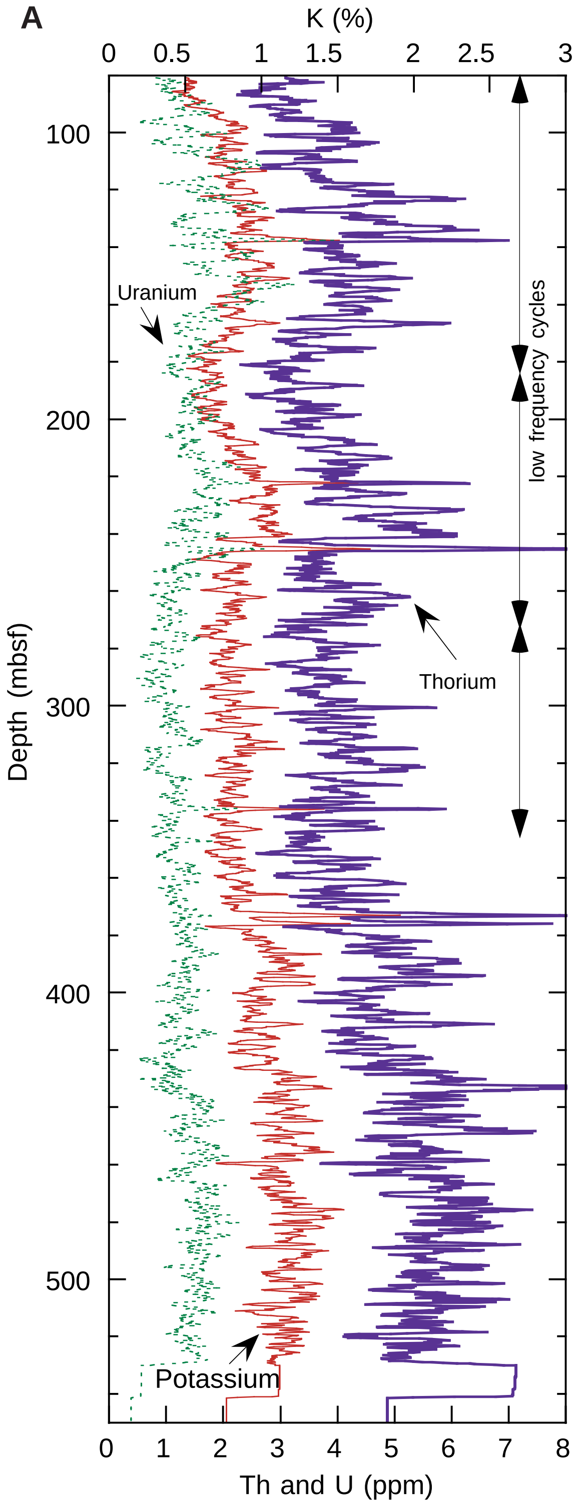

Figure F23 (continued). B. Comparison of the total natural gamma radioactivity (HSGR) with the radioactivity derived just from thorium and potassium (HCGR). Note that the nature of the gamma signal is dominated by thorium and potassium radioactivity, which are predominantly found in clay minerals.

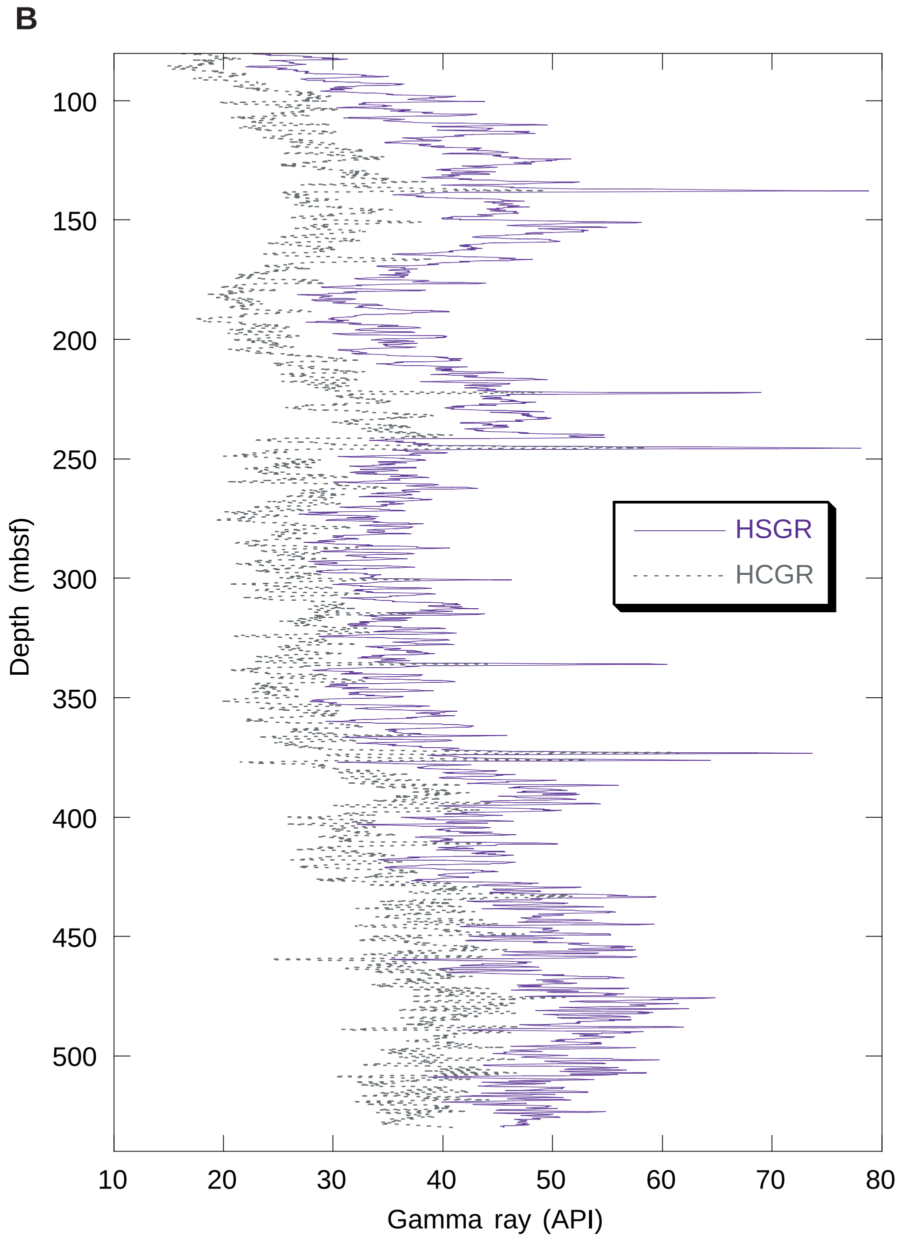

Figure F24. Crossplot of density porosity and neutron porosity. Note the slope of the regression line is close to 1. Reasons for the slight deviation from a slope of 1 are discussed in **"Data Quality/Preliminary Interpretation,"** p. 23.

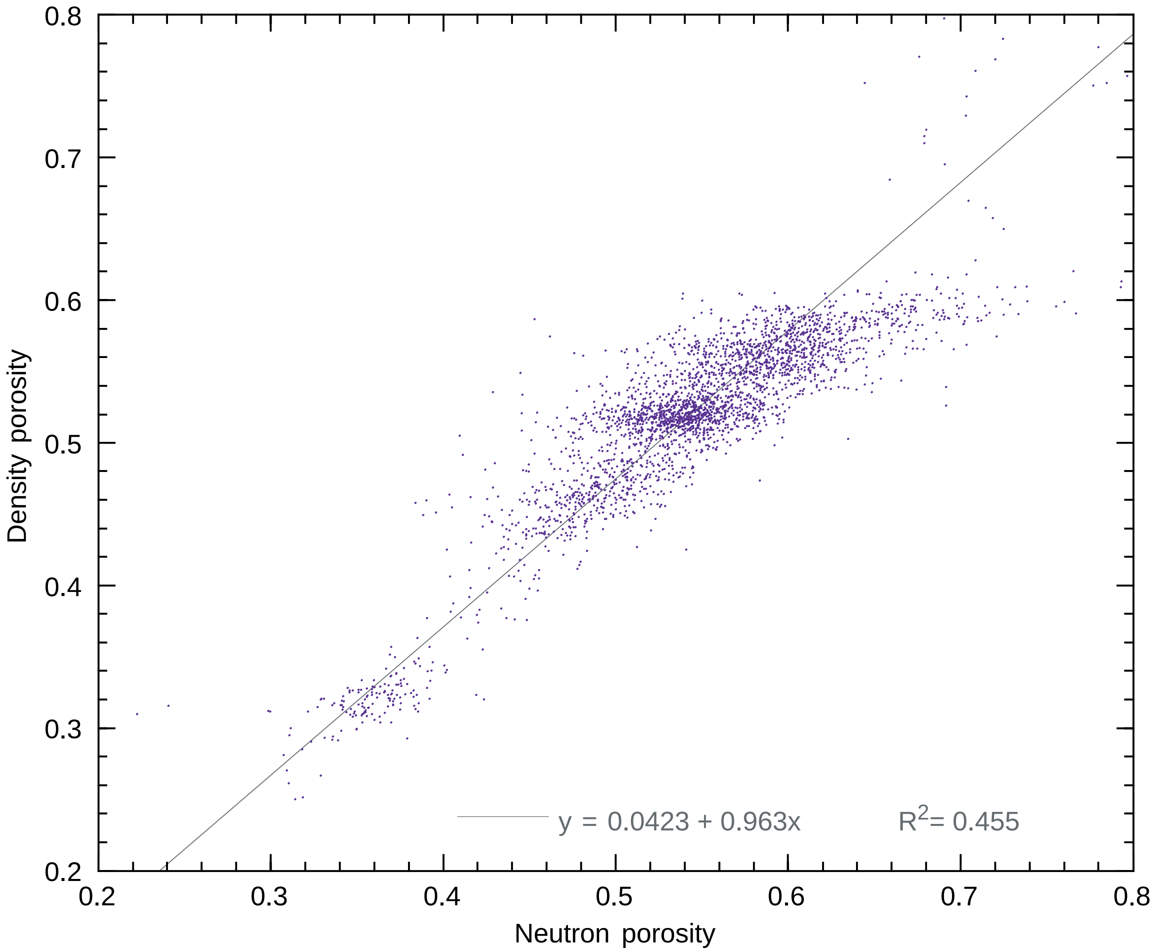

Figure F25. Downhole variations in borehole temperature. Tfast and Tslow refer to fast and slow response thermistors on the tool.

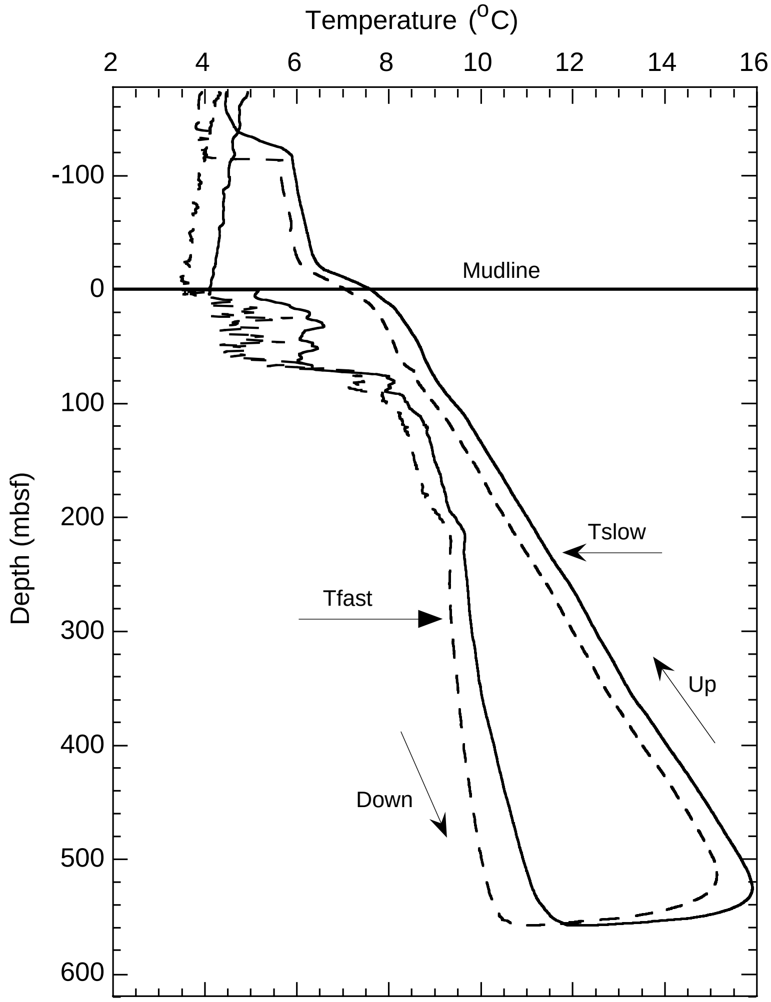

Figure F26. Cyclical fluctuations in the natural gamma results in log Unit 1. The plot on the right shows the results after they have been band-pass filtered to capture the low (~100 m) and high (~10 m) frequency cyclicities.

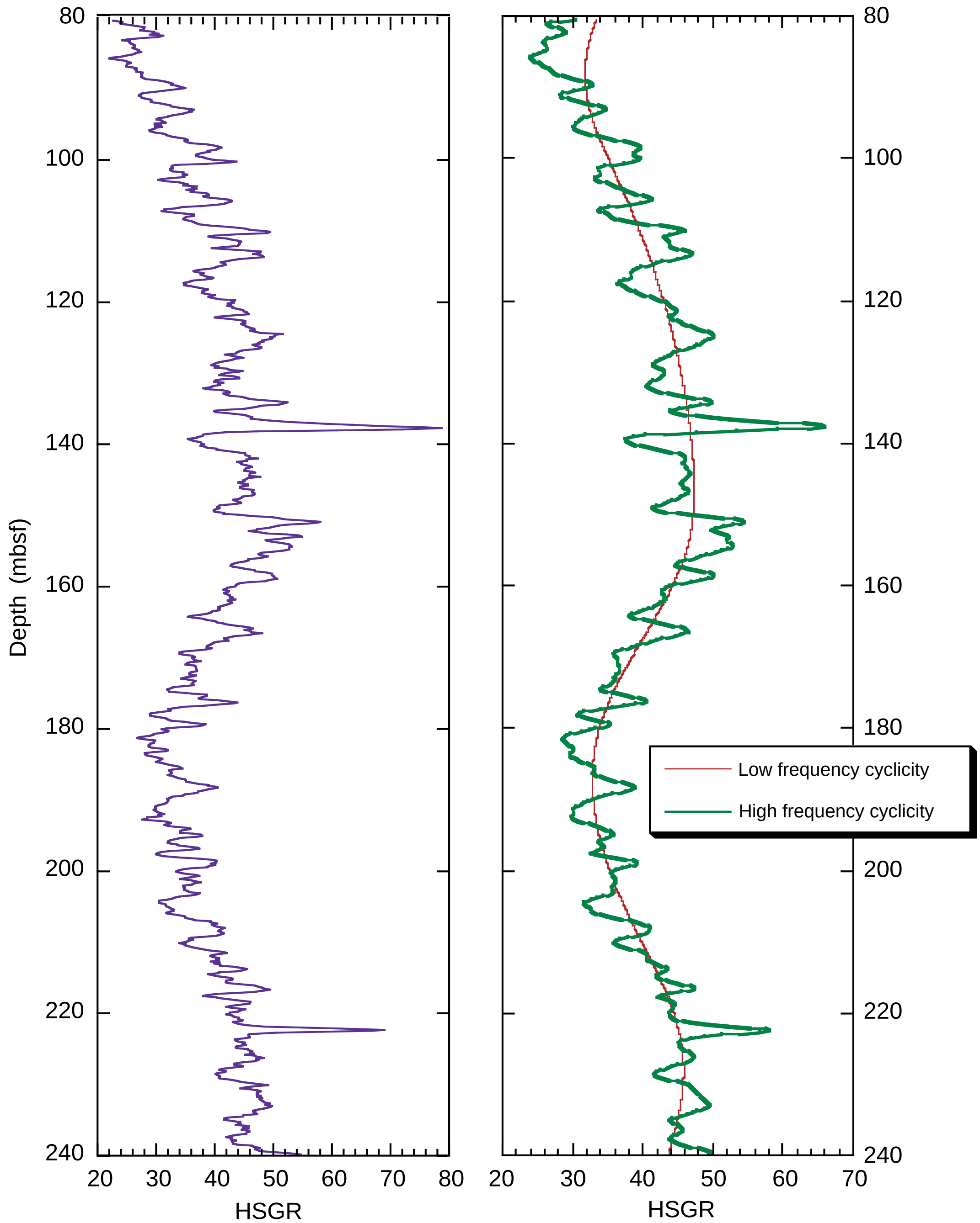

Figure F27. Comparison of recorded tephra horizons and selective log responses in the intervals 200–250 and 350–400 mbsf. The minor offset of the two may be because of depth discrepancies between core and log depths. Note the fact that the logs fail to record the tephra horizon at ~386 mbsf but indicate an additional tephra at ~245 mbsf.

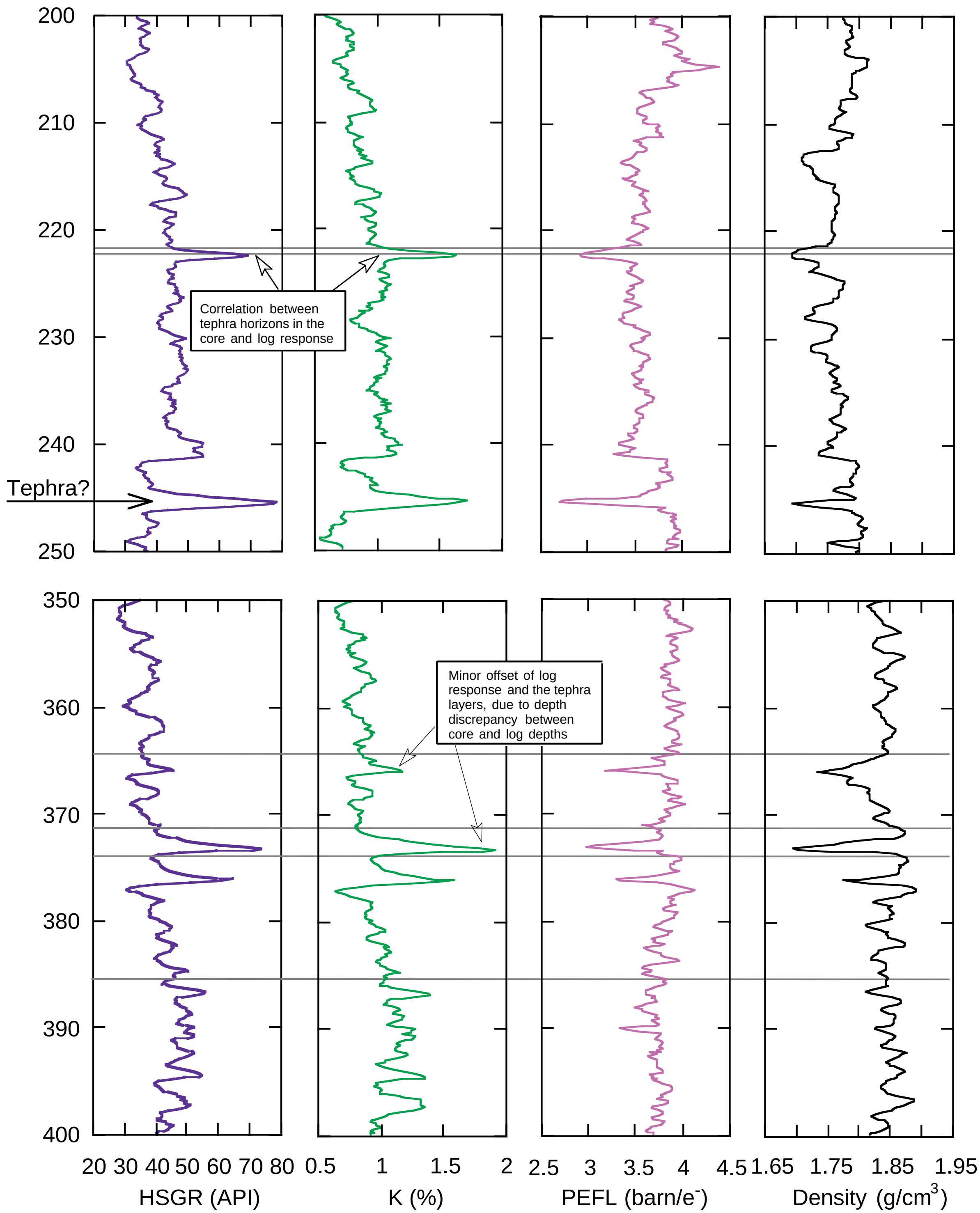

Table T1. Site 1125 expanded coring summary. (**See table note**. Continued on next 15 pages.)

Core	Date (October 1998)	Time (UTC)	Core depth (mbsf) Top	Core depth (mbsf) Bottom	Length (m) Cored	Length (m) Recovered	Recovery (%)	Section	Length (m) Liner	Length (m) Curated	Section depth (mbsf) Top	Section depth (mbsf) Bottom	Catwalk samples	Comment
181-1125A-														
1H	2	1605	0.0	4.3	4.3	4.31	100.2							
								1	1.5	1.5	0.0	1.5		
								2	1.5	1.5	1.5	3.0	IW	
								3	1.06	1.06	3.0	4.1	HS	
								CC	0.25	0.25	4.06	4.31	PAL	
									4.31	4.31				
2H	2	1645	4.3	13.8	9.5	9.17	96.5							
								1	1.5	1.5	4.3	5.8		
								2	1.5	1.5	5.8	7.3		
								3	1.5	1.5	7.3	8.8		
								4	1.5	1.5	8.8	10.3		
								5	1.5	1.5	10.3	11.8	HS	
								6	1.45	1.45	11.8	13.25		
								CC	0.22	0.22	13.25	13.47	PAL	
									9.17	9.17				
3H	2	1715	13.8	23.3	9.5	9.9	104.2							
								1	1.5	1.5	13.8	15.3		
								2	1.5	1.5	15.3	16.8		
								3	1.5	1.5	16.8	18.3		
								4	1.5	1.5	18.3	19.8	IW	
								5	1.5	1.5	19.8	21.3	HS	
								6	1.5	1.5	21.3	22.8		
								7	0.68	0.68	22.8	23.48		
								CC	0.22	0.22	23.48	23.7	PAL	
									9.90	9.90				
4H	2	1750	23.3	32.8	9.5	9.63	101.4							
								1	1.5	1.5	23.3	24.8		
								2	1.5	1.5	24.8	26.3		
								3	1.5	1.5	26.3	27.8		
								4	1.5	1.5	27.8	29.3		
								5	1.5	1.5	29.3	30.8	HS	
								6	1.5	1.5	30.8	32.3		
								7	0.4	0.4	32.3	32.7		
								CC	0.23	0.23	32.7	32.93	PAL	
									9.63	9.63				
5H	2	1840	32.8	42.3	9.5	9.88	104							
								1	1.5	1.5	32.8	34.3		
								2	1.5	1.5	34.3	35.8		
								3	1.5	1.5	35.8	37.3		
								4	1.5	1.5	37.3	38.8	IW	
								5	1.5	1.5	38.8	40.3	HS	
								6	1.5	1.5	40.3	41.8		
								7	0.67	0.67	41.8	42.47		
								CC	0.21	0.21	42.47	42.68	PAL	
									9.88	9.88				
6H	2	1915	42.3	51.8	9.5	9.42	99.2							
								1	1.5	1.5	42.3	43.8		

Table T1 (continued).

Core	Date (October 1998)	Time (UTC)	Core depth (mbsf)		Length (m)		Recovery (%)	Section	Length (m)		Section depth (mbsf)		Catwalk samples	Comment
			Top	Bottom	Cored	Recovered			Liner	Curated	Top	Bottom		
								2	1.5	1.5	43.8	45.3		
								3	1.5	1.5	45.3	46.8		
								4	1.5	1.5	46.8	48.3		
								5	1.5	1.5	48.3	49.8	HS	
								6	1.5	1.5	49.8	51.3		
								7	0.27	0.27	51.3	51.57		
								CC	0.15	0.15	51.57	51.72	PAL	
									9.42	9.42				
7H	2	2005	51.8	61.3	9.5	10.07	106							
								1	1.5	1.5	51.8	53.3		
								2	1.5	1.5	53.3	54.8		
								3	1.5	1.5	54.8	56.3		
								4	1.5	1.5	56.3	57.8	IW	
								5	1.5	1.5	57.8	59.3	HS	
								6	1.5	1.5	59.3	60.8		
								7	0.69	0.69	60.8	61.49		
								CC	0.38	0.38	61.49	61.87	PAL	
									10.07	10.07				
8H	2	2040	61.3	70.8	9.5	9.18	96.6							
								1	1.5	1.5	61.3	62.8		
								2	1.5	1.5	62.8	64.3		
								3	1.5	1.5	64.3	65.8		
								4	1.5	1.5	65.8	67.3		
								5	1.5	1.5	67.3	68.8	HS	
								6	1.45	1.45	68.8	70.25		
								CC	0.23	0.23	70.25	70.48	PAL	
									9.18	9.18				
9H	2	2130	70.8	80.3	9.5	10.06	105.9							
								1	1.5	1.5	70.8	72.3		
								2	1.5	1.5	72.3	73.8		
								3	1.5	1.5	73.8	75.3		
								4	1.5	1.5	75.3	76.8	IW	
								5	1.5	1.5	76.8	78.3	HS	
								6	1.5	1.5	78.3	79.8		
								7	0.7	0.7	79.8	80.5		
								CC	0.36	0.36	80.5	80.86	PAL	
									10.06	10.06				
10H	2	2215	80.3	89.8	9.5	9.71	102.2							
								1	1.5	1.5	80.3	81.8		
								2	1.5	1.5	81.8	83.3		
								3	1.5	1.5	83.3	84.8		
								4	1.5	1.5	84.8	86.3		
								5	1.5	1.5	86.3	87.8	HS	
								6	1.5	1.5	87.8	89.3		
								7	0.46	0.46	89.3	89.76		
								CC	0.25	0.25	89.76	90.01	PAL	
									9.71	9.71				

Table T1 (continued).

Core	Date (October 1998)	Time (UTC)	Core depth (mbsf) Top	Core depth (mbsf) Bottom	Length (m) Cored	Length (m) Recovered	Recovery (%)	Section	Length (m) Liner	Length (m) Curated	Section depth (mbsf) Top	Section depth (mbsf) Bottom	Catwalk samples	Comment
11H	2	2255	89.8	99.3	9.5	10.12	106.5							
								1	1.5	1.5	89.8	91.3		
								2	1.5	1.5	91.3	92.8		
								3	1.5	1.5	92.8	94.3		
								4	1.5	1.5	94.3	95.8	IW	
								5	1.5	1.5	95.8	97.3	HS	
								6	1.5	1.5	97.3	98.8		
								7	0.72	0.72	98.8	99.52		
								CC	0.4	0.4	99.52	99.92	PAL	
									10.12	10.12				
12H	2	2330	99.3	108.8	9.5	9.88	104							
								1	1.5	1.5	99.3	100.8		
								2	1.5	1.5	100.8	102.3		
								3	1.5	1.5	102.3	103.8		
								4	1.5	1.5	103.8	105.3		
								5	1.5	1.5	105.3	106.8	HS	
								6	1.5	1.5	106.8	108.3		
								7	0.64	0.64	108.3	108.94		
								CC	0.24	0.24	108.94	109.18	PAL	
									9.88	9.88				
13H	3	0015	108.8	118.3	9.5	10.09	106.2							
								1	1.5	1.5	108.8	110.3		
								2	1.55	1.55	110.3	111.85	IW	
								3	1.5	1.5	111.85	113.35	HS	
								4	1.5	1.5	113.35	114.85		
								5	1.5	1.5	114.85	116.35		
								6	1.5	1.5	116.35	117.85		
								7	0.64	0.64	117.85	118.49		
								CC	0.4	0.4	118.49	118.89	PAL	
									10.09	10.09				
14H	3	0050	118.3	127.8	9.5	9.91	104.3							
								1	1.5	1.5	118.3	119.8		
								2	1.5	1.5	119.8	121.3		
								3	1.5	1.5	121.3	122.8		
								4	1.5	1.5	122.8	124.3		
								5	1.5	1.5	124.3	125.8		
								6	1.5	1.5	125.8	127.3		
								7	0.66	0.66	127.3	127.96		
								CC	0.25	0.25	127.96	128.21	PAL	
									9.91	9.91				
15H	3	0135	127.8	137.3	9.5	10	105.3							
								1	1.5	1.5	127.8	129.3		
								2	1.5	1.5	129.3	130.8		
								3	1.5	1.5	130.8	132.3		
								4	1.55	1.55	132.3	133.85	IW	
								5	1.5	1.5	133.85	135.35	HS	

Table T1 (continued).

Core	Date (October 1998)	Time (UTC)	Core depth (mbsf) Top	Core depth (mbsf) Bottom	Length (m) Cored	Length (m) Recovered	Recovery (%)	Section	Length (m) Liner	Length (m) Curated	Section depth (mbsf) Top	Section depth (mbsf) Bottom	Catwalk samples	Comment
								6	1.5	1.5	135.35	136.85		
								7	0.73	0.73	136.85	137.58		
								CC	0.22	0.22	137.58	137.8	PAL	
									10.00	10.00				
16H	3	0215	137.3	146.8	9.5	9.45	99.5							
								1	1.47	1.47	137.3	138.77		
								2	1.5	1.5	138.77	140.27		
								3	1.5	1.5	140.27	141.77		
								4	1.5	1.5	141.77	143.27		
								5	1.5	1.5	143.27	144.77		
								6	1.5	1.5	144.77	146.27		
								7	0.28	0.28	146.27	146.55	HS	
								CC	0.2	0.2	146.55	146.75	PAL	
									9.45	9.45				
17H	3	0255	146.8	156.3	9.5	9.99	105.2							
								1	1.5	1.5	146.8	148.3		
								2	1.5	1.5	148.3	149.8		
								3	1.5	1.5	149.8	151.3		
								4	1.55	1.55	151.3	152.85	IW	
								5	1.5	1.5	152.85	154.35	HS	
								6	1.5	1.5	154.35	155.85		
								7	0.74	0.74	155.85	156.59		
								CC	0.2	0.2	156.59	156.79	PAL	
									9.99	9.99				
18H	3	0335	156.3	165.8	9.5	9.82	103.4							
								1	1.5	1.5	156.3	157.8		
								2	1.5	1.5	157.8	159.3		
								3	1.5	1.5	159.3	160.8		
								4	1.5	1.5	160.8	162.3		
								5	1.5	1.5	162.3	163.8		
								6	1.5	1.5	163.8	165.3		
								7	0.58	0.58	165.3	165.88	HS	
								CC	0.24	0.24	165.88	166.12	PAL	
									9.82	9.82				
19H	3	0420	165.8	175.3	9.5	9.92	104.4							
								1	1.5	1.5	165.8	167.3		
								2	1.5	1.5	167.3	168.8		
								3	1.5	1.5	168.8	170.3		
								4	1.53	1.53	170.3	171.83	IW	
								5	1.5	1.5	171.83	173.33	HS	
								6	1.5	1.5	173.33	174.83		
								7	0.67	0.67	174.83	175.5		
								CC	0.22	0.22	175.5	175.72	PAL	
									9.92	9.92				
20H	3	0450	175.3	184.8	9.5	9.72	102.3							
								1	1.3	1.3	175.3	176.6		
								2	1.5	1.5	176.6	178.1		

Table T1 (continued).

Core	Date (October 1998)	Time (UTC)	Core depth (mbsf) Top	Core depth (mbsf) Bottom	Length (m) Cored	Length (m) Recovered	Recovery (%)	Section	Length (m) Liner	Length (m) Curated	Section depth (mbsf) Top	Section depth (mbsf) Bottom	Catwalk samples	Comment
								3	1.5	1.5	178.1	179.6		
								4	1.5	1.5	179.6	181.1		
								5	1.5	1.5	181.1	182.6		
								6	1.5	1.5	182.6	184.1		
								7	0.72	0.72	184.1	184.82	HS	
								CC	0.2	0.2	184.82	185.02	PAL	
									9.72	9.72				
21H	3	0530	184.8	194.3	9.5	9.62	101.3							
								1	1.5	1.5	184.8	186.3		
								2	1.5	1.5	186.3	187.8		
								3	1.5	1.5	187.8	189.3		
								4	1.5	1.5	189.3	190.8	IW	
								5	1.5	1.5	190.8	192.3	HS	
								6	1.4	1.4	192.3	193.7		
								7	0.53	0.53	193.7	194.23		
								CC	0.19	0.19	194.23	194.42	PAL	
									9.62	9.62				
22H	3	0620	194.3	203.5	9.2	9.22	100.2							
								1	1.5	1.5	194.3	195.8		Crushed liner
								2	1.5	1.5	195.8	197.3	HS	Split liner
								3	1.5	1.5	197.3	198.8		Split liner
								4	1.5	1.5	198.8	200.3		Split liner
								5	1.5	1.5	200.3	201.8		Split liner
								6	1.41	1.41	201.8	203.21		Split liner
								CC	0.31	0.31	203.21	203.52	PAL	
									9.22	9.22				
				Totals:	203.5	209.07	102.70							
181-1125B-														
1H	3	0945	0.0	8.3	8.3	8.3	100.0							
								1	1.5	1.5	0.0	1.5		
								2	1.5	1.5	1.5	3.0		
								3	1.5	1.5	3.0	4.5		
								4	1.5	1.5	4.5	6.0	EDDY	
								5	1.5	1.5	6.0	7.5		
								6	0.66	0.66	7.5	8.2		
								CC	0.14	0.14	8.16	8.3	PAL	
									8.30	8.30				
2H	3	1010	8.3	17.8	9.5	9.65	101.6							
								1	1.5	1.5	8.3	9.8		
								2	1.5	1.5	9.8	11.3		
								3	1.5	1.5	11.3	12.8		
								4	1.5	1.5	12.8	14.3		
								5	1.5	1.5	14.3	15.8	EDDY	
								6	1.5	1.5	15.8	17.3		
								7	0.47	0.47	17.3	17.77		
								CC	0.18	0.18	17.77	17.95	PAL	
									9.65	9.65				

Table T1 (continued).

Core	Date (October 1998)	Time (UTC)	Core depth (mbsf) Top	Core depth (mbsf) Bottom	Length (m) Cored	Length (m) Recovered	Recovery (%)	Section	Length (m) Liner	Length (m) Curated	Section depth (mbsf) Top	Section depth (mbsf) Bottom	Catwalk samples	Comment
3H	3	1045	17.8	27.3	9.5	9.51	100.1							
								1	1.5	1.5	17.8	19.3		
								2	1.5	1.5	19.3	20.8		
								3	1.5	1.5	20.8	22.3		
								4	1.5	1.5	22.3	23.8		
								5	1.5	1.5	23.8	25.3	EDDY	
								6	1.5	1.5	25.3	26.8		
								7	0.41	0.41	26.8	27.21		
								CC	0.1	0.1	27.21	27.31	PAL	All to PAL
									9.51	9.51				
4H	3	1120	27.3	36.8	9.5	9.38	98.7							
								1	1.5	1.5	27.3	28.8		
								2	1.5	1.5	28.8	30.3		
								3	1.5	1.5	30.3	31.8		
								4	1.5	1.5	31.8	33.3		
								5	1.5	1.5	33.3	34.8	EDDY	
								6	1.5	1.5	34.8	36.3		
								7	0.17	0.17	36.3	36.47		
								CC	0.21	0.21	36.47	36.68	PAL	
									9.38	9.38				
5H	3	1155	36.8	46.3	9.5	9.86	103.8							
								1	1.5	1.5	36.8	38.3		
								2	1.5	1.5	38.3	39.8		
								3	1.5	1.5	39.8	41.3		
								4	1.5	1.5	41.3	42.8		
								5	1.5	1.5	42.8	44.3	EDDY	
								6	1.5	1.5	44.3	45.8		
								7	0.66	0.66	45.8	46.46		
								CC	0.2	0.2	46.46	46.66	PAL	
									9.86	9.86				
6H	3	1235	46.3	55.8	9.5	9.73	102.4							
								1	1.5	1.5	46.3	47.8		
								2	1.5	1.5	47.8	49.3		
								3	1.5	1.5	49.3	50.8		
								4	1.5	1.5	50.8	52.3	EDDY	
								5	1.5	1.5	52.3	53.8		
								6	1.5	1.5	53.8	55.3		
								7	0.5	0.5	55.3	55.8		
								CC	0.23	0.23	55.8	56.03	PAL	
									9.73	9.73				
7H	3	1310	55.8	65.3	9.5	9.95	104.7							
								1	1.5	1.5	55.8	57.3		
								2	1.5	1.5	57.3	58.8		
								3	1.5	1.5	58.8	60.3		
								4	1.5	1.5	60.3	61.8		
								5	1.5	1.5	61.8	63.3		
								6	1.5	1.5	63.3	64.8	EDDY	

Table T1 (continued).

Core	Date (October 1998)	Time (UTC)	Core depth (mbsf) Top	Core depth (mbsf) Bottom	Length (m) Cored	Length (m) Recovered	Recovery (%)	Section	Length (m) Liner	Length (m) Curated	Section depth (mbsf) Top	Section depth (mbsf) Bottom	Catwalk samples	Comment
								7	0.72	0.72	64.8	65.52		
								CC	0.23	0.23	65.52	65.75	PAL	
									9.95	9.95				
8H	3	1345	65.3	74.8	9.5	9.12	96							
								1	1.5	1.5	65.3	66.8		
								2	1.5	1.5	66.8	68.3	EDDY	
								3	1.5	1.5	68.3	69.8		
								4	1.5	1.5	69.8	71.3		
								5	1.5	1.5	71.3	72.8		
								6	1.41	1.41	72.8	74.21		
								CC	0.21	0.21	74.21	74.42	PAL	
									9.12	9.12				
9H	3	1430	74.8	84.3	9.5	9.85	103.7							
								1	1.5	1.5	74.8	76.3		
								2	1.5	1.5	76.3	77.8		
								3	1.5	1.5	77.8	79.3		
								4	1.5	1.5	79.3	80.8		
								5	1.5	1.5	80.8	82.3		
								6	1.5	1.5	82.3	83.8	EDDY	
								7	0.6	0.6	83.8	84.4		
								CC	0.25	0.25	84.4	84.65	PAL	
									9.85	9.85				
10H	3	1505	84.3	93.8	9.5	8.5	89.5							
								1	1.5	1.5	84.3	85.8		
								2	1.5	1.5	85.8	87.3		
								3	1.5	1.5	87.3	88.8		
								4	1.5	1.5	88.8	90.3		
								5	1.5	1.5	90.3	91.8	EDDY	
								6	0.88	0.88	91.8	92.68		
								CC	0.12	0.12	92.68	92.8	PAL	
									8.50	8.50				
11H	3	1545	93.8	103.3	9.5	9.93	104.5							
								1	1.5	1.5	93.8	95.3		
								2	1.5	1.5	95.3	96.8		
								3	1.5	1.5	96.8	98.3	EDDY	
								4	1.5	1.5	98.3	99.8		
								5	1.5	1.5	99.8	101.3		
								6	1.5	1.5	101.3	102.8		
								7	0.68	0.68	102.8	103.48		
								CC	0.25	0.25	103.48	103.73	PAL	
									9.93	9.93				
12H	3	1620	103.3	112.8	9.5	9.65	101.6							
								1	1.5	0.9	103.3	104.2		Replaced liner
								2	1.5	1.5	104.2	105.7		
								3	1.5	1.5	105.7	107.2		
								4	1.5	1.5	107.2	108.7		
								5	1.5	1.5	108.7	110.2	EDDY	
								6	1.5	1.5	110.2	111.7		

Table T1 (continued).

Core	Date (October 1998)	Time (UTC)	Core depth (mbsf) Top	Core depth (mbsf) Bottom	Length (m) Cored	Length (m) Recovered	Recovery (%)	Section	Length (m) Liner	Length (m) Curated	Section depth (mbsf) Top	Section depth (mbsf) Bottom	Catwalk samples	Comment
								7	0.4	0.4	111.7	112.1		
								CC	0.25	0.25	112.1	112.35	PAL	
									9.65	9.05				
13H	3	1655	112.8	122.3	9.5	9.9	104.2							
								1	1.5	1.5	112.8	114.3		
								2	1.5	1.5	114.3	115.8		
								3	1.5	1.5	115.8	117.3		
								4	1.5	1.5	117.3	118.8		
								5	1.5	1.5	118.8	120.3		
								6	1.5	1.5	120.3	121.8	EDDY	
								7	0.69	0.69	121.8	122.49		
								CC	0.21	0.21	122.49	122.7	PAL	
									9.90	9.90				
14H	3	1735	122.3	131.8	9.5	9.94	104.6							
								1	1.5	1.5	122.3	123.8		
								2	1.5	1.5	123.8	125.3		
								3	1.5	1.5	125.3	126.8		
								4	1.5	1.5	126.8	128.3		
								5	1.5	1.5	128.3	129.8	EDDY	
								6	1.5	1.5	129.8	131.3		
								7	0.64	0.64	131.3	131.94		
								CC	0.3	0.3	131.94	132.24	PAL	
									9.94	9.94				
15H	3	1820	131.8	141.3	9.5	9.92	104.4							
								1	1.5	1.5	131.8	133.3		
								2	1.5	1.5	133.3	134.8	EDDY	
								3	1.5	1.5	134.8	136.3		
								4	1.5	1.5	136.3	137.8		
								5	1.5	1.5	137.8	139.3		
								6	1.5	1.5	139.3	140.8		
								7	0.71	0.71	140.8	141.51		
								CC	0.21	0.21	141.51	141.72	PAL	
									9.92	9.92				
16H	3	1955	141.3	150.8	9.5	9.97	104.9							
								1	1.5	1.5	141.3	142.8		
								2	1.5	1.5	142.8	144.3		
								3	1.5	1.5	144.3	145.8		
								4	1.5	1.5	145.8	147.3		
								5	1.5	1.5	147.3	148.8		
								6	1.5	1.5	148.8	150.3	EDDY	
								7	0.73	0.73	150.3	151.03		
								CC	0.24	0.24	151.03	151.27	PAL	
									9.97	9.97				
17H	3	2040	150.8	160.3	9.5	10.06	105.9							
								1	1.5	1.5	150.8	152.3		
								2	1.5	1.5	152.3	153.8	EDDY	
								3	1.5	1.5	153.8	155.3		

Table T1 (continued).

Core	Date (October 1998)	Time (UTC)	Core depth (mbsf)		Length (m)		Recovery (%)	Section	Length (m)		Section depth (mbsf)		Catwalk samples	Comment
			Top	Bottom	Cored	Recovered			Liner	Curated	Top	Bottom		
								4	1.5	1.5	155.3	156.8		
								5	1.5	1.5	156.8	158.3		
								6	1.5	1.5	158.3	159.8		
								7	0.79	0.79	159.8	160.59		
								CC	0.27	0.27	160.59	160.86	PAL	
									10.06	10.06				
18H	3	2120	160.3	169.8	9.5	9.39	98.8							
								1	1.5	1.5	160.3	161.8		
								2	1.5	1.5	161.8	163.3		
								3	1.5	1.5	163.3	164.8		
								4	1.5	1.5	164.8	166.3	EDDY	
								5	1.5	1.5	166.3	167.8		
								6	1.3	1.3	167.8	169.1		
								7	0.31	0.31	169.1	169.41		
								CC	0.28	0.28	169.41	169.69	PAL	
									9.39	9.39				
19H	3	2205	169.8	179.3	9.5	9.98	105.1							
								1	1.5	1.5	169.8	171.3		
								2	1.5	1.5	171.3	172.8		
								3	1.5	1.5	172.8	174.3		
								4	1.5	1.5	174.3	175.8		
								5	1.5	1.5	175.8	177.3	EDDY	
								6	1.5	1.5	177.3	178.8		
								7	0.7	0.7	178.8	179.5		
								CC	0.28	0.28	179.5	179.78	PAL	
									9.98	9.98				
20H	3	2300	179.3	188.8	9.5	9.03	95.1							
								1	1.5	1.5	179.3	180.8		
								2	1.5	1.5	180.8	182.3		
								3	1.5	1.5	182.3	183.8		
								4	1.5	1.5	183.8	185.3	EDDY, EDDY	
								5	1.5	1.5	185.3	186.8		
								6	1.26	1.26	186.8	188.06		Split liner
								CC	0.27	0.27	188.06	188.33	PAL	
									9.03	9.03				
21X	4	35	188.8	197.2	8.4	9.74	116.0							
								1	1.5	1.5	188.8	190.3		
								2	1.5	1.5	190.3	191.8		
								3	1.5	1.5	191.8	193.3		
								4	1.5	1.5	193.3	194.8	IW	
								5	1.5	1.5	194.8	196.3	HS	
								6	1.5	1.5	196.3	197.8		
								7	0.38	0.38	197.8	198.18		
								CC	0.36	0.36	198.18	198.54	PAL	
									9.74	9.74				
22X	4	115	197.2	206.8	9.6	9.81	102.2							
								1	1.5	1.5	197.2	198.7		
								2	1.5	1.5	198.7	200.2		

Table T1 (continued).

Core	Date (October 1998)	Time (UTC)	Core depth (mbsf) Top	Core depth (mbsf) Bottom	Length (m) Cored	Length (m) Recovered	Recovery (%)	Section	Length (m) Liner	Length (m) Curated	Section depth (mbsf) Top	Section depth (mbsf) Bottom	Catwalk samples	Comment
								3	1.5	1.5	200.2	201.7		
								4	1.5	1.5	201.7	203.2		
								5	1.5	1.5	203.2	204.7		
								6	1.5	1.5	204.7	206.2		
								7	0.47	0.47	206.2	206.67		
								CC	0.34	0.34	206.67	207.01	PAL	
									9.81	9.81				
23X	4	200	206.8	216.4	9.6	9.47	98.6							
								1	1.5	1.5	206.8	208.3		
								2	1.5	1.5	208.3	209.8		
								3	1.5	1.5	209.8	211.3		
								4	1.5	1.5	211.3	212.8	IW	
								5	1.5	1.5	212.8	214.3	HS	
								6	1.5	1.5	214.3	215.8		
								7	0.18	0.18	215.8	215.98		
								CC	0.29	0.29	215.98	216.27	PAL	
									9.47	9.47				
24X	4	235	216.4	226	9.6	7.5	78.1							
								1	1.5	1.5	216.4	217.9		
								2	1.5	1.5	217.9	219.4		
								3	1.5	1.5	219.4	220.9		
								4	1.5	1.5	220.9	222.4		
								5	1.12	1.12	222.4	223.52	HS	
								CC	0.38	0.38	223.52	223.9	PAL	
									7.50	7.50				
25X	4	320	226	235.6	9.6	8.82	91.9							
								1	1.5	1.5	226	227.5		
								2	1.5	1.5	227.5	229		
								3	1.5	1.5	229	230.5		
								4	1.5	1.5	230.5	232	IW	
								5	1.5	1.5	232	233.5	HS	
								6	1.13	1.13	233.5	234.63		
								CC	0.19	0.19	234.63	234.82	PAL	
									8.82	8.82				
26X	4	400	235.6	245.2	9.6	9.72	101.3							
								1	1.5	1.5	235.6	237.1		
								2	1.5	1.5	237.1	238.6		
								3	1.5	1.5	238.6	240.1		
								4	1.5	1.5	240.1	241.6		
								5	1.5	1.5	241.6	243.1	HS	
								6	1.5	1.5	243.1	244.6		
								7	0.45	0.45	244.6	245.05		
								CC	0.27	0.27	245.05	245.32	PAL	
									9.72	9.72				
27X	4	440	245.2	254.8	9.6	8.75	91.1							
								1	1.5	1.5	245.2	246.7		
								2	1.5	1.5	246.7	248.2		
								3	1.5	1.5	248.2	249.7		

Table T1 (continued).

Core	Date (October 1998)	Time (UTC)	Core depth (mbsf)		Length (m)		Recovery (%)	Section	Length (m)		Section depth (mbsf)		Catwalk samples	Comment
			Top	Bottom	Cored	Recovered			Liner	Curated	Top	Bottom		
								4	1.5	1.5	249.7	251.2	IW	
								5	1.5	1.5	251.2	252.7	HS	
								6	0.96	0.96	252.7	253.66		
								CC	0.29	0.29	253.66	253.95	PAL	
									8.75	8.75				
28X	4	525	254.8	264.4	9.6	9.74	101.5							
								1	1.5	1.5	254.8	256.3		
								2	1.5	1.5	256.3	257.8		
								3	1.5	1.5	257.8	259.3		
								4	1.5	1.5	259.3	260.8		
								5	1.5	1.5	260.8	262.3	HS	
								6	1.5	1.5	262.3	263.8		
								7	0.42	0.42	263.8	264.22		
								CC	0.32	0.32	264.22	264.54	PAL	
									9.74	9.74				
29X	4	610	264.4	274.1	9.7	9.64	99.4							
								1	1.5	1.5	264.4	265.9		
								2	1.5	1.5	265.9	267.4		
								3	1.5	1.5	267.4	268.9		
								4	1.5	1.5	268.9	270.4	IW	
								5	1.5	1.55	270.4	271.95	HS	
								6	1.5	1.5	271.95	273.45		
								7	0.31	0.31	273.45	273.76		
								CC	0.33	0.33	273.76	274.09	PAL	
									9.64	9.69				
30X	4	700	274.1	283.7	9.6	8.23	85.7							
								1	1.5	1.5	274.1	275.6		
								2	1.5	1.5	275.6	277.1		
								3	1.5	1.5	277.1	278.6		
								4	1.5	1.5	278.6	280.1		
								5	1.5	1.5	280.1	281.6	HS	
								6	0.63	0.63	281.6	282.23		
								CC	0.1	0.1	282.23	282.33	PAL	All to PAL
									8.23	8.23				
31X	4	745	283.7	293.3	9.6	4.68	48.8							
								1	1.5	1.5	283.7	285.2		
								2	1.5	1.5	285.2	286.7	IW	
								3	1.3	1.3	286.7	288.0	HS	
								CC	0.38	0.38	288.0	288.38	PAL	
									4.68	4.68				
32X	4	830	293.3	303.0	9.7	9.82	101.2							
								1	1.5	1.5	293.3	294.8		
								2	1.5	1.5	294.8	296.3		
								3	1.5	1.5	296.3	297.8		
								4	1.5	1.5	297.8	299.3		
								5	1.5	1.5	299.3	300.8	HS	
								6	1.5	1.5	300.8	302.3		

Table T1 (continued).

Core	Date (October 1998)	Time (UTC)	Core depth (mbsf) Top	Core depth (mbsf) Bottom	Length (m) Cored	Length (m) Recovered	Recovery (%)	Section	Length (m) Liner	Length (m) Curated	Section depth (mbsf) Top	Section depth (mbsf) Bottom	Catwalk samples	Comment
								7	0.49	0.49	302.3	302.79		
								CC	0.33	0.33	302.79	303.12	PAL	
									9.82	9.82				
33X	4	910	303.0	312.6	9.6	9.79	102.0							
								1	1.5	1.5	303.0	304.5		
								2	1.5	1.5	304.5	306.0		
								3	1.5	1.5	306.0	307.5		
								4	1.5	1.5	307.5	309.0	IW	
								5	1.5	1.5	309.0	310.5	HS	
								6	1.5	1.5	310.5	312.0		
								7	0.45	0.45	312.0	312.5		
								CC	0.34	0.34	312.45	312.79	PAL	
									9.79	9.79				
34X	4	1005	312.6	321.9	9.3	8.44	90.8							
								1	1.5	1.5	312.6	314.1		
								2	1.5	1.5	314.1	315.6		
								3	1.5	1.5	315.6	317.1		
								4	1.5	1.5	317.1	318.6		
								5	1.5	1.5	318.6	320.1	HS	
								6	0.56	0.56	320.1	320.66		
								CC	0.38	0.38	320.66	321.04	PAL	
									8.44	8.44				
35X	4	1055	321.9	331.5	9.6	9.89	103.0							
								1	1.5	1.5	321.9	323.4		
								2	1.5	1.5	323.4	324.9		
								3	1.5	1.5	324.9	326.4		
								4	1.5	1.5	326.4	327.9	IW	
								5	1.5	1.5	327.9	329.4	HS	
								6	1.5	1.5	329.4	330.9		
								7	0.49	0.49	330.9	331.39		
								CC	0.4	0.4	331.39	331.79	PAL	
									9.89	9.89				
36X	4	1140	331.5	341.1	9.6	1.28	13.3							
								1	0.62	0.62	331.5	332.12		
								CC	0.66	0.66	332.12	332.78	PAL	
									1.28	1.28				
37X	4	1255	341.1	350.7	9.6	7.31	76.1							
								1	1.5	1.5	341.1	342.6		
								2	1.5	1.5	342.6	344.1		
								3	1.5	1.5	344.1	345.6	IW	
								4	1.5	1.5	345.6	347.1	HS	
								5	0.91	0.91	347.1	348.01		
								CC	0.4	0.4	348.01	348.41	PAL	
									7.31	7.31				
38X	4	1350	350.7	360.4	9.7	9.77	100.7							
								1	1.5	1.5	350.7	352.2		
								2	1.5	1.5	352.2	353.7		

Table T1 (continued).

Core	Date (October 1998)	Time (UTC)	Core depth (mbsf) Top	Core depth (mbsf) Bottom	Length (m) Cored	Length (m) Recovered	Recovery (%)	Section	Length (m) Liner	Length (m) Curated	Section depth (mbsf) Top	Section depth (mbsf) Bottom	Catwalk samples	Comment
								3	1.5	1.5	353.7	355.2		
								4	1.5	1.5	355.2	356.7		
								5	1.5	1.5	356.7	358.2	HS	
								6	1.5	1.5	358.2	359.7		
								7	0.44	0.44	359.7	360.14		
								CC	0.33	0.33	360.14	360.47	PAL	
									9.77	9.77				
39X	4	1435	360.4	370.1	9.7	9.69	99.9							
								1	1.5	1.5	360.4	361.9		Out of order
								2	1.5	1.5	361.9	363.4		
								3	1.5	1.5	363.4	364.9		
								4	1.5	1.5	364.9	366.4	IW	
								5	1.5	1.5	366.4	367.9	HS	
								6	1.5	1.5	367.9	369.4		
								7	0.38	0.38	369.4	369.78		
								CC	0.31	0.31	369.78	370.09	PAL	
									9.69	9.69				
40X	4	1520	370.1	379.7	9.6	9.02	94							
								1	1.5	1.5	370.1	371.6		
								2	1.5	1.5	371.6	373.1		
								3	1.5	1.5	373.1	374.6		
								4	1.5	1.5	374.6	376.1		
								5	1.5	1.5	376.1	377.6	HS	
								6	1.13	1.13	377.6	378.73		
								CC	0.39	0.39	378.73	379.12	PAL	
									9.02	9.02				
41X	4	1605	379.7	389.4	9.7	9.76	100.6							
								1	1.5	1.5	379.7	381.2		
								2	1.5	1.5	381.2	382.7		
								3	1.5	1.5	382.7	384.2		
								4	1.5	1.5	384.2	385.7	IW	
								5	1.5	1.5	385.7	387.2	HS	
								6	1.5	1.5	387.2	388.7		
								7	0.43	0.43	388.7	389.13		
								CC	0.33	0.33	389.13	389.46	PAL	
									9.76	9.76				
42X	4	1650	389.4	399	9.6	6.67	69.5							
								1	1.5	1.5	389.4	390.9		
								2	1.5	1.5	390.9	392.4		
								3	1.5	1.5	392.4	393.9		
								4	1.5	1.5	393.9	395.4	HS	
								5	0.55	0.55	395.4	395.95		
								CC	0.12	0.12	395.95	396.07	PAL	
									6.67	6.67				
43X	4	1735	399.0	408.6	9.6	7.83	81.6							
								1	1.5	1.5	399.0	400.5		
								2	1.5	1.5	400.5	402.0		

Table T1 (continued).

Core	Date (October 1998)	Time (UTC)	Core depth (mbsf) Top	Core depth (mbsf) Bottom	Length (m) Cored	Length (m) Recovered	Recovery (%)	Section	Length (m) Liner	Length (m) Curated	Section depth (mbsf) Top	Section depth (mbsf) Bottom	Catwalk samples	Comment
								3	1.5	1.5	402.0	403.5	IW	
								4	1.5	1.5	403.5	405.0	HS	
								5	1.4	1.4	405.0	406.4		
								CC	0.43	0.43	406.4	406.83	PAL	
									7.83	7.83				
44X	4	1820	408.6	418.3	9.7	3.53	36.4							
								1	0.82	0.82	408.6	409.42		
								2	1.5	1.5	409.42	410.92		
								3	0.8	0.8	410.92	411.72	HS	
								CC	0.41	0.41	411.72	412.13	PAL	
									3.53	3.53				
45X	4	1935	418.3	427.9	9.6	9.61	100.1							
								1	1.5	1.5	418.3	419.8		
								2	1.5	1.5	419.8	421.3		
								3	1.5	1.5	421.3	422.8	IW	
								4	1.5	1.5	422.8	424.3	HS	
								5	1.5	1.5	424.3	425.8		
								6	1.5	1.5	425.8	427.3		
								7	0.37	0.37	427.3	427.67		
								CC	0.24	0.24	427.67	427.91	PAL	
									9.61	9.61				
46X	4	2030	427.9	437.5	9.6	9.82	102.3							
								1	1.5	1.5	427.9	429.4		
								2	1.5	1.5	429.4	430.9		
								3	1.5	1.5	430.9	432.4		
								4	1.5	1.5	432.4	433.9		
								5	1.5	1.5	433.9	435.4	HS	
								6	1.5	1.5	435.4	436.9		
								7	0.45	0.45	436.9	437.35		
								CC	0.37	0.37	437.35	437.72	PAL	
									9.82	9.82				
47X	4	2115	437.5	446.8	9.3	9.63	103.5							
								1	1.5	1.5	437.5	439.0		
								2	1.5	1.5	439.0	440.5		
								3	1.5	1.5	440.5	442.0		
								4	1.5	1.5	442.0	443.5	IW	
								5	1.5	1.5	443.5	445.0	HS	
								6	1.5	1.5	445.0	446.5		
								CC	0.63	0.63	446.5	447.13	PAL	
									9.63	9.63				
48X	4	2230	446.8	456.4	9.6	4.07	42.4							
								1	1.5	1.5	446.8	448.3		
								2	1.5	1.5	448.3	449.8		
								3	0.71	0.71	449.8	450.51		
								CC	0.36	0.36	450.51	450.87	PAL	
									4.07	4.07				
49X	4	2345	456.4	466.0	9.6	9.6	100.0							
								1	1.5	1.5	456.4	457.9		

Table T1 (continued).

Core	Date (October 1998)	Time (UTC)	Core depth (mbsf) Top	Core depth (mbsf) Bottom	Length (m) Cored	Length (m) Recovered	Recovery (%)	Section	Length (m) Liner	Length (m) Curated	Section depth (mbsf) Top	Section depth (mbsf) Bottom	Catwalk samples	Comment
								2	1.5	1.5	457.9	459.4		
								3	1.5	1.5	459.4	460.9		
								4	1.5	1.5	460.9	462.4	IW	
								5	1.5	1.5	462.4	463.9	HS	
								6	1.5	1.5	463.9	465.4		
								7	0.23	0.23	465.4	465.63		
								CC	0.37	0.37	465.63	466.0	PAL	
									9.60	9.60				
50X	5	55	466.0	475.2	9.2	9.15	99.5							
								1	1.5	1.5	466.0	467.5		
								2	1.5	1.5	467.5	469.0		
								3	1.5	1.5	469.0	470.5		
								4	1.5	1.5	470.5	472.0	HS	
								5	1.5	1.5	472.0	473.5		
								6	1.5	1.5	473.5	475.0		
								CC	0.15	0.15	475.0	475.2	PAL	All to PAL
									9.15	9.15				
51X	5	205	475.2	484.9	9.7	9.8	101.0							
								1	1.5	1.5	475.2	476.7		
								2	1.5	1.5	476.7	478.2		
								3	1.5	1.5	478.2	479.7		
								4	1.5	1.5	479.7	481.2		
								5	1.5	1.5	481.2	482.7	HS	
								6	1.5	1.5	482.7	484.2		
								7	0.34	0.34	484.2	484.54		
								CC	0.46	0.46	484.54	485.0	PAL	
									9.80	9.80				
52X	5	315	484.9	494.5	9.6	9.69	100.9							
								1	1.5	1.5	484.9	486.4		
								2	1.5	1.5	486.4	487.9		
								3	1.5	1.5	487.9	489.4		
								4	1.5	1.5	489.4	490.9	IW	
								5	1.5	1.5	490.9	492.4	HS	
								6	1.5	1.5	492.4	493.9		
								7	0.39	0.39	493.9	494.29		
								CC	0.3	0.3	494.29	494.59	PAL	
									9.69	9.69				
53X	5	425	494.5	504.1	9.6	9.13	95.1							
								1	1.5	1.5	494.5	496.0		
								2	1.5	1.5	496.0	497.5		
								3	1.5	1.5	497.5	499.0		
								4	1.5	1.5	499.0	500.5		
								5	1.5	1.5	500.5	502.0	HS	
								6	1.12	1.12	502.0	503.1		
								CC	0.51	0.51	503.12	503.63	PAL	
									9.13	9.13				

Table T1 (continued).

Core	Date (October 1998)	Time (UTC)	Core depth (mbsf) Top	Core depth (mbsf) Bottom	Length (m) Cored	Length (m) Recovered	Recovery (%)	Section	Length (m) Liner	Length (m) Curated	Section depth (mbsf) Top	Section depth (mbsf) Bottom	Catwalk samples	Comment
54X	5	555	504.1	513.8	9.7	8.73	90.0							
								1	1.5	1.5	504.1	505.6		
								2	1.5	1.5	505.6	507.1		
								3	1.5	1.5	507.1	508.6		
								4	1.5	1.5	508.6	510.1		
								5	1.5	1.5	510.1	511.6	HS	
								6	0.91	0.91	511.6	512.51		
								CC	0.32	0.32	512.51	512.83	PAL	
									8.73	8.73				
55X	5	805	513.8	523.4	9.6	7.28	75.8							
								1	1.5	1.5	513.8	515.3		
								2	1.5	1.5	515.3	516.8		
								3	1.5	1.5	516.8	518.3		
								4	1.5	1.5	518.3	519.8	IW	
								5	1.18	1.18	519.8	520.98	HS	
								CC	0.1	0.1	520.98	521.08	PAL	All to PAL
									7.28	7.28				
56X	5	1030	523.4	533.0	9.6	9.59	99.9							
								1	1.5	1.5	523.4	524.9		
								2	1.5	1.5	524.9	526.4		
								3	1.5	1.5	526.4	527.9		
								4	1.5	1.5	527.9	529.4		
								5	1.5	1.5	529.4	530.9	HS	
								6	1.5	1.5	530.9	532.4		
								7	0.23	0.23	532.4	532.63		
								CC	0.36	0.36	532.63	532.99	PAL	
									9.59	9.59				
57X	15	1230	533.0	542.6	9.6	9.32	97.1							
								1	1.5	1.5	533	534.5		
								2	1.5	1.5	534.5	536		
								3	1.5	1.5	536	537.5	HS	
								4	1.5	1.5	537.5	539		
								5	1.5	1.5	539	540.5		
								6	1.47	1.47	540.5	541.97		
								CC	0.35	0.35	541.97	542.32	PAL	
									9.32	9.32				
58X	5	1515	542.6	552.1	9.5	5.62	59.2							
								1	1.5	1.5	542.6	544.1		
								2	1.5	1.5	544.1	545.6	IW	
								3	1.5	1.5	545.6	547.1	HS	
								4	1.12	1.12	547.1	548.22		
								CC	0.1	0.1	548.22	548.32	PAL	
									5.62	5.62				
				Totals:	552.1	511.66	92.70							

Note: IW = interstitial water, HS = headspace, PAL = paleontology, EDDY = geotechnical samples. This table is also available in **ASCII format.**

Table T2. Macroscopic tephra for Holes 1125A and 1125B.

Hole	Core, section	Depth of tephra at base of section (cm)	Depth of tephra at base of section (mbsf)	Thickness of tephra (cm)	Comments
1125A	1H-1	74	0.74	11	Color: 5Y 5/1
1125A	1H-1	93	0.93	5	Blebs only
1125B	1H-3	143	4.43	9	Color: 5B 6/1
1125A	2H-4	19.5	8.995	14	
1125B	2H-4	4	12.84	17	Color: 5B 6/1
1125A	3H-4	67	18.97	13	
1125A	3H-5	127	21.07	14	
1125A	3H-6	60	21.9	10	
1125A	3H-6	108	22.38	8	
1125B	3H-3	32	21.12	13	Color: 5B 7/1
1125B	3H-5	90	24.7	5	Tephra burrow
1125A	4H-3	34	26.64	7	
1125A	4H-3	75	27.05	2	
1125A	4H-4	117.5	28.975	13	Color: 5YR 6/1 (base), 5YR 7/1 (top)
1125B	4H-2	13	28.93	3	Color: 5Y 6/1
1125A	5H-6	39	40.69	11.5	Color: 5YR 7/1 (base), 5YR 8/1 (top)
1125A	5H-6	68	40.98	14	Color: 5YR 7/1 (base), 5YR 8/1 (top)
1125A	5H-6	108	41.38	2	Color: 5YR 7/1 (base and top), 5YR 6/1 (middle)
1125B	5H-2	138.5	39.685	5.5	Color: 5YR 6/1 (base), 5YR 6/1 (top)
1125B	5H-3	20.5	40.005	5	Color: 5YR 6/1 (base), 5YR 6/1 (top)
1125B	5H-3	123	41.03	14	Color: 5YR 6/1 (bottom 2/3), 5YR 8/1 (top)
1125B	5H-4	65.5	41.955	7	Color: 5YR 4/1 (base), 5YR 5/1 (top)
1125A	6H-5	73.5	49.035	5.5	Color: 5YR 8/1
1125B	6H-1	150	47.8	8.5	Color: 5YR 6/1 (basal 9/10ths), 5YR 8/1 (top)
1125B	6H-5	135	53.65	5.5	Color: 5YR 8/1
1125A	7H-2	138	54.68	0.5	
1125A	9H-5	30	77.1	10	Color: 5GY 5/1, dispersed
1125A	9H-5	66	77.46	11	Color: 5GY 5/1, dispersed
1125A	9H-5	93	77.73	4	Color: 5GY 5/1, dispersed
1125B	11H-4	69	98.99	9	
1125B	15H-3	112	135.92	6	
1125B	19X-4	50	174.8	10	
1125A	20H-3	32	178.42	1	
1125A	20H-2	150	178.1	1	Bioturbated tephra
1125A	20H-3	5	178.15	1	Bioturbated tephra
1125B	24X-4	75	221.65	5	
1125B	24X-4	86	221.76	7	
1125B	24X-4	133	222.23	7	
1125B	28X-5	41.5	261.215	1	
1125B	34X-1	137.5	313.975	2	Nannofossil tephra
1125B	34X-6	42	320.52	2.5	
1125B	36X-CC	45	332.57	1	
1125B	39X-3	138	364.78	8	
1125B	40X-2	1	371.61	9	
1125B	40X-3	133	374.43	8	
1125B	41X-5	26	385.96	10	
1125B	43X-2	122	401.72	10	
1125B	46X-3	75	431.65	3	
1125B	47X-1	26	437.76	4	
1125B	47X-4	62	442.62	3	
1125B	48X-2	22	448.52	5	
1125B	49X-3	95	460.35	5	
1125B	49X-5	14	462.54	2	
1125B	49X-6	20	464.1	3	
1125B	50X-3	16	469.16	3	
1125B	50X-4	72	471.22	4	
1125B	52X-3	87	488.77	2	
1125B	52X-5	120	492.1	6	
1125B	53X-4	17	499.17	5	
1125B	54X-1	81	504.91	1	
1125B	57X-5	149	540.49	2	

Table T3. Identification and relative abundance of nannofossils observed at Site 1125. (See table note. Continued on next page.)

Core, section, interval (cm)	Depth (mbsf)	Preservation	Group abundance	*Amaurolithus delicatus*	*Amaurolithus primus*	*Amaurolithus tricorniculatus*	*Calcidiscus leptoporus*	*Calcidiscus macintyrei*	*Calcidiscus premacintyrei*	*Calcidiscus tropicus*	*Ceratolithus cristatus*	*Chiasmolithus* spp.	*Coccolithus miopelagicus*	*Coccolithus pelagicus*	*Coronocyclus nitescens*	*Cyclicargolithus abisectus*	*Cyclicargolithus floridanus*	*Dictyococcites antarcticus*	*Dictyococcites bisectus*	*Dictyococcites productus*	*Discoaster asymmetricus*	*Discoaster bellus*	*Discoaster brouweri*	*Discoaster exilis*	*Discoaster intercalcaris*	*Discoaster moorei*	*Discoaster pentaradiatus*	*Discoaster pseudovariabilis*	*Discoaster quinqueramus*	*Discoaster subsurculus*	*Discoaster surculus*	*Discoaster tamalis*	*Discoaster triradiatus*	*Discoaster variabilis*	*Emiliania huxleyi*	*Geminilithella rotula*	*Gephyrocapsa* (medium)	*Gephyrocapsa parallela*	*Gephyrocapsa* (small)	*Helicosphaera carteri*	*Helicosphaera intermedia*	*Helicosphaera inversa*	*Helicosphaera pacifica*	*Helicosphaera sellii*	*Markalius inversus*	*Minylitha convallis*	*Pontosphaera* spp.	*Pseudoemiliania lacunosa*	*Pyrocyclus* spp.	*Reticulofenestra asanoi*	*Reticulofenestra* (medium)	*Reticulofenestra pseudoumbilicus*	*Reticulofenestra* (small)	*Reticulofenestra umbilicus*	*Rhabdosphaera clavigera*	*Sphenolithus abies*	*Sphenolithus heteromorphus*	*Sphenolithus moriformis*	*Sphenolithus neoabies*	*Syracosphaera* spp.	*Umbellosphaera irregularis*	*Umbilicosphaera sibogae*
181-1125A-																																																														
1H-CC, 15-25	4.21	G	A				C							A				F			A														R		D	F		C		F					F						R					R		F	R	F
2H-CC, 12-22	13.37	G	A				C				R			A						C																	C	F	A	C		R			R		C	C			C										R	F
3H-CC, 12-22	23.60	G	A				C							C				R																			C	C	A	F								C		C	C											
4H-CC, 13-23	32.83	G	A				F							C				F																			A		C	C				C			R	C	R	F	C									R		
5H-CC, 11-21	42.58	G	VA				C	C						C			R	F	R				C											C						C				C			F	C			C		A							C		
6H-CC, 0-15	51.57	G	A				C	C				R		C		R		C		A			F		F		F					F				R				C				C			F	C			C	F	D	F		R		R				
7H-CC, 28-38	61.77	G	A				F	C				R		C				F	R	C			R											R		F				F				C			F	C	F		A	F				R				F		
8H-CC, 13-23	70.38	G	A				F	C						A			R	F					R													C				C				F			F	C				F	A			R				F		
9H-CC, 26-36	80.76	G	A				C	C						A						C	F		F								F					C			A	C				C				C				C	A									
10H-CC, 15-25	89.91	G	A				C	C					R	C				F	R	C																C				C				C			F	F				F	A						C	C		
11H-CC, 30-40	99.82	G	A				C	C						A				F			F		C		F		F				C		R	C		C				C							C		C			C	A		C			R	C	C		
12H-CC, 14-24	109.08	G	A				C	C	R	F				A			R						C		C		C			F	C			C		F				C												C	A					F	C	C		
13H-CC, 30-40	118.79	G	A				C	C				R		F				F		A			R													F				F							F		F			C	D			C			C			
14H-CC, 15-25	128.11	G	A				C	C						C			R	F		A			A		C		F				C			A		C				C							F					F	A			C			C			
15H-CC, 12-22	137.70	G	A	C			C	C						C				F		A			C		F		R				C			C		C				C							F					C	A			C			C			
16H-CC, 10-20	146.65	G	A	F			C	F			R	R	R	C				F		A			C		F		F				F			A		F				C											C	C	A		F	C			C	F		
17H-CC, 10-20	156.69	G	A				C	C						F			R	F		C			C				C				C			C		F				C	F						F				C	F	C		R	C			C			
18H-CC, 14-24	166.02	G	A				C	C						C				R		A			F				F				F			C		C				C							R				F	C	C			C			C			
19H-CC, 11-22	175.61	G	A		R		C	C						C				C		C			C		C		C				C			F		C				C							C				A	C	A			C		F	C	C		
20H-CC, 10-20	184.92	G	A				C	C						C				F		C			C		F		F				C			C		F				F							C				A	C	A			C		R	C			
21H-CC, 9-19	194.32	VG	VA	C		R	C	C						C			R	F		D			C				C				C			F		C				R							C				A	C	D		C	C		F	C			
22H-CC, 21-31	203.42	G	A	A			C	C				R		C			R		R	A	R		C				C				C			A		F				F							C				C	C	A			C			C			
181-1125B-																																																														
23X-CC, 19-29	216.17	G	A	C			C	C						A				F		A			C			R	C				C			A		C				C							C				C	F	C			C	R		C			
24X-CC, 28-38	223.80	G	A	C			F	C						C				F		C			F		F		C				C			C		C				C							C				C	C	A			C			C			
25X-CC, 9-19	234.72	G	A	F			C	C						C				C		C			C				F				C			F		C				F							C				C	C	C			C			C			
26X-CC, 17-27	245.22	G	A	C	R		C	C						C				F		C			C		R		C				C			C		F				C							F				C	F	A			C			F			
27X-CC, 19-29	253.85	G	A				C	C				R		C			R	F		C														R		C				F							R				C	F	C			F		R	F			
28X-CC, 22-32	264.44	G	A			R		A				R		C	F			C		C			C		F		F							C		C				C							C				C	C	A			C			C			
29X-CC, 23-33	273.99	G	A	F			C	C						C				F		A			F				F							C		F				C							R				C	F	A			C			C			
30X-CC, 0-10	282.23	VG	VA	C			C	C		F				C				R	R	A			C		F		F	F						C		F				C	F						F				C	F	A			C		F	C			
31X-CC, 28-38	288.28	G	A	C			C	C		C				C				F		D									C		R			C		C				C							C				A	C	A			C			C			
32X-CC, 23-33	303.02	G	A	C			C	C		R				C				F		A							F		C					C		F				F							F				A	F	A			C			C			
33X-CC, 24-34	312.69	G	A				F	A						C				C		A			C		F				F					C		C				C											C	C	A			C			C			
34X-CC, 28-38	320.94	VG	A				C	C						C				F		A			R											C		C				C							R				C	C	A			C			F			
35X-CC, 30-40	331.69	G	A				C	C		F				A				F		A			R		R									C		F				C	R						F		R		C	F	C			C			C	F		
36X-CC, 56-66	332.68	G	VA				C	F		C				A		R	R	C	R	D					F									C		C				C	F						F		F		C	C	F			C	R		C	C		
37X-CC, 30-40	348.31	G	A				C	C						C				C		A			F											F		C				C											C	C	A			C			C			

Table T3 (continued).

Core, section, interval (cm)	Depth (mbsf)	Preservation	Group abundance	*Amaurolithus delicatus*	*Amaurolithus primus*	*Amaurolithus tricorniculatus*	*Calcidiscus leptoporus*	*Calcidiscus macintyrei*	*Calcidiscus premacintyrei*	*Calcidiscus tropicus*	*Ceratolithus cristatus*	*Chiasmolithus* spp.	*Coccolithus miopelagicus*	*Coccolithus pelagicus*	*Coronocyclus nitescens*	*Cyclicargolithus abisectus*	*Cyclicargolithus floridanus*	*Dictyococcites antarcticus*	*Dictyococcites bisectus*	*Dictyococcites productus*	*Discoaster asymmetricus*	*Discoaster bellus*	*Discoaster brouweri*
38X-CC, 23-33	360.37	G	A				A	C		F				C				F		A			R
39X-CC, 21-31	369.99	G	VA				C	C				R		F				R		C			C
40X-CC, 29-39	379.02	G	A				C	C	R	C				C				F		C			
41X-CC, 23-33	389.36	G	VA				C	F		C				A						C			
42X-CC, 0-12	395.95	G	A				C	C					R	A				C		A			
43X-CC, 33-43	406.73	G	A				A	C		C		R		C			R	F		A			
44X-CC, 31-41	412.03	G	A				C	C		R				C				C		A			
45X-CC, 14-24	427.81	G	A				C	C				R		C				C		A			F
46X-CC, 27-37	437.62	G	A				C	F						C				C		A			R
47X-CC, 53-63	447.03	G	A				A							A				C		A			F
48X-CC, 26-36	450.77	M	C				C	C						C				C		C			R
49X-CC, 27-37	465.90	M	C				C	C		F				A				C	R	C			R
50X-CC, 0-15	475.00	M	A				C	C		C				C				F		C			R
51X-CC, 36-46	484.90	G	A				C	C		F				C				C		C			F
52X-CC, 20-30	494.49	M	C				C	F		C				C				C		C		C	C
53X-CC, 41-51	503.53	G	A				C	C	R					C				C		F		C	C
54X-CC, 22-32	512.73	G	A				C	F						C			R	F	R	C		R	
55X-CC, 0-10	520.98	M	C				C	C		F				C				F		F			R
56X-CC, 26-36	532.89	G	A				C	C						C				C		C			
57X-CC, 25-35	542.22	M	A				C	C		C				C				C	R	C			
58X-CC	542.20	M	A				C	C		C				F				A		C			

Core, section, interval (cm)	*Discoaster exilis*	*Discoaster intercalcaris*	*Discoaster moorei*	*Discoaster pentaradiatus*	*Discoaster pseudovariabilis*	*Discoaster quinqueramus*	*Discoaster subsurculus*	*Discoaster surculus*	*Discoaster tamalis*	*Discoaster triradiatus*	*Discoaster variabilis*	*Emiliania huxleyi*	*Geminilithella rotula*	*Gephyrocapsa* (medium)	*Gephyrocapsa parallela*	*Gephyrocapsa* (small)	*Helicosphaera carteri*	*Helicosphaera intermedia*	*Helicosphaera inversa*	*Helicosphaera pacifica*
38X-CC, 23-33											F		C				C			
39X-CC, 21-31		F									C		C				A			
40X-CC, 29-39		C									C		F				C			
41X-CC, 23-33		C									C		C				C	C		
42X-CC, 0-12											C		C				C			
43X-CC, 33-43		F									C		C				C			
44X-CC, 31-41											F		C				C			
45X-CC, 14-24					R						F		C				C			
46X-CC, 27-37													F				C			
47X-CC, 53-63													C				C			
48X-CC, 26-36													F				C			
49X-CC, 27-37													C				C			
50X-CC, 0-15	R										R		F				C	F		C
51X-CC, 36-46											F		C				C	F		C
52X-CC, 20-30											C		C				F			
53X-CC, 41-51											C		R				C			
54X-CC, 22-32											F						F			
55X-CC, 0-10													F				C			
56X-CC, 26-36											R		C				C			
57X-CC, 25-35											R		R				F			
58X-CC													F				F			

Core, section, interval (cm)	*Helicosphaera sellii*	*Markalius inversus*	*Minylitha convallis*	*Pontosphaera* spp.	*Pseudoemiliania lacunosa*	*Pyrocyclus* spp.	*Reticulofenestra asanoi*	*Reticulofenestra* (medium)	*Reticulofenestra pseudoumbilicus*	*Reticulofenestra* (small)	*Reticulofenestra umbilicus*	*Rhabdosphaera clavigera*	*Sphenolithus abies*	*Sphenolithus heteromorphus*	*Sphenolithus moriformis*	*Sphenolithus neoabies*	*Syracosphaera* spp.	*Umbellosphaera irregularis*	*Umbilicosphaera sibogae*
38X-CC, 23-33								C	C	A			C			C			
39X-CC, 21-31				C		C		C	C	C			C		F	C			
40X-CC, 29-39		R	C	C		C		C	C	C			C			C			
41X-CC, 23-33			C	C		C		F	C	C			C			C			
42X-CC, 0-12			C	F		F		F	C	C			C			C			
43X-CC, 33-43			C	F		C		C	A	C			C			C			
44X-CC, 31-41			F	R		C		C	A	C			C			C			
45X-CC, 14-24			F			R		A	C	A			C			F			
46X-CC, 27-37								F	C	A			C			C			
47X-CC, 53-63				F				C	C	C			C			C			
48X-CC, 26-36								C	C				C		F	C			
49X-CC, 27-37								C	C				C		F	C			
50X-CC, 0-15				F					C				C			C			
51X-CC, 36-46				C					C				F			F			
52X-CC, 20-30				F					C				C						
53X-CC, 41-51									C				C		R	C			
54X-CC, 22-32						F			C				C		R				
55X-CC, 0-10									C						R	C			
56X-CC, 26-36								C	C	F					R	C			
57X-CC, 25-35								C	F						R	C			
58X-CC								A	F				C		R	C			

Note: Preservation: VG = very good, G = good, and M = moderate; total (group) and relative abundance of calcareous nannofossils: VA = very abundant, A = abundant, C = common, R = rare, and F = few.

Table T4. Nannofossil datum levels identified and age estimates used at Site 1125.

Depth (mbsf)	Bioevent	Age (Ma)	Reference
2.05	LO *Helicosphaera inversa*	0.16	Sato and Kameo, 1996
4.53	LO *Pseudoemiliania lacunosa*	0.42	Sato and Kameo, 1996
23.60	LO *Reticulofenestra asanoi*	0.85	Sato and Kameo, 1996
23.60	FO *Gephyrocapsa parallela*	0.95	Sato and Kameo, 1996
28.22	LO *Helicosphaera sellii*	1.26	Sato and Kameo, 1996
35.80	FO *Gephyrocapsa* (medium)	1.67	Raffi and Flores, 1995
42.00	LO *Discoaster brouweri*	1.96	Raffi and Flores, 1995
47.08	LO *Discoaster tamalis*	2.76	Raffi and Flores, 1995
80.76	Acme *Gephyrocapsa* (small)	3.88	Rio, 1982
94.87	FO *Pseudoemiliania lacunosa*	4.00	Gartner, 1990
285.25	LO *Discoaster quinqueramus*	5.56	Raffi and Flores, 1995
374.50	LO *Minylitha convallis*	7.73	Shackleton et al., 1995
432.40	FO *Minylitha convallis*	9.34	Raffi and Flores, 1995
516.85	FO *Discoaster bellus*	10.50	Gartner, 1990

Note: The depth of each datum level is placed at the midpoint between samples.

Table T5. Significant foraminiferal and bolboformid datums at Site 1125.

Foraminiferal and bolboformid events	Epoch	NZ stage	Age (Ma)	Core, section, interval (cm)	Depth (mbsf)
				181-	
LO *Globorotalia puncticuloides*	Pleistocene	Wc	~0.6	1125A-1H-CC	4.2
LO *Stilostomella* spp.	Pleistocene	Wc	0.6-0.8	1125A-2H-CC	13.4
LO *Plectofrondicularia advena*	Pleistocene	Wc	0.6-0.8	1125A-2H-CC	13.4
FO *Globorotalia truncatulinoides*	Pleistocene	Wn	~0.8*	1125A-3H-CC	23.6
LO *Globorotalia inflata triangula*	late Pliocene	Wn	~2	1125A-5H-CC	42.6
FO *Globorotalia crassula*	late Pliocene	Wm/Wn	2.6	1125A-5H-CC	42.6
LO *Globorotalia crassaformis* (dextral)	late Pliocene	Wn	2.1	1125A-6H-2, 130-135	45.1
FO *Globorotalia crassaformis* (dextral)	early Pliocene	Wp/Wm	3.0	1125A-7H-CC	61.8
LO *Globorotalia crassaconica*	early Pliocene	Wp/Wm	3.0	1125A-8H-CC	74.4
FO *Globorotalia puncticuloides*	early Pliocene	Wp	3.6	1125A-11H-CC	99.8
FO *Globorotalia inflata*	early Pliocene	Wo/Wp	3.7	1125A-11H-CC	99.8
FO *Globorotalia inflata triangula*	early Pliocene	Wo/Wp	3.6	1125A-11H-CC	99.8
LCO *Globorotalia pliozea*	early Pliocene	Wo/Wp	3.6	1125A-13H-CC	118.8
LO *Globorotalia puncticulata*	early Pliocene	Wo/Wp	3.7	1125A-13H-CC	118.8
FO *Globorotalia crassaconica*	early Pliocene	Wo	4.7	1125A-17H-CC	156.7
LO *Globorotalia mons*	early Pliocene	Wo	4.8	1125A-17H-CC	156.7
FO *Globorotalia puncticulata*	Miocene/Pliocene	Tk/Wo	5.2	1125B-25X-CC	234.7
FO *Globorotalia crassaformis*	Miocene/Pliocene	Tk/Wo	5.2	1125B-25X-CC	234.7
LO *Globorotalia sphericomiozea*	Miocene/Pliocene	Tk/Wo	5.2	1125B-25X-CC	234.7
LO *Globorotalia juanai*	Miocene/Pliocene	Tk/Wo	5.2	1125B-26X-CC	245.2
LO *Globorotalia miotumida*	late Miocene	Tk	5.6	1125B-26X-CC	245.2
FO *Globorotalia pliozea*	late Miocene	Tk	5.4	1125B-26X-CC	244.2
FO *Globorotalia mons*	late Miocene	Tk	5.5	1125B-27X-CC	253.9
FO *Globorotalia sphericomiozea*	late Miocene	Tk	5.6	1125B-29X-CC	274.0
FO *Globorotalia juanai*	late Miocene	Tt	6.6	1125B-45X-CC	427.8
LO *Bolboforma* aff. *metzmacheri*	late Miocene	Tt	8.5	1125B-45X-CC	427.8
FCO *Neogloboquadrina pachyderma*	late Miocene	Tt	9.2	1125B-45X-CC	427.8
LO *Globoquadrina dehiscens*	late Miocene	e Tt	9.9	1125B-48X-CC	450.8
LO *Globorotalia panda*	late Miocene	e Tt	10.3	1125B-57X-CC	542.2
LO *Globorotalia miotumida* (dextral)	late Miocene	e Tt	10.7	1125B-58X-CC	548.2
FO *Globorotalia miotumida* (dextral)	late Miocene	e Tt	10.9	1125B-58X-CC	548.2

Note: Wc = Castlecliffian, Wn = Nukumaruan, Wm = Mangapanian, Wp = Waipipian, Wo = Opoitian, Tk = Kapitean, Tt = Tongaporutuan. * = in subantarctic.

Table T6. Identification and abundance of planktonic foraminifers and bolboformids observed at Site 1125. (Continued on next page.)

Core, section, interval (cm)	Depth (mbsf)	Preservation	Group abundance	*Globigerina bulloides*	*Globigerina falconensis*	*Globigerina quinqueloba*	*Globorotalia crassula*	*Globorotalia inflata*	*Globorotalia puncticuloides*	*Globorotalia scitula*	*Globorotalia truncatulinoides*	*Neogloboquadrina pachyderma*	*Orbulina universa*	*Globorotalia crassacarina*	*Globigerinella aequilateralis*	*Globigerinoides extremus*	*Neogloboquadrina humerosa*	*Globorotalia inflata triangula*	*Zeaglobigerina woodi*	*Globorotalia crassaconica*	*Globigerinoides ruber*	*Globorotalia crassaformis* (dextral)	*Globorotalia crassaformis*	*Dentoglobigerina altispira altispira*	*Globorotalia puncticulata*	*Globorotalia pliozea*	*Neogloboquadrina acostaensis*	*Globorotalia mons*	*Globorotalia sphericomiozea*	*Globorotalia juanai*	*Globorotalia miotumida*	*Zeaglobigerina nepenthes*	*Globorotalia explicationis*	*Globorotalia menardii*	*Globorotalia miotumida conoidea*	*Catapsydrax parvulus*	*Globorotalia partimlabiata*	*Bolboforma* aff. *metzmacheri*	*Bolboforma pentaspinosa*	*Globigerinoides quadrilobatus*	*Paragloborotalia mayeri*	*Zeaglobigerina decoraperta*	*Globigerinoides trilobus*	*Globoquadrina dehiscens*	*Neogloboquadrina continuosa*	*Globorotalia panda*	*Globorotalia miotumida* (dextral)	*Globorotalia pseudopima*	*Sphaeroidinellopsis seminulina*
181-1125A-																																																	
1H-CC, 15-25	4.21	P	F	R	P	R	P	R	P	P	P	R	R																																				
2H-CC, 12-22	13.37	G	C	R	R	F	R	F	F	P	P			R																																			
4H-CC, 13-23	32.83	M	C	R	R	R	R	A				R		R	P	P	P																																
5H-CC, 11-21	42.58	G	A	A			R	A	F	P		A	R		P			F	P																														
6H-CC, 0-15	51.57	M	C				R	R	R									R		P																													
7H-6, 42-44	59.72	VG	A	A				F	A			A	P		P			R			P	F																											
7H-CC, 28-38	61.77	VG	A	F		R		F	A	P		F	R		P			P			P	F		P																									
8H-CC		VG	A	A				F	F	R		A	R		P				R	R			R																										
9H-CC, 26-36	80.76	VG	A	A				F	A	P		A	R		P			R	R	P			R																										
11H-CC, 30-40	99.82	G	A	R		F		F				R	R							F					F																								
13H-CC, 30-40	118.79	VG	A	D		R				R		F	R		P					R	P		P		F	P																							
15H-CC, 12-22	137.70	VG	A	D		F				R		F	P							R	P		R		F	R	P																						
17H-CC, 10-20	156.69	VG	A	F	F	F							R						R	R			F		F	R		R																					
18H-CC, 14-24	166.02	VG	A	F	F	R				F		R	P										R		F	R		R																					
20H-CC, 10-20	184.92	VG	A	F		F				P		F	P		P				R				R		F	F	P	P																					
21H-CC, 9-19	194.32	VG	A	F	F							F	P		R										F		P	R																					
22H-CC, 21-31	203.42	VG	A	F						P		D	R												F	R	R	R																					
181-1125B-																																																	
23X-CC, 19-29	216.17	VG	C	R								A	R										F		F	F		P																					
25X-CC, 9-19	234.72	VG	C	R						R		A	R		P										R	F		P	P																				
26X-CC, 17-27	245.22	VG	C	R						R		F	R						R							F	R	F		R	F																		
27X-CC, 19-29	253.85	VG	A	F		R				R		A	F															R	R	R	F																		
29X-CC, 23-33	273.99	G	A	R						P		A	P						R										F		A																		
31X-CC, 28-38	288.28	G	A	F	F	F				P		A	P						R											P	A																		
33X-CC, 24-34	312.69	G	A	F	F					P		A	R						P								P				F	P																	
35X-CC, 30-40	331.69	G	C	A						P		D							R												R	P																	
37X-CC, 30-40	348.31	M	C									R	R																	P	R		P	P	R														
39X-CC, 21-31	369.99	M	C										R																		R			P	R	P													
41X-CC, 23-33	389.36	M	C	R		F							R																		P	P			P		P												
43X-CC, 33-43	406.73	M	C									P	R																		R	R			P	P	P												
44X-CC, 31-41	412.03	M	C									R	F																		R				R	P													
45X-CC, 14-24	427.81	M	A									R	F																		A	R			F			P	R	R									
48X-CC, 26-36	450.77	P	C									R	F																		R	R			R	P	R				P	R		P					
50X-CC, 0-15	475.00	M	F	R						P		P	R						F												F	F											P	P	P				
52X-CC, 20-30	494.49	G	R	A						R		P	P						R												F	R												F	R				
54X-CC, 22-32	512.73	M	C	A									P						F												A	F												F	P				
55X-CC, 0-10	520.98	M	A	A																											A													F					
56X-CC, 26-36	532.89	M	A																												F													F					

Table T6 (continued).

Core, section, interval (cm)	Depth (mbsf)	Preservation	Group abundance	*Globigerina bulloides*	*Globigerina falconensis*	*Globigerina quinqueloba*	*Globorotalia crassula*	*Globorotalia inflata*	*Globorotalia puncticuloides*	*Globorotalia scitula*	*Globorotalia truncatulinoides*	*Neogloboquadrina pachyderma*	*Orbulina universa*	*Globorotalia crassacarina*	*Globigerinella aequilateralis*	*Globigerinoides extremus*	*Neogloboquadrina humerosa*	*Globorotalia inflata triangula*	*Zeaglobigerina woodi*	*Globorotalia crassaconica*	*Globigerinoides ruber*	*Globorotalia crassaformis* (dextral)	*Globorotalia crassaformis*	*Dentoglobigerina altispira altispira*	*Globorotalia puncticulata*	*Globorotalia pliozea*	*Neogloboquadrina acostaensis*	*Globorotalia mons*	*Globorotalia sphericomiozea*	*Globorotalia juanai*	*Globorotalia miotumida*	*Zeaglobigerina nepenthes*	*Globorotalia explicationis*	*Globorotalia menardii*	*Globorotalia miotumida conoidea*	*Catapsydrax parvulus*	*Globorotalia partimlabiata*	*Bolboforma* aff. *metzmacheri*	*Bolboforma pentaspinosa*	*Globigerinoides quadrilobatus*	*Paragloborotalia mayeri*	*Zeaglobigerina decoraperta*	*Globigerinoides trilobus*	*Globoquadrina dehiscens*	*Neogloboquadrina continuosa*	*Globorotalia panda*	*Globorotalia miotumida* (dextral)	*Globorotalia pseudopima*	*Sphaeroidinellopsis seminulina*
57X-CC, 25-35	542.22	P	C										R																			F							R		P			R		R			
58X-CC, 0-10	548.22	P	C	R									R																			R												F			F	P	P

Note: Preservation: VG = very good, G = good, M = moderate, and P = poor; total (group) and relative abundance of planktonic foraminifers: D = dominant, A = abundant, C = common, F = few/frequent, R = rare, and P = present.

Table T7. Composite depth section, Site 1125. (See table note. Continued on next five pages.)

Leg	Site	Hole	Core	Type	Section	Section length (m)	Depth (mbsf)	Offset (m)	Composite depth (mcd)
181	1125	A	1	H	1	1.50	0.00	0.00	0.00
181	1125	A	1	H	2	1.50	1.50	0.00	1.50
181	1125	A	1	H	3	1.06	3.00	0.00	3.00
181	1125	A	1	H	CC	0.25	4.06	0.00	4.06
181	1125	A	2	H	1	1.50	4.30	1.57	5.87
181	1125	A	2	H	2	1.50	5.80	1.57	7.37
181	1125	A	2	H	3	1.50	7.30	1.57	8.87
181	1125	A	2	H	4	1.50	8.80	1.57	10.37
181	1125	A	2	H	5	1.50	10.30	1.57	11.87
181	1125	A	2	H	6	1.45	11.80	1.57	13.37
181	1125	A	2	H	CC	0.22	13.25	1.57	14.82
181	1125	A	3	H	1	1.50	13.80	–0.11	13.69
181	1125	A	3	H	2	1.50	15.30	–0.11	15.19
181	1125	A	3	H	3	1.50	16.80	–0.11	16.69
181	1125	A	3	H	4	1.50	18.30	–0.11	18.19
181	1125	A	3	H	5	1.50	19.80	–0.11	19.69
181	1125	A	3	H	6	1.50	21.30	–0.11	21.19
181	1125	A	3	H	7	0.68	22.80	–0.11	22.69
181	1125	A	3	H	CC	0.22	23.48	–0.11	23.37
181	1125	A	4	H	1	1.50	23.30	3.09	26.39
181	1125	A	4	H	2	1.50	24.80	3.09	27.89
181	1125	A	4	H	3	1.50	26.30	3.09	29.39
181	1125	A	4	H	4	1.50	27.80	3.09	30.89
181	1125	A	4	H	5	1.50	29.30	3.09	32.39
181	1125	A	4	H	6	1.50	30.80	3.09	33.89
181	1125	A	4	H	7	0.40	32.30	3.09	35.39
181	1125	A	4	H	CC	0.23	32.70	3.09	35.79
181	1125	A	5	H	1	1.50	32.80	5.05	37.85
181	1125	A	5	H	2	1.50	34.30	5.05	39.35
181	1125	A	5	H	3	1.50	35.80	5.05	40.85
181	1125	A	5	H	4	1.50	37.30	5.05	42.35
181	1125	A	5	H	5	1.50	38.80	5.05	43.85
181	1125	A	5	H	6	1.50	40.30	5.05	45.35
181	1125	A	5	H	7	0.67	41.80	5.05	46.85
181	1125	A	5	H	CC	0.21	42.47	5.05	47.52
181	1125	A	6	H	1	1.50	42.30	8.43	50.73
181	1125	A	6	H	2	1.50	43.80	8.43	52.23
181	1125	A	6	H	3	1.50	45.30	8.43	53.73
181	1125	A	6	H	4	1.50	46.80	8.43	55.23
181	1125	A	6	H	5	1.50	48.30	8.43	56.73
181	1125	A	6	H	6	1.50	49.80	8.43	58.23
181	1125	A	6	H	7	0.27	51.30	8.43	59.73
181	1125	A	6	H	CC	0.15	51.57	8.43	60.00
181	1125	A	7	H	1	1.50	51.80	10.18	61.98
181	1125	A	7	H	2	1.50	53.30	10.18	63.48
181	1125	A	7	H	3	1.50	54.80	10.18	64.98
181	1125	A	7	H	4	1.50	56.30	10.18	66.48
181	1125	A	7	H	5	1.50	57.80	10.18	67.98
181	1125	A	7	H	6	1.50	59.30	10.18	69.48
181	1125	A	7	H	7	0.69	60.80	10.18	70.98
181	1125	A	7	H	CC	0.38	61.49	10.18	71.67
181	1125	A	8	H	1	1.50	61.30	11.45	72.75
181	1125	A	8	H	2	1.50	62.80	11.45	74.25
181	1125	A	8	H	3	1.50	64.30	11.45	75.75
181	1125	A	8	H	4	1.50	65.80	11.45	77.25
181	1125	A	8	H	5	1.50	67.30	11.45	78.75
181	1125	A	8	H	6	1.45	68.80	11.45	80.25
181	1125	A	8	H	CC	0.23	70.25	11.45	81.70
181	1125	A	9	H	1	1.50	70.80	11.92	82.72
181	1125	A	9	H	2	1.50	72.30	11.92	84.22
181	1125	A	9	H	3	1.50	73.80	11.92	85.72
181	1125	A	9	H	4	1.50	75.30	11.92	87.22
181	1125	A	9	H	5	1.50	76.80	11.92	88.72
181	1125	A	9	H	6	1.50	78.30	11.92	90.22
181	1125	A	9	H	7	0.70	79.80	11.92	91.72
181	1125	A	9	H	CC	0.36	80.50	11.92	92.42
181	1125	A	10	H	1	1.50	80.30	12.87	93.17

Table T7 (continued).

Leg	Site	Hole	Core	Type	Section	Section length (m)	Depth (mbsf)	Offset (m)	Composite depth (mcd)
181	1125	A	10	H	2	1.50	81.80	12.87	94.67
181	1125	A	10	H	3	1.50	83.30	12.87	96.17
181	1125	A	10	H	4	1.50	84.80	12.87	97.67
181	1125	A	10	H	5	1.50	86.30	12.87	99.17
181	1125	A	10	H	6	1.50	87.80	12.87	100.67
181	1125	A	10	H	7	0.46	89.30	12.87	102.17
181	1125	A	10	H	CC	0.25	89.76	12.87	102.63
181	1125	A	11	H	1	1.50	89.80	13.58	103.38
181	1125	A	11	H	2	1.50	91.30	13.58	104.88
181	1125	A	11	H	3	1.50	92.80	13.58	106.38
181	1125	A	11	H	4	1.50	94.30	13.58	107.88
181	1125	A	11	H	5	1.50	95.80	13.58	109.38
181	1125	A	11	H	6	1.50	97.30	13.58	110.88
181	1125	A	11	H	7	0.72	98.80	13.58	112.38
181	1125	A	11	H	CC	0.40	99.52	13.58	113.10
181	1125	A	12	H	1	1.50	99.30	14.81	114.11
181	1125	A	12	H	2	1.50	100.80	14.81	115.61
181	1125	A	12	H	3	1.50	102.30	14.81	117.11
181	1125	A	12	H	4	1.50	103.80	14.81	118.61
181	1125	A	12	H	5	1.50	105.30	14.81	120.11
181	1125	A	12	H	6	1.50	106.80	14.81	121.61
181	1125	A	12	H	7	0.64	108.30	14.81	123.11
181	1125	A	12	H	CC	0.24	108.94	14.81	123.75
181	1125	A	13	H	1	1.50	108.80	16.23	125.03
181	1125	A	13	H	2	1.55	110.30	16.23	126.53
181	1125	A	13	H	3	1.50	111.85	16.23	128.08
181	1125	A	13	H	4	1.50	113.35	16.23	129.58
181	1125	A	13	H	5	1.50	114.85	16.23	131.08
181	1125	A	13	H	6	1.50	116.35	16.23	132.58
181	1125	A	13	H	7	0.64	117.85	16.23	134.08
181	1125	A	13	H	CC	0.40	118.49	16.23	134.72
181	1125	A	14	H	1	1.50	118.30	17.07	135.37
181	1125	A	14	H	2	1.50	119.80	17.07	136.87
181	1125	A	14	H	3	1.50	121.30	17.07	138.37
181	1125	A	14	H	4	1.50	122.80	17.07	139.87
181	1125	A	14	H	5	1.50	124.30	17.07	141.37
181	1125	A	14	H	6	1.50	125.80	17.07	142.87
181	1125	A	14	H	7	0.66	127.30	17.07	144.37
181	1125	A	14	H	CC	0.25	127.96	17.07	145.03
181	1125	A	15	H	1	1.50	127.80	17.98	145.78
181	1125	A	15	H	2	1.50	129.30	17.98	147.28
181	1125	A	15	H	3	1.50	130.80	17.98	148.78
181	1125	A	15	H	4	1.55	132.30	17.98	150.28
181	1125	A	15	H	5	1.50	133.85	17.98	151.83
181	1125	A	15	H	6	1.50	135.35	17.98	153.33
181	1125	A	15	H	7	0.73	136.85	17.98	154.83
181	1125	A	15	H	CC	0.22	137.58	17.98	155.56
181	1125	A	16	H	1	1.47	137.30	19.17	156.47
181	1125	A	16	H	2	1.50	138.77	19.17	157.94
181	1125	A	16	H	3	1.50	140.27	19.17	159.44
181	1125	A	16	H	4	1.50	141.77	19.17	160.94
181	1125	A	16	H	5	1.50	143.27	19.17	162.44
181	1125	A	16	H	6	1.50	144.77	19.17	163.94
181	1125	A	16	H	7	0.28	146.27	19.17	165.44
181	1125	A	16	H	CC	0.20	146.55	19.17	165.72
181	1125	A	17	H	1	1.50	146.80	18.75	165.55
181	1125	A	17	H	2	1.50	148.30	18.75	167.05
181	1125	A	17	H	3	1.50	149.80	18.75	168.55
181	1125	A	17	H	4	1.55	151.30	18.75	170.05
181	1125	A	17	H	5	1.50	152.85	18.75	171.60
181	1125	A	17	H	6	1.50	154.35	18.75	173.10
181	1125	A	17	H	7	0.74	155.85	18.75	174.60
181	1125	A	17	H	CC	0.20	156.59	18.75	175.34
181	1125	A	18	H	1	1.50	156.30	22.44	178.74
181	1125	A	18	H	2	1.50	157.80	22.44	180.24
181	1125	A	18	H	3	1.50	159.30	22.44	181.74
181	1125	A	18	H	4	1.50	160.80	22.44	183.24
181	1125	A	18	H	5	1.50	162.30	22.44	184.74
181	1125	A	18	H	6	1.50	163.80	22.44	186.24
181	1125	A	18	H	7	0.58	165.30	22.44	187.74

Table T7 (continued).

Leg	Site	Hole	Core	Type	Section	Section length (m)	Depth (mbsf)	Offset (m)	Composite depth (mcd)
181	1125	A	18	H	CC	0.24	165.88	22.44	188.32
181	1125	A	19	H	1	1.50	165.80	22.80	188.60
181	1125	A	19	H	2	1.50	167.30	22.80	190.10
181	1125	A	19	H	3	1.50	168.80	22.80	191.60
181	1125	A	19	H	4	1.53	170.30	22.80	193.10
181	1125	A	19	H	5	1.50	171.83	22.80	194.63
181	1125	A	19	H	6	1.50	173.33	22.80	196.13
181	1125	A	19	H	7	0.67	174.83	22.80	197.63
181	1125	A	19	H	CC	0.22	175.50	22.80	198.30
181	1125	A	20	H	1	1.30	175.30	25.10	200.40
181	1125	A	20	H	2	1.50	176.60	25.10	201.70
181	1125	A	20	H	3	1.50	178.10	25.10	203.20
181	1125	A	20	H	4	1.50	179.60	25.10	204.70
181	1125	A	20	H	5	1.50	181.10	25.10	206.20
181	1125	A	20	H	6	1.50	182.60	25.10	207.70
181	1125	A	20	H	7	0.72	184.10	25.10	209.20
181	1125	A	20	H	CC	0.20	184.82	25.10	209.92
181	1125	A	21	H	1	1.50	184.80	25.86	210.66
181	1125	A	21	H	2	1.50	186.30	25.86	212.16
181	1125	A	21	H	3	1.50	187.80	25.86	213.66
181	1125	A	21	H	4	1.50	189.30	25.86	215.16
181	1125	A	21	H	5	1.50	190.80	25.86	216.66
181	1125	A	21	H	6	1.40	192.30	25.86	218.16
181	1125	A	21	H	7	0.53	193.70	25.86	219.56
181	1125	A	21	H	CC	0.19	194.23	25.86	220.09
181	1125	A	22	H	1	1.50	194.30	27.70	222.00
181	1125	A	22	H	2	1.50	195.80	27.70	223.50
181	1125	A	22	H	3	1.50	197.30	27.70	225.00
181	1125	A	22	H	4	1.50	198.80	27.70	226.50
181	1125	A	22	H	5	1.50	200.30	27.70	228.00
181	1125	A	22	H	6	1.41	201.80	27.70	229.50
181	1125	A	22	H	CC	0.31	203.21	27.70	230.91
181	1125	B	1	H	1	1.50	0.00	1.54	1.54
181	1125	B	1	H	2	1.50	1.50	1.54	3.04
181	1125	B	1	H	3	1.50	3.00	1.54	4.54
181	1125	B	1	H	4	1.50	4.50	1.54	6.04
181	1125	B	1	H	5	1.50	6.00	1.54	7.54
181	1125	B	1	H	6	0.66	7.50	1.54	9.04
181	1125	B	1	H	CC	0.14	8.16	1.54	9.70
181	1125	B	2	H	1	1.50	8.30	3.05	11.35
181	1125	B	2	H	2	1.50	9.80	3.05	12.85
181	1125	B	2	H	3	1.50	11.30	3.05	14.35
181	1125	B	2	H	4	1.50	12.80	3.05	15.85
181	1125	B	2	H	5	1.50	14.30	3.05	17.35
181	1125	B	2	H	6	1.50	15.80	3.05	18.85
181	1125	B	2	H	7	0.47	17.30	3.05	20.35
181	1125	B	2	H	CC	0.18	17.77	3.05	20.82
181	1125	B	3	H	1	1.50	17.80	4.09	21.89
181	1125	B	3	H	2	1.50	19.30	4.09	23.39
181	1125	B	3	H	3	1.50	20.80	4.09	24.89
181	1125	B	3	H	4	1.50	22.30	4.09	26.39
181	1125	B	3	H	5	1.50	23.80	4.09	27.89
181	1125	B	3	H	6	1.50	25.30	4.09	29.39
181	1125	B	3	H	7	0.41	26.80	4.09	30.89
181	1125	B	3	H	CC	0.10	27.21	4.09	31.30
181	1125	B	4	H	1	1.50	27.30	4.58	31.88
181	1125	B	4	H	2	1.50	28.80	4.58	33.38
181	1125	B	4	H	3	1.50	30.30	4.58	34.88
181	1125	B	4	H	4	1.50	31.80	4.58	36.38
181	1125	B	4	H	5	1.50	33.30	4.58	37.88
181	1125	B	4	H	6	1.50	34.80	4.58	39.38
181	1125	B	4	H	7	0.17	36.30	4.58	40.88
181	1125	B	4	H	CC	0.21	36.47	4.58	41.05
181	1125	B	5	H	1	1.50	36.80	9.16	45.96
181	1125	B	5	H	2	1.50	38.30	9.16	47.46
181	1125	B	5	H	3	1.50	39.80	9.16	48.96
181	1125	B	5	H	4	1.50	41.30	9.16	50.46
181	1125	B	5	H	5	1.50	42.80	9.16	51.96
181	1125	B	5	H	6	1.50	44.30	9.16	53.46
181	1125	B	5	H	7	0.66	45.80	9.16	54.96

Table T7 (continued).

Leg	Site	Hole	Core	Type	Section	Section length (m)	Depth (mbsf)	Offset (m)	Composite depth (mcd)
181	1125	B	5	H	CC	0.20	46.46	9.16	55.62
181	1125	B	6	H	1	1.50	46.30	9.93	56.23
181	1125	B	6	H	2	1.50	47.80	9.93	57.73
181	1125	B	6	H	3	1.50	49.30	9.93	59.23
181	1125	B	6	H	4	1.50	50.80	9.93	60.73
181	1125	B	6	H	5	1.50	52.30	9.93	62.23
181	1125	B	6	H	6	1.50	53.80	9.93	63.73
181	1125	B	6	H	7	0.50	55.30	9.93	65.23
181	1125	B	6	H	CC	0.23	55.80	9.93	65.73
181	1125	B	7	H	1	1.50	55.80	12.12	67.92
181	1125	B	7	H	2	1.50	57.30	12.12	69.42
181	1125	B	7	H	3	1.50	58.80	12.12	70.92
181	1125	B	7	H	4	1.50	60.30	12.12	72.42
181	1125	B	7	H	5	1.50	61.80	12.12	73.92
181	1125	B	7	H	6	1.50	63.30	12.12	75.42
181	1125	B	7	H	7	0.72	64.80	12.12	76.92
181	1125	B	7	H	CC	0.23	65.52	12.12	77.64
181	1125	B	8	H	1	1.50	65.30	11.20	76.50
181	1125	B	8	H	2	1.50	66.80	11.20	78.00
181	1125	B	8	H	3	1.50	68.30	11.20	79.50
181	1125	B	8	H	4	1.50	69.80	11.20	81.00
181	1125	B	8	H	5	1.50	71.30	11.20	82.50
181	1125	B	8	H	6	1.41	72.80	11.20	84.00
181	1125	B	8	H	CC	0.21	74.21	11.20	85.41
181	1125	B	9	H	1	1.50	74.80	11.54	86.34
181	1125	B	9	H	2	1.50	76.30	11.54	87.84
181	1125	B	9	H	3	1.50	77.80	11.54	89.34
181	1125	B	9	H	4	1.50	79.30	11.54	90.84
181	1125	B	9	H	5	1.50	80.80	11.54	92.34
181	1125	B	9	H	6	1.50	82.30	11.54	93.84
181	1125	B	9	H	7	0.60	83.80	11.54	95.34
181	1125	B	9	H	CC	0.25	84.40	11.54	95.94
181	1125	B	10	H	1	1.50	84.30	13.67	97.97
181	1125	B	10	H	2	1.50	85.80	13.67	99.47
181	1125	B	10	H	3	1.50	87.30	13.67	100.97
181	1125	B	10	H	4	1.50	88.80	13.67	102.47
181	1125	B	10	H	5	1.50	90.30	13.67	103.97
181	1125	B	10	H	6	0.88	91.80	13.67	105.47
181	1125	B	10	H	CC	0.12	92.68	13.67	106.35
181	1125	B	11	H	1	1.50	93.80	14.06	107.86
181	1125	B	11	H	2	1.50	95.30	14.06	109.36
181	1125	B	11	H	3	1.50	96.80	14.06	110.86
181	1125	B	11	H	4	1.50	98.30	14.06	112.36
181	1125	B	11	H	5	1.50	99.80	14.06	113.86
181	1125	B	11	H	6	1.50	101.30	14.06	115.36
181	1125	B	11	H	7	0.68	102.80	14.06	116.86
181	1125	B	11	H	CC	0.25	103.48	14.06	117.54
181	1125	B	12	H	1	0.90	103.30	16.00	119.30
181	1125	B	12	H	2	1.50	104.20	16.00	120.20
181	1125	B	12	H	3	1.50	105.70	16.00	121.70
181	1125	B	12	H	4	1.50	107.20	16.00	123.20
181	1125	B	12	H	5	1.50	108.70	16.00	124.70
181	1125	B	12	H	6	1.50	110.20	16.00	126.20
181	1125	B	12	H	7	0.40	111.70	16.00	127.70
181	1125	B	12	H	CC	0.25	112.10	16.00	128.10
181	1125	B	13	H	1	1.50	112.80	16.08	128.88
181	1125	B	13	H	2	1.50	114.30	16.08	130.38
181	1125	B	13	H	3	1.50	115.80	16.08	131.88
181	1125	B	13	H	4	1.50	117.30	16.08	133.38
181	1125	B	13	H	5	1.50	118.80	16.08	134.88
181	1125	B	13	H	6	1.50	120.30	16.08	136.38
181	1125	B	13	H	7	0.69	121.80	16.08	137.88
181	1125	B	13	H	CC	0.21	122.49	16.08	138.57
181	1125	B	14	H	1	1.50	122.30	17.62	139.92
181	1125	B	14	H	2	1.50	123.80	17.62	141.42
181	1125	B	14	H	3	1.50	125.30	17.62	142.92

Table T7 (continued).

Leg	Site	Hole	Core	Type	Section	Section length (m)	Depth (mbsf)	Offset (m)	Composite depth (mcd)
181	1125	B	14	H	4	1.50	126.80	17.62	144.42
181	1125	B	14	H	5	1.50	128.30	17.62	145.92
181	1125	B	14	H	6	1.50	129.80	17.62	147.42
181	1125	B	14	H	7	0.64	131.30	17.62	148.92
181	1125	B	14	H	CC	0.30	131.94	17.62	149.56
181	1125	B	15	H	1	1.50	131.80	18.81	150.61
181	1125	B	15	H	2	1.50	133.30	18.81	152.11
181	1125	B	15	H	3	1.50	134.80	18.81	153.61
181	1125	B	15	H	4	1.50	136.30	18.81	155.11
181	1125	B	15	H	5	1.50	137.80	18.81	156.61
181	1125	B	15	H	6	1.50	139.30	18.81	158.11
181	1125	B	15	H	7	0.71	140.80	18.81	159.61
181	1125	B	15	H	CC	0.21	141.51	18.81	160.32
181	1125	B	16	H	1	1.50	141.30	19.27	160.57
181	1125	B	16	H	2	1.50	142.80	19.27	162.07
181	1125	B	16	H	3	1.50	144.30	19.27	163.57
181	1125	B	16	H	4	1.50	145.80	19.27	165.07
181	1125	B	16	H	5	1.50	147.30	19.27	166.57
181	1125	B	16	H	6	1.50	148.80	19.27	168.07
181	1125	B	16	H	7	0.73	150.30	19.27	169.57
181	1125	B	16	H	CC	0.24	151.03	19.27	170.30
181	1125	B	17	H	1	1.50	150.80	20.37	171.17
181	1125	B	17	H	2	1.50	152.30	20.37	172.67
181	1125	B	17	H	3	1.50	153.80	20.37	174.17
181	1125	B	17	H	4	1.50	155.30	20.37	175.67
181	1125	B	17	H	5	1.50	156.80	20.37	177.17
181	1125	B	17	H	6	1.50	158.30	20.37	178.67
181	1125	B	17	H	7	0.79	159.80	20.37	180.17
181	1125	B	17	H	CC	0.27	160.59	20.37	180.96
181	1125	B	18	H	1	1.50	160.30	24.51	184.81
181	1125	B	18	H	2	1.50	161.80	24.51	186.31
181	1125	B	18	H	3	1.50	163.30	24.51	187.81
181	1125	B	18	H	4	1.50	164.80	24.51	189.31
181	1125	B	18	H	5	1.50	166.30	24.51	190.81
181	1125	B	18	H	6	1.30	167.80	24.51	192.31
181	1125	B	18	H	7	0.31	169.10	24.51	193.61
181	1125	B	18	H	CC	0.28	169.41	24.51	193.92
181	1125	B	19	H	1	1.50	169.80	25.26	195.06
181	1125	B	19	H	2	1.50	171.30	25.26	196.56
181	1125	B	19	H	3	1.50	172.80	25.26	198.06
181	1125	B	19	H	4	1.50	174.30	25.26	199.56
181	1125	B	19	H	5	1.50	175.80	25.26	201.06
181	1125	B	19	H	6	1.50	177.30	25.26	202.56
181	1125	B	19	H	7	0.70	178.80	25.26	204.06
181	1125	B	19	H	CC	0.28	179.50	25.26	204.76
181	1125	B	20	H	1	1.50	179.30	26.81	206.11
181	1125	B	20	H	2	1.50	180.80	26.81	207.61
181	1125	B	20	H	3	1.50	182.30	26.81	209.11
181	1125	B	20	H	4	1.50	183.80	26.81	210.61
181	1125	B	20	H	5	1.50	185.30	26.81	212.11
181	1125	B	20	H	6	1.26	186.80	26.81	213.61
181	1125	B	20	H	CC	0.27	188.06	26.81	214.87
181	1125	B	21	X	1	1.50	188.80	27.06	215.86
181	1125	B	21	X	2	1.50	190.30	27.06	217.36
181	1125	B	21	X	3	1.50	191.80	27.06	218.86
181	1125	B	21	X	4	1.50	193.30	27.06	220.36
181	1125	B	21	X	5	1.50	194.80	27.06	221.86
181	1125	B	21	X	6	1.50	196.30	27.06	223.36
181	1125	B	21	X	7	0.38	197.80	27.06	224.86
181	1125	B	21	X	CC	0.36	198.18	27.06	225.24
181	1125	B	22	X	1	1.50	197.20	31.07	228.27
181	1125	B	22	X	2	1.50	198.70	31.07	229.77
181	1125	B	22	X	3	1.50	200.20	31.07	231.27
181	1125	B	22	X	4	1.50	201.70	31.07	232.77
181	1125	B	22	X	5	1.50	203.20	31.07	234.27
181	1125	B	22	X	6	1.50	204.70	31.07	235.77
181	1125	B	22	X	7	0.47	206.20	31.07	237.27

Table T7 (continued).

Leg	Site	Hole	Core	Type	Section	Section length (m)	Depth (mbsf)	Offset (m)	Composite depth (mcd)
181	1125	B	22	X	CC	0.34	206.67	31.07	237.74
181	1125	B	23	X	1	1.50	206.80	31.07	237.87
181	1125	B	23	X	2	1.50	208.30	31.07	239.37
181	1125	B	23	X	3	1.50	209.80	31.07	240.87
181	1125	B	23	X	4	1.50	211.30	31.07	242.37
181	1125	B	23	X	5	1.50	212.80	31.07	243.87
181	1125	B	23	X	6	1.50	214.30	31.07	245.37
181	1125	B	23	X	7	0.18	215.80	31.07	246.87
181	1125	B	23	X	CC	0.29	215.98	31.07	247.05
181	1125	B	24	X	1	1.50	216.40	31.07	247.47
181	1125	B	24	X	2	1.50	217.90	31.07	248.97
181	1125	B	24	X	3	1.50	219.40	31.07	250.47
181	1125	B	24	X	4	1.50	220.90	31.07	251.97
181	1125	B	24	X	5	1.12	222.40	31.07	253.47
181	1125	B	24	X	CC	0.38	223.52	31.07	254.59
181	1125	B	25	X	1	1.50	226.00	31.07	257.07
181	1125	B	25	X	2	1.50	227.50	31.07	258.57
181	1125	B	25	X	3	1.50	229.00	31.07	260.07
181	1125	B	25	X	4	1.50	230.50	31.07	261.57
181	1125	B	25	X	5	1.50	232.00	31.07	263.07
181	1125	B	25	X	6	1.13	233.50	31.07	264.57
181	1125	B	25	X	CC	0.19	234.63	31.07	265.70

Note: This table is also available in **ASCII format.**

Table T8. Splice tie points, Site 1125.

Site	Hole	Core	Type	Section	Depth in section (cm)	Depth (mbsf)	Depth (mcd)		Site	Hole	Core	Type	Section	Depth in section (cm)	Depth (mbsf)	Depth (mcd)
1125	A	1	H	2	120	2.70	2.70	Tie to	1125	B	1	H	1	114.0	1.16	2.70
1125	B	1	H	4	116	5.66	7.20	Tie to	1125	A	2	H	1	131.5	5.63	7.20
1125	A	2	H	5	74	11.04	12.61	Tie to	1125	B	2	H	1	124.0	9.56	12.61
1125	B	2	H	5	96	15.26	18.31	Tie to	1125	A	3	H	4	12.0	18.42	18.31
1125	A	3	H	7	12	22.92	22.81	Tie to	1125	B	3	H	1	92.0	18.72	22.81
1125	B	3	H	5	124	25.04	29.13	Tie to	1125	A	4	H	2	124.0	26.04	29.13
1125	A	4	H	5	96	30.26	33.35	Tie to	1125	B	4	H	1	147.0	28.77	33.35
1125	B	4	H	5	113	34.43	39.01	Tie to	1125	A	5	H	1	116.0	33.96	39.01
1125	A	5	H	6	144	41.74	46.79	Tie to	1125	B	5	H	1	82.0	37.63	46.79
1125	B	5	H	5	97	43.77	52.93	Tie to	1125	A	6	H	2	69.0	44.50	52.93
1125	A	6	H	5	88	49.18	57.61	Tie to	1125	B	6	H	1	136.5	47.68	57.61
1125	B	6	H	5	137	53.67	63.60	Tie to	1125	A	7	H	2	12.0	53.42	63.60
1125	A	7	H	5	144	59.24	69.42	Tie to	1125	B	7	H	1	150.0	57.30	69.42
1125	B	7	H	5	116	62.96	75.08	Tie to	1125	A	8	H	2	82.5	63.63	75.08
1125	A	8	H	5	136	68.66	80.11	Tie to	1125	B	8	H	3	59.0	68.91	80.11
1125	B	8	H	5	124	72.54	83.74	Tie to	1125	A	9	H	1	101.0	71.82	83.74
1125	A	9	H	6	12	78.42	90.34	Tie to	1125	B	9	H	3	98.0	78.80	90.34
1125	B	9	H	6	95	83.25	94.79	Tie to	1125	A	10	H	2	12.0	81.92	94.79
1125	A	10	H	5	44	86.74	99.61	Tie to	1125	B	10	H	2	14.0	85.94	99.61
1125	B	10	H	5	105	91.35	105.02	Tie to	1125	A	11	H	2	14.0	91.44	105.02
1125	A	11	H	7	12	98.92	112.50	Tie to	1125	B	11	H	4	14.0	98.44	112.50
1125	B	11	H	6	39	101.69	115.75	Tie to	1125	A	12	H	2	13.0	100.94	115.75
1125	A	12	H	6	44	107.24	122.05	Tie to	1125	B	12	H	3	33.0	106.05	122.05
1125	B	12	H	5	119	109.89	125.89	Tie to	1125	A	13	H	1	85.0	109.66	125.89
1125	A	13	H	4	128	114.63	130.86	Tie to	1125	B	13	H	2	47.0	114.78	130.86
1125	B	13	H	6	59	120.89	136.97	Tie to	1125	A	14	H	2	9.0	119.90	136.97
1125	A	14	H	5	48	124.78	141.85	Tie to	1125	B	14	H	2	42.0	124.23	141.85
1125	B	14	H	5	99	129.29	146.91	Tie to	1125	A	15	H	1	111.5	128.93	146.91
1125	A	15	H	6	92	136.27	154.25	Tie to	1125	B	15	H	3	63.5	135.44	154.25
1125	B	15	H	5	105	138.85	157.66	Tie to	1125	A	16	H	1	118.5	138.49	157.66
1125	A	16	H	6	4	144.81	163.98	Tie to	1125	B	16	H	3	39.5	144.71	163.98
1125	B	16	H	5	34	147.64	166.91	Tie to	1125	A	17	H	1	136.0	148.16	166.91
1125	A	17	H	6	144	155.79	174.54	Tie to	1125	B	17	H	3	36.0	154.17	174.54
1125	B	17	H	6	95	159.25	179.62	Tie to	1125	A	18	H	1	88.0	157.18	179.62
1125	A	18	H	6	4	163.84	186.28	Tie to	1125	B	18	H	1	147.0	161.77	186.28
1125	B	18	H	4	129	166.09	190.60	Tie to	1125	A	19	H	2	49.0	167.80	190.60
1125	A	19	H	6	112	174.45	197.25	Tie to	1125	B	19	H	2	66.5	171.99	197.25
1125	B	19	H	5	74	176.54	201.80	Tie to	1125	A	20	H	2	9.0	176.70	201.80
1125	A	20	H	6	32	182.92	208.02	Tie to	1125	B	20	H	2	39.0	181.21	208.02
1125	B	20	H	4	115	184.95	211.76	Tie to	1125	A	21	H	1	109.0	185.90	211.76
1125	A	21	H	5	80	191.60	217.46	Tie to	1125	B	21	X	2	7.5	190.40	217.46
1125	B	21	X	6	95	197.25	224.31	Tie to	1125	A	22	H	2	80.5	196.61	224.31
1125	A	22	H	6	48	202.28	229.98	Tie to	1125	B	22	X	2	19.0	198.91	229.98
1125	B	22	X	7	46	206.66	237.73									

Note: This table is also available in **ASCII format.**

Table T9. Biostratigraphic events identified at Site 1125.

	Events	Group	Age (Ma)	Sample	Depth (mbsf)
1	LO *Helicosphaera inversa*	N	0.16	1125A-1H-CC	4.21
2	LO *Pseudoemiliania lacunosa*	N	0.42	1125A-2H-CC	13.37
3	FO *Globorotalia truncatulinoides*	F	~0.8*	1125A-2H-CC	13.4
4	LO *Reticulofenestra asanoi*	N	0.85	1125A-3H-CC	23.6
5	FO *Gephyrocapsa parallela*	N	0.98	1125A-3H-CC	23.6
6	LO *Helicosphaera sellii*	N	1.26	1125A-4H-CC	32.83
7	FO *Gephyrocapsa* (medium)	N	1.67	1125A-4H-CC	32.83
8	LO *Discoaster brouweri*	N	1.96	1125A-5H-CC	42.58
9	LO *Discoaster tamalis*	N	2.76	1125A-6H-CC	51.57
10	FO *Globorotalia crassula*	F	2.6	1125A-6H-CC	51.57
11	LO *Globorotalia crassaformis* (dextral)	F	2.1	1125A-7H-6, 42-44 cm	59.7
12	FO *Globorotalia crassaformis* (dextral)	F	3.0	1125A-7H-CC	61.8
13	Acme *Gephyrocapsa* (small)	N	3.88	1125A-9H-CC	80.67
14	FO *Globorotalia puncticuloides*	F	3.6	1125A-9H-CC	80.8
15	FO *Globorotalia inflata triangula*	F	3.6	1125A-9H-CC	80.8
16	FO *Pseudoemiliania lacunosa*	N	4.0	1125A-10H-CC	89.91
17	FO *Globorotalia inflata*	F	3.7	1125A-11H-CC	99.8
18	LO *Globorotalia puncticulata*	F	3.7	1125A-11H-CC	99.8
19	LCO *Globorotalia pliozea*	F	3.6	1125A-13H-CC	118.8
20	FO *Globorotalia crassaconica*	F	~4.7	1125A-17H-CC	156.7
21	LO *Globorotalia mons*	F	~4.8	1125A-17H-CC	156.7
22	FO *Globorotalia puncticulata*	F	5.2	1125B-25X-CC	234.7
23	FO *Globorotalia crassaformis*	F	5.2	1125B-25X-CC	234.7
24	LO *Globorotalia sphericomiozea*	F	5.2	1125B-25X-CC	234.7
25	LO *Globorotalia juanai*	F	5.2	1125B-26X-CC	245.2
26	LO *Globorotalia miotumida*	F	5.6	1125B-26X-CC	245.2
27	FO *Globorotalia pliozea*	F	5.4	1125B-26X-CC	245.2
28	FO *Globorotalia sphericomiozea*	F	5.6	1125B-27X-CC	253.9
29	FO *Globorotalia mons*	F	5.5	1125B-29X-CC	274.0
30	LO *Discoaster quinqueramus*	N	5.56	1125B-31X-CC	288.28
31	FO *Globorotalia juanai*	F	~6.6	1125B-37X-CC	348.3
32	LO *Minylitha convallis*	N	7.73	1125B-40X-CC	379.02
33	LO *Bolboforma* aff. *metzmacheri*	F	8.5	1125B-41X-CC	389.4
34	FO *Minylitha convallis*	N	9.43	1125B-45X-CC	427.81
35	LO *Globoquadrina dehiscens*	F	9.9	1125B-48X-CC	450.8
36	LO *Globorotalia panda*	F	~10.3	1125B-50X-CC	475
37	FO *Discoaster bellus*	N	10.5	1125B-54X-CC	512.73
38	Acme Kaiti *Globorotalia miotumida* (dextral) event	F	10.8–10.9	1125B-58X-CC	548.2

Note: * = in subantarctic.

Table T10. Composition of interstitial waters at Site 1125.

Core, section, interval (cm)	Depth (mbsf)	Depth (mcd)	Salinity	Cl^- (mM)	pH	Alkalinity (mM)	Na^+ (mM)	Mg^{2+} (mM)	Ca^{2+} (mM)	SO_4^{2-} (mM)	HPO_4^{2-} (µM)	NH_4^+ (µM)	H_4SiO_4 (µM)	K^+ (mM)
1125A-														
1H-2, 145-150	2.95	2.95	34.5	556	7.51	3.95	472	51.7	10.0	26.1	6.8	158	447	11.8
3H-4, 145-150	19.75	19.64	34.5	559	7.38	5.82	475	49.4	9.1	22.2	6.4	463	610	11.4
5H-4, 145-150	38.75	43.80	33.5	562	7.37	7.11	477	45.9	8.6	18.1	4.8	984	727	11.5
7H-4, 140-150	57.70	67.88	33.5	563	7.32	7.19	479	44.2	7.5	16.0	4.4	1210	718	11.2
9H-4, 140-150	76.70	88.62	33.5	562	7.39	8.06	480	41.6	7.1	13.4	4.4	1327	660	10.8
11H-4, 140-150	95.70	109.28	33.0	563	7.32	8.80	479	38.8	7.5	10.5	5.2	1627	705	10.7
13H-2, 145-155	111.75	127.98	32.5	564	7.35	8.80	483	36.1	6.6	8.4	4.8	1684	694	10.5
15H-4, 145-155	133.75	151.73	32.5	564	7.32	9.33	483	33.5	6.6	5.6	5.6	1701	746	10.3
17H-4, 145-155	152.75	171.50	32.0	563	7.30	9.70	482	31.1	7.0	3.5	4.4	2165	792	10.4
19H-4, 143-153	171.73	194.53	32.0	565	7.23	9.75	487	28.3	7.0	2.4	5.2	2120	859	10.0
21H-4, 140-150	190.70	216.56	32.0	563	7.19	9.91	482	27.3	7.4	0.0	4.8	2279	879	9.8
1125B-														
21X-4, 140-150	194.70	221.76	32.0	563	7.25	10.06	483	27.3	7.8	0.9	4.4	2369	904	10.1
23X-4, 140-150	212.70	243.77	32.0	565	7.19	10.51	485	25.8	7.9	0.0	4.0	2406	947	9.8
25X-4, 140-150	231.90	262.97	31.5	565	7.32	9.28	485	25.4	8.8	0.0	5.6	2132	941	9.9
27X-4, 140-150	251.10	—	31.5	566	7.19	8.92	488	23.8	9.3	0.0	3.6	2459	922	9.4
29X-4, 140-150	270.30	—	31.5	565	7.15	8.35	489	22.3	9.9	0.0	6.0	2550	982	9.3
31X-2, 140-150	286.60	—	31.5	568	7.17	8.56	491	21.7	10.9	0.0	8.7	2541	1044	9.3
33X-4, 140-150	308.90	—	32.0	569	7.27	7.80	493	20.5	11.6	0.0	7.8	2578	1051	8.9
35X-4, 140-150	327.80	—	32.0	569	7.11	7.76	497	18.9	12.1	0.0	9.5	2488	1077	8.4
37X-3, 140-150	345.50	—	32.0	569	7.06	7.92	494	18.9	13.3	0.0	6.0	2455	1066	8.4
39X-4, 140-150	366.30	—	32.0	569	7.11	7.19	495	17.9	14.1	0.3	6.6	2566	1083	8.2
41X-4, 140-150	385.60	—	32.0	569	7.09	7.08	495	16.7	15.3	0.0	5.0	2505	1100	7.9
43X-3, 140-150	403.40	—	32.0	570	7.12	6.12	496	16.3	15.8	0.0	7.2	2345	1080	7.8
45X-3, 135-150	422.65	—	32.0	570	7.10	6.14	497	15.1	16.7	0.2	5.6	2435	1079	7.2
47X-4, 135-150	443.35	—	32.0	573	7.09	5.24	501	14.2	17.6	0.0	11.7	2198	1042	6.7
49X-4, 135-150	462.25	—	32.0	575	7.20	4.24	503	13.6	18.6	0.5	11.1	2206	1010	6.3
52X-4, 135-150	490.75	—	32.0	576	7.33	4.17	503	12.9	20.2	0.6	6.8	2128	1019	5.3
55X-4, 135-150	519.65	—	32.0	579	7.79	0.96	507	10.5	22.1	0.0	4.2	1941	181	4.3
58X-2, 135-150	545.45	—	32.5	583	7.41	1.94	510	9.1	25.2	0.8	4.4	1493	418	3.7

Note: — = not available. This table is also available in **ASCII format.**